Institut für Hydrologie
der Albert-Ludwigs-Universität Freiburg i.Br.

Combined approach of numeric groundwater modelling with classical and geophysical hydrometry to investigate runoff processes at the hillslope scale

Katrin Meusburger

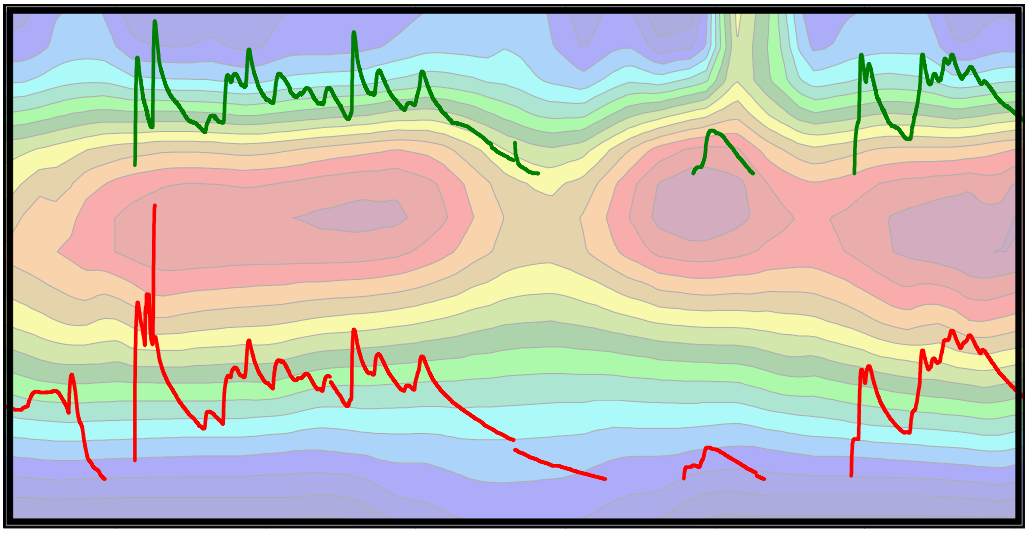

Diplomarbeit unter der Leitung von PD Dr. S. Uhlenbrook
Freiburg i.Br., Januar 2005

Institut für Hydrologie
der Albert-Ludwigs-Universität Freiburg i.Br.

Combined approach of numeric groundwater modelling with classical and geophysical hydrometry to investigate runoff processes at the hillslope scale

Katrin Meusburger

Referent: PD Dr. S. Uhlenbrook
Ko-Referent: Dr. J. Lange

Diplomarbeit unter der Leitung von PD Dr. S. Uhlenbrook
Freiburg i.Br., Januar 2005

Contents

List of figures in the text

List of tables in the text

Contents of the Appendix

Notations

ρ	[Ωm]	resistivity
ΔV	[V]	difference in voltage
A		current electrode
a	[m]	electrode spacing
a.s.l.	[m]	above see level
A_r	[m²]	area of the inner ring
B		current electrode
DFG		Deutsche Forschungsgemeinschaft
ERT		electrical resistivity tomography
ET_0	[mm]	reference evapotranspiration
F	[-]	formation factor
h	[m]	pressure head
h_1,h_2	[m]	Water table to the time t_1, t_2.
h_m	[m]	drawdown of water level above well bottom
I	[A]	current
IHF		Institute for Hydrology, Freiburg
K_{ij}^A	[-]	components of a dimensionless anisotropy tensor K^A
K_r	[m/d]	relative hydraulic conductivity
K_s	[m/d]	saturated hydraulic conductivity
l	[-]	pore connectivity parameter
L	[m]	length of the well filter
M		potential electrode
MHQ	[m³/s]	mean highest discharge
MQ	[m³/s]	mean discharge
Mq	[l/s*km²]	mean yield
m	[-]	empirical constant
min.		minutes
N		potential electrode
n	[-]	pore size distribution index
na	[m]	multiple electrode spacing
P		precipitation
p_e		effective porosity
pH	[-]	value of pH
Q	[m³/s]	pumping capacity
Q_P		channel precipitation

Q_g		groundwater flow
Q_O		overland flow
Q_t		throughflow
Q_V	[m³]	volume of infiltrated water
R	[Ωm]	resistivity
r	[m]	radius of the well filter
r^2	[-]	coefficient of determination
RES2Dinv		resistivity-2D-inversion programme
R_G	[J/cm²]	global radiation
RMS	[%]	root-mean-squared
S	[1/d]	sink term for root water uptake
s	[m]	absolute value of drawdown in the depletion curve
S_e	[m³/m³]	effective water content
t		time
T	[°C]	daily mean of air temperature
T_r	[m²/s]	transmissivity,
U	[%]	relative humidity
V	[V]	voltage
VES		vertical electrical sounding
w_i	[-]	weight associated with a particular data point
x	[m]	distance
$x_{i\ (i=1,2)}$	[m]	special coordinates
y_i	[-]	fitted value
z_i	[-]	observed value
α	[-]	inverse of the air-entry value
ε	[-]	empirical constant
Θ	[m³/m³]	volumetric water content
$Θ_r$	[m³/m³]	residual water content
$Θ_s$	[m³/m³]	saturated water content
$σ_f$	[-]	conductivity of the formation as a whole
$σ_w$	[-]	conductivity of the water
Φ	[m]	matric suction

Summary

The following thesis “Combined approach of numeric groundwater modelling with classical and geophysical hydrometry to investigate runoff processes at the hillslope scale” is based on the results from the project “Runoff generation processes and catchment modelling” which was funded by the German Research Foundation (DFG) project.

As expressed by the title the general aim of this study is to improve the comprehension of runoff generation mechanisms with the help of different methodologies. The analysis of experimental data and its integration into a physically based soil water model serves on the one hand to identify the processes at the hillslope scale and on the other hand, to assess potential and limitations of physically based modelling.

The research site is located in the Black Forest Mountains in Germany at 800 m a.s.l. elevation, where snow is an important form of precipitation, but rain is still decisive. Beside climatic factors the forest-covered steep slopes, which occupy three quarters of the catchment area, and strong Pleistocene influences, determine present hydrological processes. The material covering the crystalline bedrock is a heterogenic composition of well-conductive boulder fields with poorly conductive boulder clay as well as solifluction debris and moraine deposits.

HYDRUS-2D is a mathematical model that describes water and solute transport in porous media with physical equations such as the Richard’s equation for variably saturated-unsaturated flow and the Fickian-based dispersive-advective transport equation. The hydraulic properties of the unsaturated soil are nonlinear functions of the pressure head, which are described with the analytical van Genuchten function where water movement in the unsaturated media is defined by six independent parameters that can be derived form measurement or a soil texture database.

The focus of the experimental work was to receive data for model application and to improve the understanding of flow mechanisms by studying the soil water status and groundwater level observations for a period of three month. Soil hydraulic properties were surveyed and assigned to the finite element grid of the numeric model with help of geoelectric measurements (ERT).
The experimental work can be separated into three different parts:

- inquiry of hydrometry data (measurement of stream data, piezometric heads, soil moisture time series and hydrochemistry data)

- exploration of the subsurface (with drilling, ERT profiling and vertical electrical sounding)
- determination of soil hydraulic parameters (with infiltration and pumping tests).

A perched groundwater table that covers the main aquifer body was found at the test site. The distinct dynamic of the perched groundwater table originates from the direct influence of meteorology (precipitation and evaporation). The water flow to this shallow groundwater table occurs mainly by an vertically infiltrating wetting front but moist antecedent conditions also allow preferential flow. Although the perched water table shields the main groundwater body from local influence of evapotranspiration and precipitation its response of the piezometric heads to rainfall is slightly faster and more pronounced. As fractions of percolation to the groundwater are small, the impulses creating this distinct reactions in the groundwater are induced by an impulse of a faster infiltration component probably located at the hillslope and lateral transport through the flood plain. The transport might be possible with piston flow displacement or a subsurface pipe network as simulations assuming Darcy flow failed to reproduce the distinct dynamic of the deep groundwater. The detection of a subsurface pipe system by KOCH (2004) supports the latter hypothesis.

The results of this study indicate the need for a two-domain concept to be incorporated into simulation models. This would help to improve predictions concerning different hydrological purposes and to quantify the relevance of accelerated subsurface flow components. It is necessary to combine experimental work and model application in order to reciprocally complement one another.
The investigations at the headwater research site clearly highlight that the occurrence of throughflow does not prohibit rapid groundwater reactions, which might be of major importance for generation of stormflow hydrographs.

Keywords:
numeric groundwater model (HYDRUS)
electrical resistivity tomography (ERT)
subsurface stormflow
lateral flow
macropores
piston flow
hydrological process
perched groundwater

Zusammenfassung

Die vorliegende Diplomarbeit “Combined approach of numeric groundwater modelling with classical and geophysical hydrometry to investigate runoff processes at the hillslope scale” basiert auf den Ergebnissen des Projekts „Abflussbildung und Einzugsgebietsmodellierung“ welches von der Deutschen Forschungsgemeinschaft gefördert wurde.

Die Zielsetzung dieser Studie ist, wie der Titel besagt, das Verständnis von Abflussbildungsprozessen durch die Kombination verschiedener Methoden zu erweitern. Die Analyse experimenteller Daten und deren Einbindung in ein physikalisch basiertes Bodenwassermodell sollen zu einen verbesserten Verständnis der Abflussbildungsmechanismen an der Hangskala dienen und das Potential und Grenzen physikalisch basierter Modellierung aufzeigen.

Die Versuchsfläche befindet sich im südlichen Schwarzwald in einer Höhe von 800 m ü.NN. In dem zu drei Vierteln bewaldeten Einzugsgebiet fällt ein bedeutender Teil des Niederschlags als Schnee, was sich in einem nivo-pluvialen Regime wiederfindet. Neben klimatischen Faktoren bestimmen die steilen Hänge und der glaziale Ursprung des Gebietes die hydrologischen Prozesse. Die Überdeckung des Grundgebirges ist sehr heterogen; Gut durchlässige Blockschutthalden wechseln mit schlecht durchlässigem Geschiebelehm, periglazialen Fließerden und Moränenmaterial.

HYDRUS-2D ist ein mathematisches Modell welches Wasser- und Stoffflüsse in porösen Medien mit physikalischen Grundgleichungen, wie der Richard’s Gleichung für variablen gesättigten- ungesättigten Fluß und der auf den Fick’schen Gleichung basierenden dispersive-advektive Transportgleichung beschreibt. Die hydraulischen Eigenschaften des ungesättigten Bodens sind nicht-lineare Funktionen der Druckhöhe die mit einem analytischen Ansatz von van Genuchten beschrieben werden. Dabei wird der Wassertransport im ungesättigten Medium über sechs unabhängige Parameter definiert die aus Messungen oder aus einer Bodenarten Datenbank erhalten werden können.

Die experimentelle Arbeit diente zum einen der Datengewinnung (Eingangs- und Kalibrierungsdaten, Bodenparameter) für die Modellanwendung. Gleichzeitig soll durch die Analyse der Daten für den Untersuchungszeitraum von drei Monaten die Abflussprozesse entschlüsselt werden. Die hydraulischen Eigenschaften des Bodens wurden untersucht und mit Hilfe von Geoelektrik Messungen (ERT) auf

das Finite Elemente Grid des numerischen Modells übertragen. Der experimentelle Teil dieser Arbeit kann in drei Abschnitte eingeteilt werden:

- Erhebung von hydrometrischen Daten (wie Grundwasserhöhen, hydrochemische Daten, Bodenfeuchte- und Abflussmessungen)
- Erkundung des Untergrundes (durch Bohrung und geoelektrische Kartierung und Sondierung)
- Bestimmung von Aquiferparametern (mit Infiltrations- und Pumpversuchen)

Auf der Versuchsfläche wurde ein über dem Hauptgrundwasserleiter schwebender Grundwasserspiegel entdeckt. Die ausgeprägte Dynamik der schwebenden Grundwasserspiegels resultiert aus dem direkten Einfluß meteorologischer Faktoren (Niederschlag und Evapotranspiration). Der Wassertransport zu diesem oberflächenahen Grundwasserspiegel erfolgt hauptsächlich über eine infiltrierende Feuchtefront, jedoch tritt bei ausgeprägter Vorfeuchte auch präferentieller Fluß auf. Obwohl das schwebende Grundwasser den Aquifer von lokalem Verdunstungs- und Niederschlagseinfluß abschirmt, sind in diesem schnellere und deutlichere Reaktion zu beobachten. Da nur geringfügig Perkolation stattfindet, ist es wahrscheinlich, daß der Auslöser der dynamischen Grundwasserschwankungen schnelle Infiltrationskomponenten am Hang sind, die lateral durch die Talaue transportiert werden. Auf der Darcygleichung basierende Simulationen konnten die stärke Dynamik des tiefen Grundwassers nicht nachbilden was auf Piston Flow oder Markroporenfluß als mögliche Transportmechanismen schließen läßt. KOCH (2004) konnte das Vorhandensein eines unterirdischen Röhrensystems nachweisen, was für die letztere Hypothese spricht.

Die Ergebnisse dieser Studie bestätigen die Notwendigkeit eines Two-domain Konzepts für die Boden- und Grundwassermodellierung. Dies würde nicht nur die Vorhersagen für verschiedenste hydrologische Fragestellungen verbessern, sondern auch ermöglichen die Relevanz von schnellen Zwischen- und Grundwasserabflusskomponenten zu quantifizieren. Eine Kombination von experimenteller Arbeit und Modellanwendung ermöglicht gegenseitige Ergänzung und Verbesserungen.
Die Untersuchungen am Testfeld im Oberlauf des St. Wilhelmer Talbaches zeigten deutlich, daß trotz der Existenz eines schwebenden Grundwasserspiegels schnelle Grundwasserkomponenten auftreten können, die für die Entstehung von Hochwasserereignissen einen entscheidenden Einfluß haben.

1 Introduction

Models are a mathematical imitation of nature and an essential tool for hydrologists to describe the complex factors affecting the water cycle with the aim to make predictions e.g. water resource management or flood forecasting etc. To improve results of model predictions a comprehensive understanding of processes relating rainfall with runoff is fundamental. It is therefore crucial that modelling approaches and knowledge from process experimentation are brought together.

Therefore, within the project “Runoff generation processes and catchment modelling” supported by the German Research Foundation (DFG) experimental investigations are conducted in order to improve process-based catchment modelling.
Despite worldwide research endeavours concerning runoff generation processes, there are still open questions. Especially runoff generation mechanisms happening in the subsurface disguised form the sight of the observer are not sufficiently understood.
Various techniques are required to identify and quantify subsurface processes. The objective of the research project of Freiburg is to utilise tracer hydrology and geoelectric methods to investigate subsurface runoff generation mechanisms.

Thereby the focus is laid upon hillslope flow paths because mechanisms of rapid response at the hillslope scale affects the magnitude of storm flow peaks at small (< 10 km^2) and large (10 - 100 km^2) catchment scale not only by overland flow but also subsurface storm flow.

1.1 Theoretical background

In this section, an introduction about sources and components of runoff is presented (WARD & ROBINSON, 2000) to provide a theoretical background and introduce the used terminology.
The main part of precipitation that reaches the surface is absorbed by the soil (infiltration). The remaining precipitation flows over the surface as overland flow. Once any depression storage has been filled the infiltrated water may evaporate, or flow laterally close to the surface as throughflow, or percolate under gravity to the groundwater body.
The groundwater body can be classified into tree main types (see Figure 1-1).

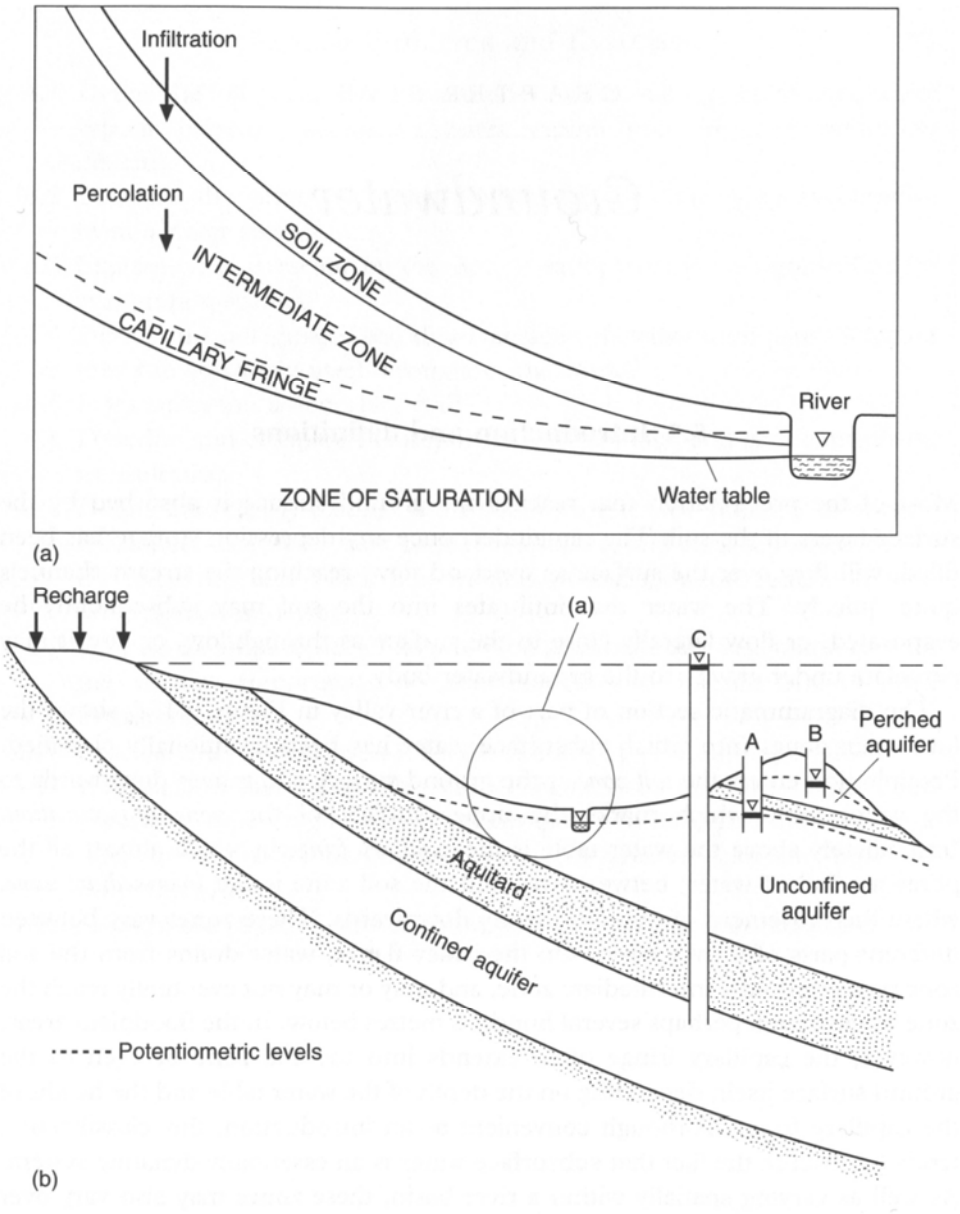

Figure 1-1: (a) main zones into which subsurface water has been traditionally classified; (b) relationship between unconfined, perched and confined aquifers where piezometric heads may be different in each of them (WARD & ROBINSON, 2000).

- Unconfined groundwater (unconfined aquifer): A water table is the upper boundary of an unconfined aquifer. The water table is defined where the porewater pressure is equal to atmospheric pressure,
- Confined groundwater has a overlying less conductive layer; because the unconfined groundwater is situated at a higher elevation it is to be concluded, that groundwater in the confined aquifer is under a pressure equivalent to the difference in the hydrostatic level between the two. The surface to which the water level of a confined aquifer rises after the drilling of a well is the height of the water table in the recharge area minus the height the of energy loss resulting from

the movement of water from the recharge area to the measurement point. This level is the piezometric surface.

- Perched groundwater is a special case of unconfined groundwater, which commonly occurs where an impermeable or semi-impermeable bed exists in a shallow depth at some height above the main groundwater body or if the surface layers of the soil are so slowly permeable as to result in saturated conditions. The perched aquifer and the main groundwater body are separated by an unsaturated zone.

Two main components contribute to the hydraulic head (i) the pore water pressure; pressure head; and (ii) height above sea level; the elevation head (see Figure 1-2).

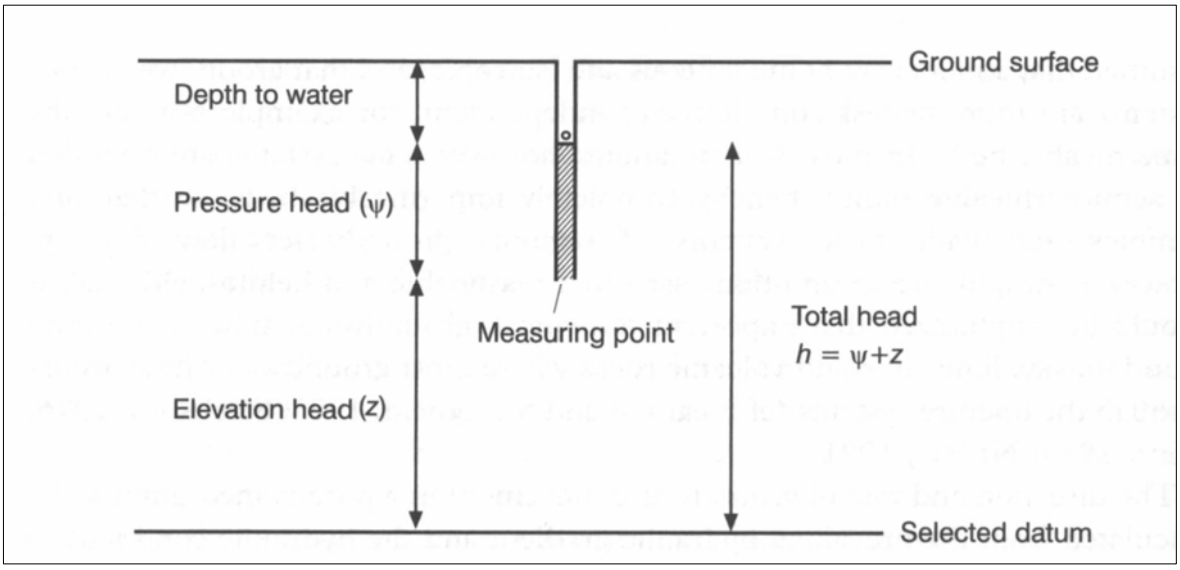

Figure 1-2: Diagram showing the elevation head (z), pressure head (ψ) and the total head (h), for a specific measurement point in a groundwater flow field (WARD & ROBINSON, 2000).

For this study, the matric pressure is expressed in terms of a pressure head as the pressure head can be converted to potential energy applying the gravitational constant.
The pressure potential is negative in the unsaturated zone due to water retention forces (matric suction), becomes zero at the water table, and gets increasingly positive with depth.
Water will move from a point of higher to a point of lower total potential energy.
Darcy's law describes the movement of water in the saturated zone. Whereas for unsaturated media, the Richards equation is valid (see chapter 3.1).

The reaction of streamflow to rainfall is variable in space (due to drainage basin characteristics) and time (seasonally and even during a single storm event). This indicates the existence of different flow paths of precipitation towards the stream. These flow paths are direct precipitation onto stream surface (Q_P: channel precipitation); direct

precipitation on the surface (Q_O: overland flow); shallow subsurface flow (Q_t: throughflow); and deep subsurface flow (Q_g: groundwater flow).
The variability during a single event is exemplary displayed in Figure 1-3: in the beginning of rainfall (a), subsurface flow dominates but as rainfall proceeds (b), an additional flow path occur $Q_O(s)$ (saturation overland flow) and the contribution of the different flow component to stream runoff changes.

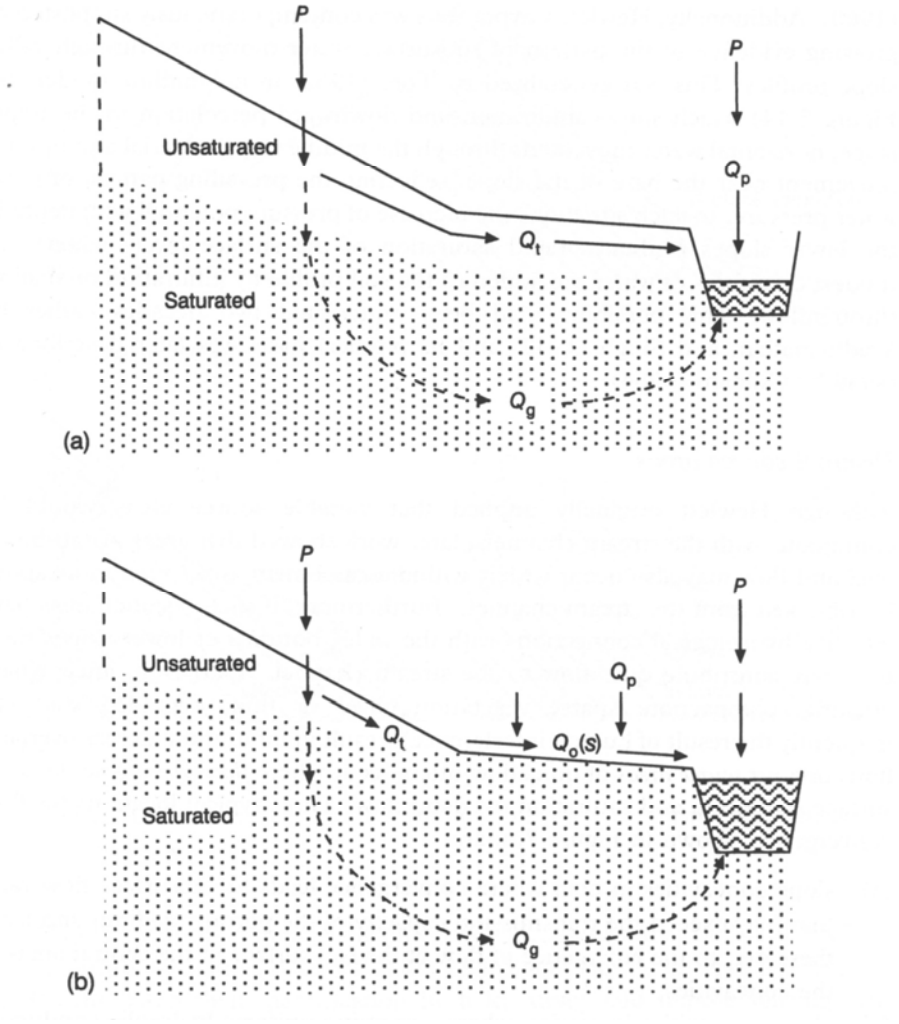

Figure 1-3: Schematically display of different pathways of precipitation to the stream; a: at the beginning of rainfall, b: after a longer rainfall duration (WARD & ROBINSON, 2000).

The amount of precipitation falling direct on water surfaces (channel precipitation) is usually very small because the surface of the perennial channel system is only small compared to the total catchment area and thus is neglected in the following.
There are two causes of overland flow: excess of infiltration capacity of the surface or, more common in humid and sub-humid areas a rise of shallow water tables to the ground surface during rainfall; saturation overland flow.
The subsurface runoff consists of throughflow and groundwater flow. Infiltrated water that moves laterally through the upper horizons of the soil toward the stream, either as unsaturated flow or as shallow perched saturated flow is known as throughflow. Lateral

instead of vertical movement is supported by topography and stratification e.g. hillslopes or even in isotropy soil, the hydraulic conductivity is bigger near the surface than in deeper compacted parts. Throughflow is regarded as probably the most important runoff generation process in steeply sloping terrain of the headwaters as for example the St. Wilhelmer Talbach. In flat terrain, infiltrated rainfall percolates through the soil layer to the groundwater and eventually reaches the stream as groundwater flow through the saturated zone. Once it was thought that subsurface flow is too slow to influence the short-term response of stream flow, however in humid areas high proportions of quickflow are generated by subsurface flow.

The focus of this study is the quick components of subsurface flow. An explanation for the occurrence of rapid subsurface flow is that throughflow from lower slopes closest to the channel contribute in the beginning of an event and as rainfall proceeds, the riparian area of surface saturation expands and shortens the flow path for throughflow from more distant parts of the slope.

Responsible for the rapid arrival of throughflow in headwater catchments are flow in macropores or a process called piston flow or translatory flow, whereby a new increment of rainfall displaces all preceding increments, causing the oldest water to exit from the bottom end of the hillslope profile. This is only possible, if the available moisture storage capacity is almost filled in order to conduct a pressure wave through the coherent groundwater body. These processes may also induce a fast reaction of groundwater.

Throughflow does not always reach the stream directly but surfaces at some point and continues to flow over the surface to the stream (return flow).

Another process that allows groundwater to contribute significantly to a storm hydrograph is the formation of a groundwater ridge near the stream, because comparatively modest input of rainfall into already very moist soil causes a rapid increase in soil moisture potential. In addition, lower valley sides often have a concave profile that provokes convergence that might lead to overland flow as well as groundwater recharge.

1.2 Previous studies

In recent decades, several field studies have been conduced on hillslopes and steep headwater catchments that improved hillslope process understanding. The following reviews provide a summarisation:

- ANDERSON & BURT (1990),
- BONELL (1998),
- Uchida et al. (2001).

Thereby it could be proved that subsurface stormflow processes such as e.g. lateral macropore flow (e.g. MOSLEY,1982; MCGLYNN ET AL., 2002), perched aquifers above less conductive layers (e.g. MCDONNELL, 1990; LORENTZ, 2001), near-stream groundwater ridging effects (e.g. SKLASH & FARVOLDEN, 1979), pressure wave effects (TORRES ET AL., 1998), and transmissivity feedback mechanisms (BISHOP, 1991) have considerable affects on rapid stream hydrodynamic. The contribution of groundwater to rapid runoff response was verified by O'BRIEN (1977) and ZALTSBERG (1987).
More literature to previous studies and example applications of applied methods within this work are given prior the corresponding sections in the methodology chapter.
At the investigated area, the surface water / groundwater test site St. Wilhelm, Black Forest, Germany, three consecutive studies (WENNINGER 2002; SCHEIDLER 2002; KOCH 2004) have already been carried out. The focus of WENNINGER (2002) and SCHEIDLER (2002) was on possible occurrence of the piston flow effect and to identify the origin of water at saturated areas, in particular during events. Reasoning was established based on natural tracer data (deuterium, dissolved silica, and major anions and cations) and the dynamics in piezometric heads but concerning the observed heterogeneity knowledge of subsurface structures was assumed insufficient to provide evidence for possible piston flow.
During the work of KOCH (2004) 111 ERT measurement were carried out to gain a three dimensional picture of the subsurface structure on the test site. Three zones of different resistivity could be detected.
Because of the ERT measurements, scepticism aroused, whether the groundwater monitoring holes reach into the main aquifer body and whether the conceptual idea of processes on the test site, is comprehensive.
Therefore, additional experimental work was necessary. Beside the surveyed data of the present study, this work is also based on results of the previous diploma thesis.

1.3 Objectives and Procedure

The objective of this study is to further improve the conceptual image of runoff generation processes at the hillslope scale by experimental work and the application a numeric groundwater model. With the help of classical hydrometric data and geoelectric methods conceptualisation and parameterisation of the numeric soil water HYDRUS-2D is carried out. A simulation of observed pressure heads and soil moisture contents with focus on flood events is done.
The application of the model should help to narrow the possible hydrological concepts and should indicate whether processes are actually understood. Reciprocally with gained knowledge from field observation, the limitations of physically based modelling with the present database should be assessed.

Various steps were carried out to reach the aim of this study. First, exact positions of the groundwater wells were measured to determine the flow direction of groundwater and to identify a vertical two-dimensional modelling profile.
With pumping test and double ring infiltration experiments aquifer parameters were determined. Soil moisture probes in different depth were installed to measure the extend of local infiltration and to provide calibration data for the unsaturated zone. On 07/07/04, a deeper groundwater well was implemented with a filter device in 5m depth. With the gained soil probes from the drilling core and additional geoelectric 1-D and 2-D measurements the subsurface is further explored.
Surface / groundwater water samples are collected. The objective was to differentiate and characterise the water components on the test site. In chapter 4 a description of the applied methodologies is provided.
After a measurement period of three month, the measured water content / pressure head timeseries and water samples were analysed. The analysis and discussion of the conducted fieldwork is presented in chapter 5.
The new and previously gained knowledge is integrated into the one-dimensional soil water model HYDRUS-1D to perform a parameter calibration and to prove to which extend the observed dynamic of shallow and deep groundwater can be explained by vertical movement of subsurface water.
All collected data and information from the previous studies are integrated into a vertical two-dimensional HYDRUS-2D finite element grid in order to reproduce groundwater dynamic at the test site conducting different scenarios. The model results are presented and discussed in chapter 6 in order to assess potential and limitations of the physically based model concept of HYDRUS-2D and suggestions for an improved simulation are proposed.
A conceptual model of runoff processes, derived from the observations and model application is schematically presented in chapter 7.

2 Study area

The upper St. Wilhelmer valley was chosen for detailed investigations of runoff generation processes on hillslopes. The test site was established in 2001 it provides an on-site stream and a steep hillslope. The subject of interest is how they are linked by the flood plain. The following sections give a brief description. For a more detailed description, see LINDENLAUB (1998) and UHLENBROOK (1999).

2.1 Location

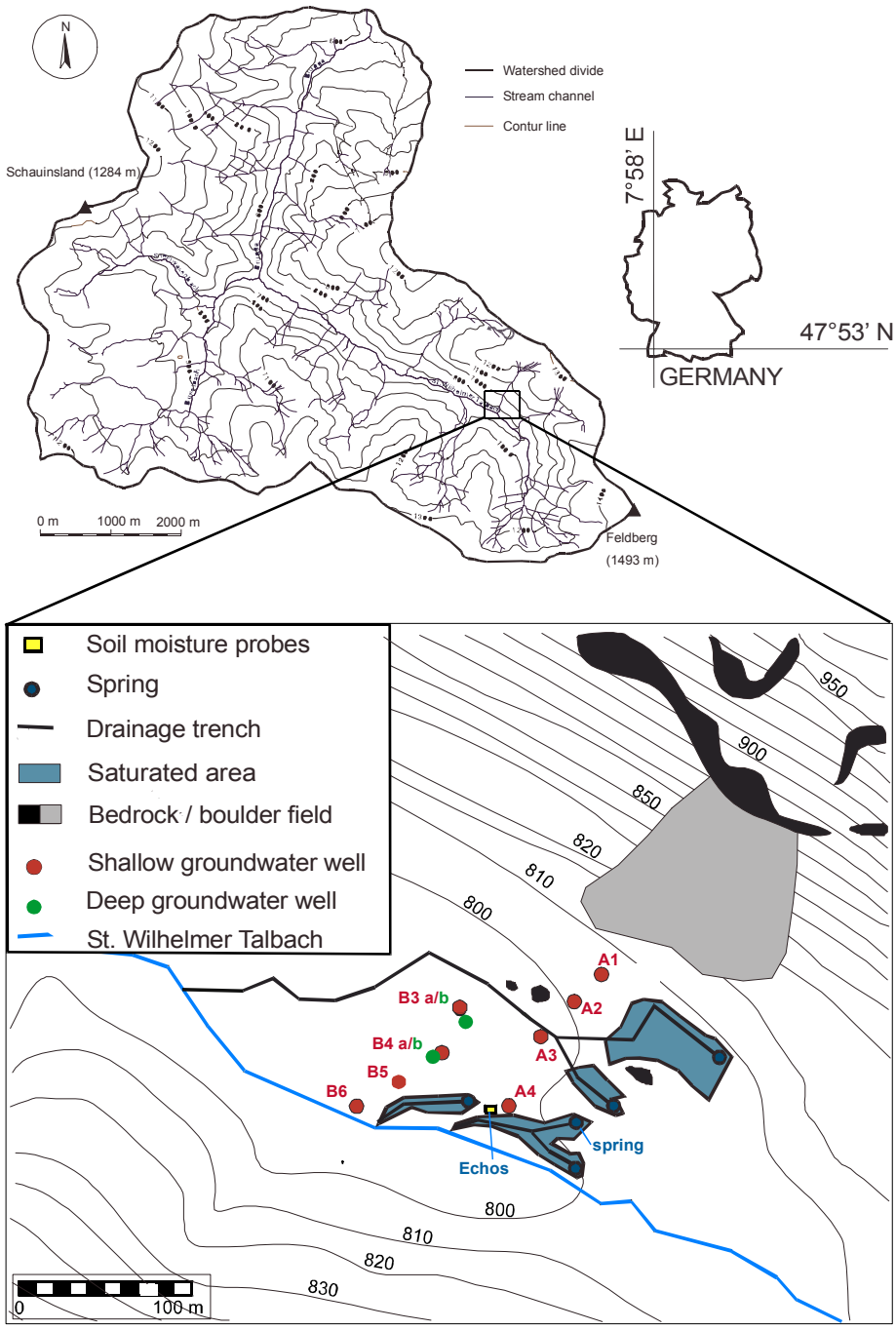

Figure 2-1: Geographical position of the research area.

The groundwater research site “Hintere Matte” is situated in the meso-scale (40 km²) Brugga catchment, located 20 km south-west of Freiburg (47°53’24’’N; 7°57’58’’E) in the southern Black Forest in Germany. Elevation of the Brugga catchment ranges between 1493 m a.s.l. at Feldberg and 434 m a.s.l. at gauge Oberried, the outlet of the basin. The elevation averages 945 m a.s.l., the elevation range is 1059 m. Figure 2-1 shows a schematic overview of the test site with the location of measurement equipment, drainage trench, boulder field and the saturated areas with its attached drainage system.

2.2 Climate and Land use

The southern Black Forest is a region with temperate-clime, at the southern outskirts of the west wind zone. As typical for mid-latitudes, hot sub-tropic and cold sub-polar air masses are interacting. This causes a high frequency of fronts so that precipitation is sufficient all over the year with maxima in May and December as displayed in the climatic chart (Figure 2-2).

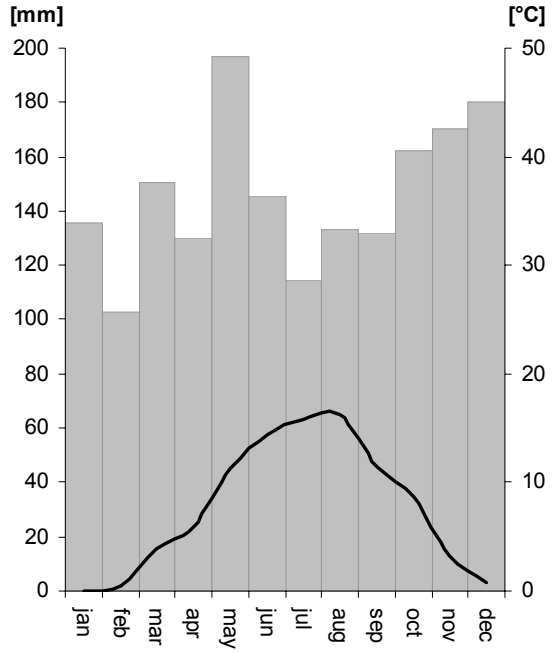

Figure 2-2: Climatic chart of Katzensteig meteorological station situated in the Brugga catchment at 765 m a.s.l. 1994 – 2004; precipitation is not corrected (KOCH, 2004).

The maximum in December is the result of cyclonal weather systems with prevailing west wind. Summer precipitation events have a different character due to the dominating influence of convective cells.

The data of the Katzensteig climate station is representative for the meteorological conditions at the test site, although distinctive topography causes high variability of rainfall.

At 765 m a.s.l. the mean annual rainfall is 1750 mm. The annual average temperature is 7.7 °C and varies from -15 °C to 25 °C (Katzensteig meteorological station, 1994 – 2004, IHF). Due to the low average temperatures during winter, snow has great impact. Above 900 m a.s.l. on more than 60 days, a snow cover is existent. More details on regional climate can be found in REKLIP (1995).

The Brugga catchment has rural character. Most of the catchment area is covered by coniferous and mixed forests (75 %); 22 % is pastureland and 3 % of the catchment area is urban land use. The study site itself is used as a pasture and the vegetation is cut two to three times a year by machines.

2.3 Topography, morphology and geology

The Black forest is a typical low mountain range developed due to a tectonic uplifting in Tertiary and Quaternary. The enhanced exposure caused total erosion of the covering Cretaceous and Tertiary sediments and crystalline bedrock lay open. The bedrock consists mainly of Gneiss and Anatexit and although it comprises different rocks, it can be regarded as homogeneous hydrological unit with a joint network.
The characteristic erosion of homogeneous Gneiss is responsible for flat landforms on hilltops and at the same time steep gorges with narrow valley bottoms (GEYER & GWINNER, 1991). While the Black Forest bedrock is relatively old, glaciers and the two river-systems of Rhine and Danube shaped the current relief.

The three morphologic units can be distinguished in the catchment (Figure 2-3):

- Flat hilltops (20 %)
- Steep hillslopes (75 %)
- Narrow valley bottoms (5 %)

Glacial influence is evident all over the basin. Especially the U-shaped valley of St. Wilhelm shows several characteristic morphologic forms such as cirques and moraines.
In Pleistocene the periglacial condition induced solifluction processes that created drift covers. These drift covers are decisive for runoff generation processes (GLA, 1981; UHLENBROOK ET AL., 2002) because compared to the almost impermeable bedrock (with a hydraulic conductivity between 10^{-10} - 10^{-5} m/s (STOBER, 1995) the hydraulic conductivity of the drift covers is higher. The drift covers are also the base material for the development of covering brown soils.

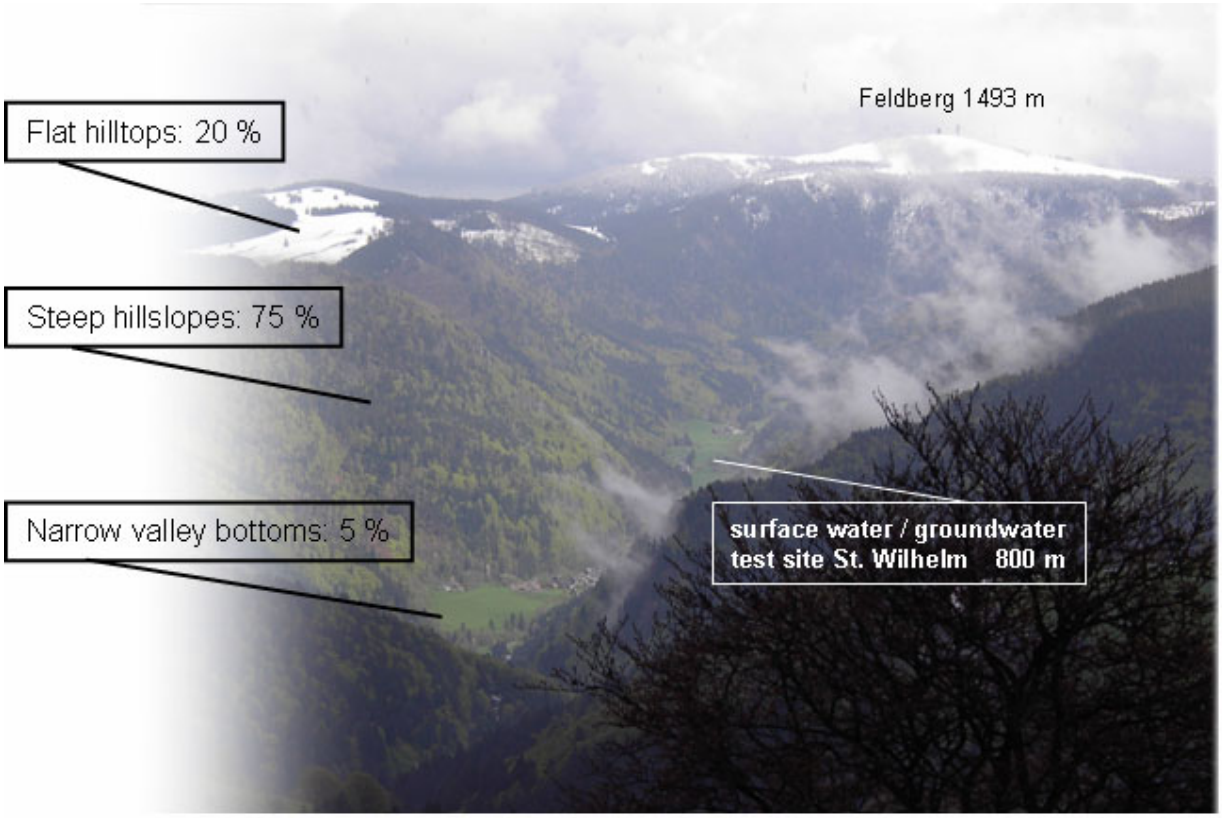

Figure 2-3: View from Schauinsland Mountain to Feldberg Mountain, May 7th 2004, together with main morphologic classes and their percentage of the total catchment area. (KOCH, 2004)

Three layers are distinguishable: The so-called base layer covers the bedrock with the autochthon-weathering zone. The matrix of this layer is riddled with tile-like orientated coarse material. It is compacted and consolidated and therefore hydraulic conductivity is low. The second layer is the main layer with a larger amount of fine material. The storage capacity of this layer is better. The upper layer is formed by coarse material due to frost and melting processes (HÄDRICH & STAHR, 1997) and washout of fine soil material.

The drift cover is not present in the entire catchment. Bedrock is exposed on slopes below which there are steep boulder fields with very high hydraulic conductivities (10^{-2} - 10^{-1} m/s) where flow velocities of several meters per hour occur (MEHLHORN *et al.*, 1998). The boulder fields might therefore be decisive for the generation of fast runoff components.

At the lower parts of the hillslopes, the periglacial hillslope layers and the fluvio-glacial material of the valley floor are mixed, often in cones of accumulated material or alluvial fans. It can be assumed that here the hydraulic conductivity is high due to deposition of coarse material. According to GLA (1981) the depth to the bedrock is about 1-4 m at the slopes and up to 10 m at the foot of the hillslopes, and unknown on the valley floor

In general, the fraction of solid rock, coarse material and boulders outweighs the proportion of fine porous media at the test site.

2.4 Hydrology

Beside the climatic boundary conditions, the hydrology of the study area is influenced to a high degree by the geology of the area. Due to the thin amounts of porous media and the low storage volume of the bedrock, the main part of precipitation drains quickly (UHLENBROOK, 1999).
This is also reflected by the characteristic water discharges of the Brugga. The difference between the mean discharge (MQ = 1,56 m³/s) and the mean highest discharge (MHQ = 17,6 m³/s) points at the low storage capacity of the catchment.

The specific surface discharge of the St. Wilhelmer Talbach is Mq = 41 l/s km^2. Reasons for this are the location in the crystalline bedrock that with its low hydraulic conductivities acts mainly as aquitard, as well as the absence of widespread valley aquifers and the higher precipitation in catchments in this altitude.

The runoff regime of the St Wilhelmer Talbach is nivo-pluvial. This is coherent with the significant influence of snowmelt on runoff generation (see peak in April Figure 2-4).

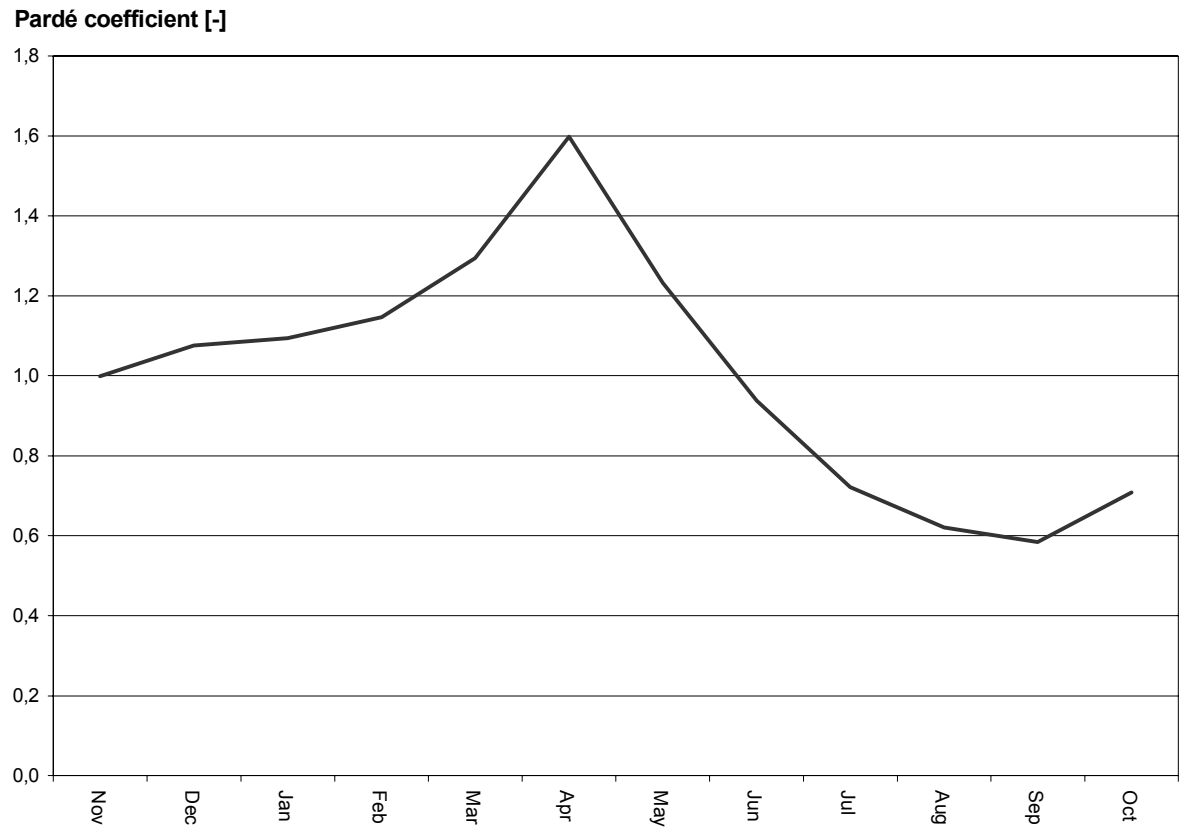

Figure 2-4: Runoff regime of the Brugga river (1934 – 1994).

2.5 Investigation area

WENNINGER (2002) proposed a division of the “Hintere Matte” investigation area into five parts.

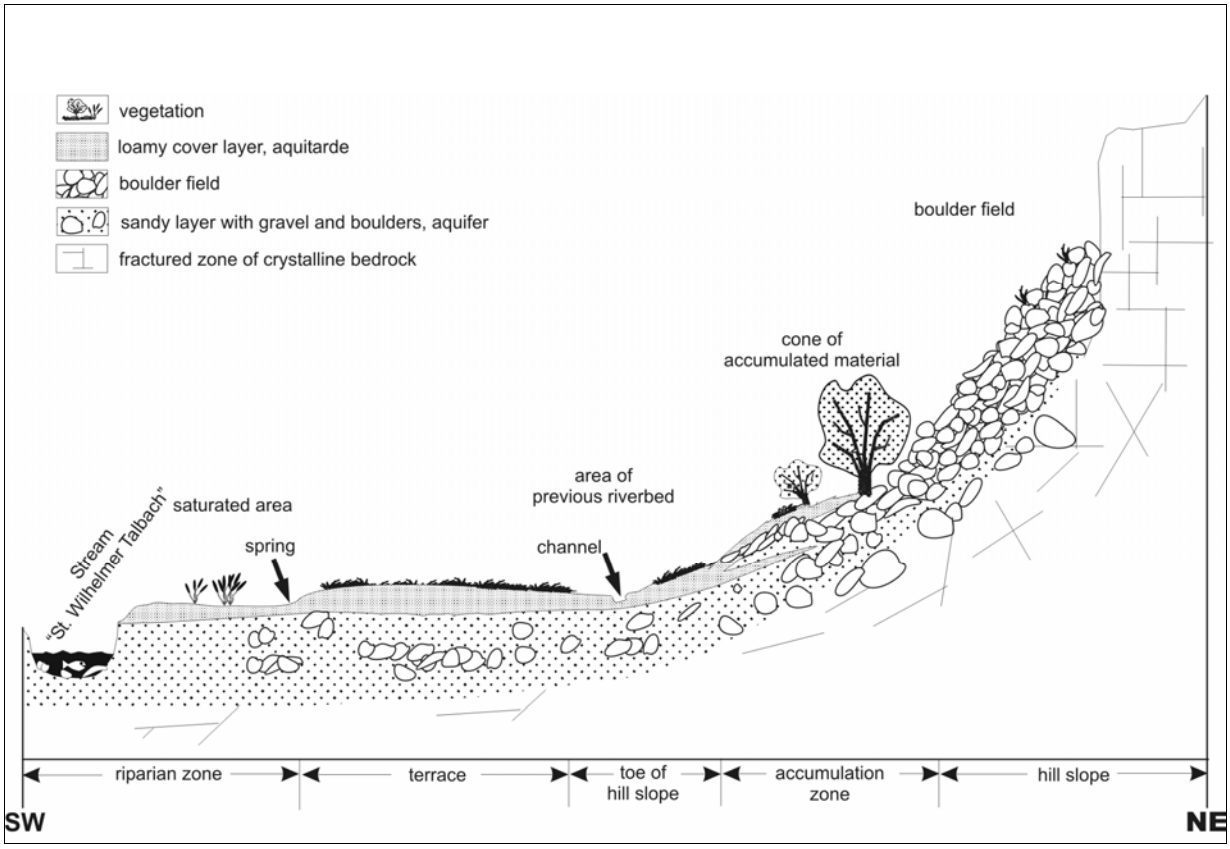

Figure 2-5: Schematic cross section of the investigation area “Hintere Matte” (WENNINGER ET AL., 2004).

- (i) the upper hillslope area with the boulder field,
- (ii) the lower hillslope area with two convex vaulted cones of accumulated material,
- (iii) the toe of the hillslope with strong micro topography from a previous river channel,
- (iv) the terrace that divides the present and previous channels,
- (v) and the riparian zone with the saturated area near the main channel.

The area at about 800 m a.s.l., is characterized by a relatively flat (~3.3°) 200 m by 130 m valley floor. According to spatial dimensions of the investigation area, it belongs to the micro-scale (DYCK & PESCHKE, 1995), where elementary processes may be directly assessed by measurements and described by fundamental physical laws. Nevertheless, the catchment responsible for hydrological processes is probably much bigger and is hard to asses due to the fractured character of the bedrock.

As Figure 2-5, shows the heterogeneity and variability of spatial units is distinctive and responsible for complex mechanisms.
A continuous loamy cover layer of 30 to 150 cm with low amounts of coarse material was found across the valley floor during intensive soil probing by WENNINGER (2002). These brown soils are thicker on the terrace due to fluvial deposits. Whereas the riparian zone with its recent fluvial dynamic does not allow the development of a thick soil cover. Therefore, its composition is different: the soil is sandier with a very high proportion of coarse material.

2.6 Conclusion

The groundwater test site is located in the Black-Forest, a typical low mountain range situated in the mid-latitudes. The steep slopes are forest-covered while the remaining part of the Brugga catchments area is characterised by pastureland and few settlements.
Precipitation is sufficient throughout the year. In winter, snow is an important part of precipitation.
Besides the climatic influences on runoff generation, the crystalline bedrock and periglacial drift covers are decisive. While the bedrock with low hydraulic conductivity mainly acts as an aquitard and valley aquifers are only occurring on 5% of the catchment the main part of precipitation drains quickly. The processes that enable the quick passage of water to the stream are investigated on a micro-scale groundwater test site that is characterised by a high spatial heterogeneity.

3 The model HYDRUS-2D

The model HYDRUS-2D was developed by J. SIMUNEK, M. SEJNA and M. T. VAN GENUCHTEN. It is documented as "The HYDRUS-2D Software Package for Simulating the Two-Dimensional Movement of Water, Heat and Multiple Solutes in Variably-Saturated Media". This report serves as a reference document and user manual. It is the basis of the following description of the model.

The software has been verified in a large number of test cases. Although in most cases, it was applied to experimental setups like infiltration tests for agricultural irrigation purposes, example applications of larger spatial dimensions and under natural conditions are rather rare. The reason for this might be that the model structure does not consider processes like snow melting, surface runoff or dynamic boundary condition e.g. switching between seepage face and atmospheric BC based on the system's status. Examples for application on hillslope are LORENTZ (2001), DÖRNER & HORN (2004), HUADE & WILSON (2003).

According to the title of the manual HYDRUS-2D is also capable to perform the movement of solutes with the Fickian-based advection-dispersion equations. Because the option is not applied in this study, it is not described in further detail.
During this thesis, the HYDRUS-1D package was also applied not only because computational time is about three times shorter, but also to obtain initial parameters for the more complex two-dimensional model and to detect possible limitations of a one-dimensional model conceptualisation. Both models are based on identical model structures.

3.1 Model Theory

The role of the unsaturated zone is decisive for runoff generation, but also for many other aspects in hydrology including groundwater recharge, irrigation, evapotranspiration, groundwater contamination and so forth.

HYDRUS-2D is capable of calculating saturated as well as unsaturated water flow in porous media with the Richard's equation. The model solves the Richard's equation numerically with the Galerkin finite element method applied to a network of triangular elements. The integration in time is done by an implicit finite difference scheme. The resulting equations are solved iterative.
The governing flow equation considers two-dimensional isothermal Darcy flow of water in variably saturated porous medium.

These conditions are given by a modified Richard's equation 3-1:

$$\frac{\partial \Theta}{\partial t} = \frac{\partial}{\partial x_i}\left[K\left(K_{ij}^{A} \frac{\partial h}{\partial x_i} + K_{iz}^{A} \right)\right] - S \qquad \textbf{3-1}$$

, where Θ = volumetric water content [m^3/m^3]
h = pressure head [m]
S = sink term for root water uptake [1/d]
$x_{i\ (i=1,2)}$ = special coordinates [m]
t = time [d]
K_{ij}^{A} = components of a dimensionless anisotropy tensor K^A [-]
K = unsaturated hydraulic conductivity function [m/d]

, given by:

$$K(h,x,z) = K_S(x,z) K_r(h,x,z) \qquad \textbf{3-2}$$

K_r = relative hydraulic conductivity [m/d]
K_s = saturated hydraulic conductivity [m/d]

The properties of the unsaturated soil, $\Theta(h)$ and $K(h)$ in equation 3-1 are generally nonlinear functions of the pressure head. The knowledge of the soil hydraulic properties is essential to model water movement in the vadose zone. Therefore, HYDRUS-2D permits the use of three different analytical models to receive the hydraulic properties:

- BROOKS & COREY, 1964;
- VAN GENUCHTEN, 1980;
- VOGEL & CISLEROVA, 1988.

Throughout the model application, the van Genuchten model was applied. The van Genuchten model uses the statistical pore size distribution model of MUALEM (1976) to obtain the equation for the unsaturated hydraulic conductivity function in terms of soil retention parameters.

The equations of van Genuchten are given by:

$$\Theta(h) = \Theta_S + \frac{\Theta_S - \Theta_r}{\left[1 + |\alpha h|^n\right]^m} \qquad h < 0 \qquad \textbf{3-3}$$

$$\Theta(h) = \Theta_S \qquad h \geq 0 \qquad \textbf{3-4}$$

$$K(h) = K_S S_e^l \left[1 - \left(1 - S_e^{1/m} \right)^m \right]^2 \qquad \textbf{3-5}$$

$$m = 1 - 1/n \qquad n \triangleright 1 \qquad \textbf{3-6}$$

Θ_r	=	residual water content [m^3/m^3]
Θ_s	=	saturated water content [m^3/m^3]
α	=	inverse of the air-entry value [-]
n	=	pore size distribution index [-]
K_s	=	saturated hydraulic conductivity [m^3/m^3]
l	=	pore connectivity parameter [-]
S_e	=	effective water content [m^3/m^3]

These six independent parameters describe the soil hydraulic properties. Where K_s, Θ_r and Θ_s can be determined by field measurements, the parameters α, n and l are merely empirical coefficients defining the shape of the hydraulic functions.

Figure 3-1 shows the dependency of water content on matric suction ($\Theta(\Phi)$) and hydraulic conductivity on pressure head ($K(h)$).

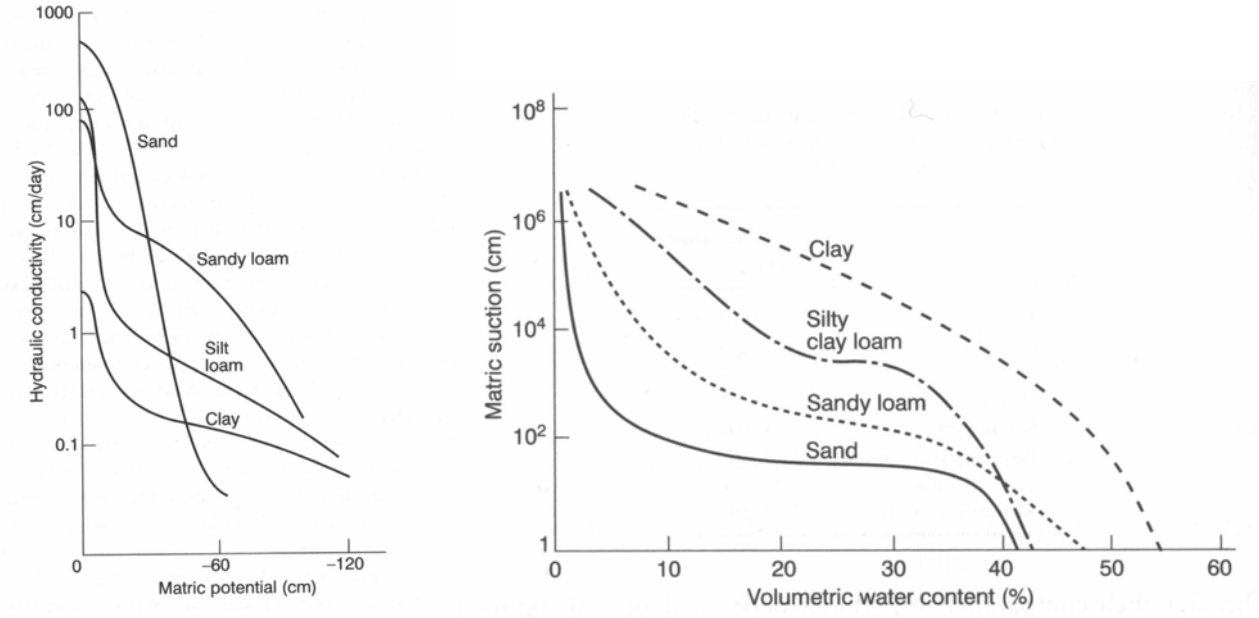

Figure 3-1: Dependency of water content on matric suction (Θ(Φ)) and hydraulic conductivity on pressure head (K(h)) for different soil textural classes (WARD & ROBINSON, 2000).

For parameter determination, HYDRUS-2D provides different possibilities:

- Estimation of parameters depending on the chosen soil textural class (based on CARSEL & PARRISH, 1988).
- Neural Network Predictions: the code can predict soil hydraulic parameters using information about textural characteristic, e.g., fraction of sand, silt and clay, bulk density etc. using the program Rosetta, which is trained on large soil databases.
- Inverse parameter estimation: HYDRUS-2D provides a Marquard-Levenberg type parameter estimation technique for inverse estimation of selected soil hydraulic parameters from cumulative boundary flux across a specified boundary, pressure head measurements at certain observation point (s), water content measurements at certain observation point (s), boundary flux across a specified boundary, concentration measurements at certain observation point (s), Θ(Φ) measurement, K(h) measurement and prior knowledge of any other parameter (s). This method combines the Newton and steepest descend methods, and generates confidence intervals for the optimized parameters. The method was found to be very effective and has become a standard in nonlinear least squares fitting among soil scientists and hydrologists. An upper and a lower limit can be defined to keep the estimated parameters in a sensible range. Decisive for the success of the parameter estimation is the choice of initial parameters. Because of possible problems related to convergence and parameter uniqueness, it is recommend, to routinely rerun the program with different initial parameter estimates to verify that the program indeed converges to the same global minimum in the objective function.

Model evaluation was done with the help of statistical information about the fitted parameters such as the mean, standard error, T-value, and the lower and upper confidence limits (given in output file FIT.OUT). Large confidence limits indicate that the results are not very sensitive to the value of a particular parameter. Moreover, the r^2-value (coefficient of determination) is an important measure of the goodness of fit of the observed, z_i, versus fitted, y_i, values:

$$r^2 = \frac{\left[\sum w_i z_i y_i - \frac{\sum z_i \sum y_i}{\sum w_i}\right]^2}{\left[\sum w_i z_i^2 - \frac{\left(\sum z_i\right)^2}{\sum w_i}\right]\left[\sum y_i^2 - \frac{\left(\sum y_i\right)^2}{\sum w_i}\right]} \qquad \textbf{3-7}$$

z_i = observed value

y_i = fitted value

w_i = weight associated with a particular data point.

The r^2 value is a measure of the relative magnitude of the total sum of squares associated with the fitted equation; a value of 1 indicates a perfect correlation between the fitted and observed values.

3.2 Problem definition

HYDRUS-2D has a graphical user interface, which allows easy management of the required data to perform a model run like time series (e.g. precipitation, potential evapotranspiration) grid design, parameter allocation and visualization of model output. In a first step, the flow region needs to be specified with a finite element mesh. To perform mesh generation the program MESHGEN-2D is supplied.
The created flow region delineated by irregular boundaries may be subdivided into different soil types with an arbitrary degree of local anisotropy and subregions. For each soil type, a set of parameters can be assumed. For each subregion, the mass balance is calculated.
Two-dimensional modelling of flow and transport is possible either along a horizontal or a vertical plane. At the boundary of the water flow region, different conditions can be defined:

- “System-independent” boundary conditions e.g. constant or time-varying pressure head or water flux,
- Atmospheric boundary condition, which allows the input of precipitation and potential evapotranspiration timeseries and calculates actual evapotranspiration according to water supply.
- “System dependent” boundary conditions such as seepage face and free drainage.
- Deep drainage can be applied as boundary condition at the bottom of the flow region but two additional empirical parameters are necessary.

Essential for model application is the proper setting of initial conditions. Numerical instability occurs, if instable initial conditions come together with time varying boundary conditions. HYDRUS-2D provides multiple possibilities to define initial conditions. One possibility is to calculate a steady state solution and import it. Alternatively, one can set initial conditions manually by selecting regions and apply a water content value or a pressure head. For the application on the hillslope no steady state solution could be found, therefore the automatic calculation of linear distributed water content / pressure head with depth proved a good alternative.

3.3 Input and calibration data

Model uncertainty is assessed comparing simulated model output with measured data. For model calibration, soil moisture and groundwater measurements were conducted for about three months Further details are given in the methodology chapter.

Climate data are provided by IHF's Katzensteig climate station. The climate station is located about 700 m west and 35 m below (at 765 m a.s.l.) the test site. Therefore, the data was applied as model input without a further regionalisation. Precipitation, temperature, short wave radiation, relative humidity, wind speed and wind direction are measured with a temporal resolution of 10 min.

Precipitation is measured using the tipping bucket technique and was applied without a correction factor as model input.

Beside precipitation also the potential evaporation and the potential transpiration is required for model application. The actual values of transpiration and evaporation are calculated by HYDRUS-2D depending on the availability of water in the profile. The subdivision into evaporation and transpiration cannot be done by the model itself, because no crop-growing module is implemented, which could do the subdivision depending on the type and growing status of the crop. ALLEN ET AL. (1998) recommend a standard approach to calculate ET_0 (reference evapotranspiration) and the single components of evaporation and transpiration with a dual crop coefficient concept. The approach is very complex and data intensive. Instead of implementing several empirical assumptions to derive missing data such as soil heat flux, long wave radiation and leaf area index it seems more reasonable to use a more simple approach - in this case the TURC model - for the calculation of potential evapotranspiration, which works with the directly measured data:

$$ETp_{Turc} = 0{,}0031 * C * (R_G + 209) * \left(\frac{T}{(T + 15)} \right) \qquad \textbf{3-8}$$

C	**=**	1*((50-U)/70) for U < 50 % and
C	**=**	1 for U > 50 %
U	**=**	relative humidity [%]
R_G	**=**	global radiation [J/cm²]
T	**=**	daily mean of air temperature [°C]

For the subdivision, a constant percentage of 25 % for evaporation and 75 % for transpiration on pastureland was applied (BAUMGARTNER & LIEBSCHER, 1988). ALLEN ET AL. (1998) remark that the subdivision coefficient is rather constant during the mid-season stage and because modelling is only carried out for three months of growing season this simplified approach is reasonable.

3.4 Conclusion

HYDRUS-2D is a mathematical model, which describes water and solute transport in porous media with physical equations such as the Richards equation for variably saturated-unsaturated flow and the Fickian-based dispersive-advective transport equation.
The hydraulic properties of the unsaturated soil are nonlinear functions of the pressure head that were received with the analytical van Genuchten model, where water movement in the unsaturated media is defined by six independent parameters. The parameters can partially be determined partially by measurement. The programme also comprises a database and a Marquard-Levenberg type parameter estimation technique for the estimation of van Genuchten parameters.
For model calibration, soil moisture and groundwater data is used.
Precipitation is applied without a correction factor as model input. Potential evapotranspiration is calculated with measured data from the Katzensteig climate station with the TURC model. For subdivision into evaporation and transpiration, a constant value is applied (BAUMGARTNER & LIEBSCHER, 1988).
HYDRUS-2D is designed for the micro-scale and experimental setups therefore some processes that usually occur in nature are not yet implemented.

4 Methodology - Experimental work

As mentioned in chapter 1.2, due to ERT measurements (KOCH, 2004), doubts whether monitoring wells are implemented in the main aquifer occurred and still reasons for the pronounced dynamic of shallow groundwater was missing.
Thus, additional fieldwork was necessary, to improve the process understanding, receive calibration data and to derive soil hydraulic parameters as basis of model application. The applied methodologies are presented in following sections.

4.1 Hydrometric and hydrochemistry data

4.1.1 Stream and groundwater measurement

Throughout the study, stream data was collected using a multiple functions probe, which measures water level, temperature, electrical conductivity and pH-value with a temporal resolution of 10 min.
The test site was already equipped with 10 groundwater wells (Figure 2-1), so-called driven wells or abyssinian wells, with a 1¼ inch diameter, slitted for the lower 100 cm with a maximum depth of 1,8 m (WENNINGER, 2002).
Within this work, two additional groundwater-monitoring holes from the same type were installed in 4 m and 5 m depth right next to shallow groundwater wells. This location was chosen to allow comparability of groundwater dynamic between the different depths. The annulus was refilled with natural backfill to pre-event artificial vertical flow along the borehole. After the installation of the groundwater wells, their hydraulic connection was checked by slug and pumping tests.
The monitoring in different depth allows determining whether groundwater is upwelling to the surface or if groundwater recharge occurs.
The groundwater wells were equipped with capacitance rods including data loggers (WT-HR 1000, TruTrack©) to continuously record groundwater levels at 10-minute intervals.
For the model application, information about the exact position and elevation of the monitoring holes was needed. The elevation of the monitoring holes was measured with a theodolite the distances with tape measure. With the exact distances and elevation of the monitoring wells (see A 1), the isopiestic surface of the shallow groundwater could be created.

4.1.2 Soil moisture measurement

Infiltration through the unsaturated zone is the controlling factor for groundwater recharge. To improve knowledge about the role and extend of infiltration on the test field five diaelectric aquameters (ECH_2O) measuring soil moisture have been installed.

Furthermore, soil moisture data should be used for model calibration of the unsaturated zone and inverse parameter estimation.
The ECH_2O probe uses the principle of the dielectric constant, since the dielectric constant of water is much higher than that of air or soil minerals. Therefore, dielectric constant of the soil is a sensitive measure of water content. The ECH_2O probe measures volumetric water content. Therefore contact between the soil and the probe mainly influences the readings.
The probes were installed with the flat side (see A 2 in the Appendix) parallel to the surface according to the calibration procedure. Although an orientation in all directions is possible, the most sensible choice is the orientation with the flat side of the probe perpendicular to the soil surface. This causes only minimal effects on the downward movement of water and no water can cumulate on the top.
The accuracy is typically +-3 % but can be improved by a soil specific calibration by up to +-1 %. As standard calibration, produced negative water contents, a soil specific gravimetric calibration as outlined in “Calibrating ECH_2O Soil Moisture Probes”. CAMPBELL (1997) was necessary. Soil material for calibration of the ECH_2O was extracted during the implementation of the probes.

4.1.3 Hydrochemistry measurement

In previous studies, water from saturated areas, groundwater monitoring wells, springs and stream water was sampled and analysed (deuterium, dissolved silica, and major anions and cations) by WENNINGER (2002) and SCHEIDLER (2002).
Within the present work the surface and groundwater was additionally sampled three times to differentiate the groundwater of the new groundwater monitoring wells from shallow groundwater stations. The first sample was collected during a summer storm event on 06/08/04. The second and third samples were collected during dry weather conditions on 22/08/04 and 01/10/04. Comparing event and pre-event samples might give a hint on variability of surface / groundwater water composition.
The groundwater samples were extracted from the bottom of the well with a motor pump. Pumping was applied until momentary measurements of temperature and conductivity reached a constant value before the sample was collected.
The samples were analyzed for major anions (Cl^-, NO_3^-, SO_4^{2-}), cations (Na^+, K^+, Mg^{2+}, Ca^{2+}), and dissolved silica. To ascertain silica concentrations a photometer (Spectronic-Unicam®, model Aqua Mate) according to the German Institute for Standardisation (DIN) (DEV D21; DIN 38405 part 21) was employed. The mean analytical error was about ± 10 %. The anions and the cations were analysed by ion exchange chromatography with a DIONEX DX 500. A mean analytical error of ± 10 % for the anions and ± 5 % for the cations was determined.

These geogenic tracers were used to gain information about the origin and the footpaths of the water. However, these ions are involved in several processes such as e.g. biochemical cycles and sorption, i.e. they are not conservative. Silicate was additionally analysed, because it is less variable than major ions. The erosion of rock determines the input of silicate. Because of this attribute it is suitable for the separation of different water components (UHLENBROOK, 1999).
The major input of chloride in the study area is through precipitation. In the winter month, also de-icing salt may play a role (WENNINGER, 2002). Nitrate and sulphate are subject to complex reactions which are difficult to quantify, but generally, increased values of nitrate indicate a surface near runoff component. Calcium and magnesium inputs result from erosion and precipitation and are important nutrients for plants, which act as a sink. Input of sodium occurs mainly with precipitation, but also fertiliser is an important source. Erosion of mica and feldspar determines the input of potassium but also precipitation and liquid manure may play a role (SCHACHTSCHABEL ET AL. 2002).
WENNINGER (2002) and SCHEIDLER (2002) provide an extended description of the properties of major ions.

4.2 Determination of subsurface structure

4.2.1 Soil probing

Intensive soil probing at 50 spots to a depth of between 100 cm and 200 cm was performed by WENNINGER (2002). The grain size distribution was determined every 20 cm.
During the drilling of two additional groundwater monitoring holes, soil probes were collected every 20 cm out of the drilling core to a depth of 4 m and 5 m. The soil samples were analysed by feel method (AG BODEN, 1996) to gain information about the depth of different soil horizons.
Another soil profile could be obtained as the ECH_2O were installed up to a depth of 90 cm (see Figure 5-5).

4.2.2 Electrical Resistivity Tomography (ERT)

The purpose of the electrical survey is to determine the resistivity distribution of the subsurface by making measurements on the surface (LOKE, 2000). This method provides insight to the subsurface structure without affecting or even destroying it.

4.2.2.1 ERT in hydrology

The most common application of ERT in hydrology is the exploration of the thickness and depth of an aquifer. The procedure is described in many educational books (KNÖDEL, 1997; MEYER DE STADELHOFEN, 1994; VOGELSANG, 1993). In addition, ERT also provides the possibility to determine aquifer parameters such as transmissivity (SRI

NIWAS & SINGHAL, 1985) or hydraulic conductivity (KEMNA ET AL., 2002). A further possibility is to monitor a tracer experiment with ERT to improve the understanding of water and solute movement in the groundwater body or in the unsaturated zone (WHITE, 1988; BATTLE-AGUILAR ET AL., 2004; KEMNA ET AL., 2002).

The approach for determination of aquifer parameter with ERT is that current in analogy to water flows the way of lowest resistivity. Due to the high density of ions inside a matrix pore, it can be assumed that electric conductivity is stronger influenced by porosity and water conductivity than by the surrounding matrix material. Therefore, SRI NIWAS & SINGHAL (1985), conclude that measured resistivity mainly reflects hydrologic conditions.

4.2.2.2 Basics of Electrical Resistivity Tomography

During an ERT measurement, current is injected into the conductive underground with two electrodes A and B as can be seen in Figure 4-1. The current flows in a semicircle from the positive potential at electrode A to the negative potential at electrode B.
The result is a three dimensional potential field that depends on the different resistivities occurring in the subsurface. The electric resistivity is a characteristic physical material parameter. Its value is not only defined by the composition of the rock, but also primarily by the contained water and the proportion of dissolved substances, as well as the porosity and permeability of the rock.
The effect of porosity and water content on the electrical resistivity is expressed by Archie's law (KNÖDEL, 1997):

$$\frac{\sigma_W}{\sigma_f} = F = \varepsilon * p_e^{-m} \qquad \textbf{4-1}$$

σ_w = conductivity of the water [-],
σ_f = conductivity of the formation as a whole [-],
F = „formation factor", related to the volume and tortuosity of the pore space,
ε = empirical constant, typically 1 for unconsolidated sediments,
m = empirical constant, typically 2 for unconsolidated sediments,
p_e = effective porosity, the fraction of interconnected pore space.

The conductivity of many geological even crystalline rocks formations is well represented by this simple function of porosity.
The originating potential field is detected by two additional electrodes M and N.

The basis of the measurement is Ohm's law:

$$R = \frac{\Delta V}{I} \qquad \textbf{4-2}$$

, where ***I*** is the current induced through the current electrodes A and B and ***V*** is the voltage measured between electrodes M and N. In other words, ***V*** is the difference between the equipotential line at electrode M to the equipotential line at electrode N and ***R*** is resistivity (BERCKHEMER, 1997).

To account for the different electrode arrays a correction factor has to be included. Hence, for a homogenous half space the specific resistivity can be calculated.

4.2.2.3 Electrode array

Current follows circular pathways through the subsurface. The radius of the cycles depends on the distance between the injecting electrodes.

The radius becomes bigger with increasing distance between electrodes and therefore reaches greater depth. Current is influenced to a growing extent by the resistivity of deeper material. At the same time, the current flow at the surface decreases gets and information about the upper material decreases. Thus, variation of the electrodes position is necessary to detect different subsurface structures and associate them to a certain depth. This principle is illustrated in Figure 4-1.

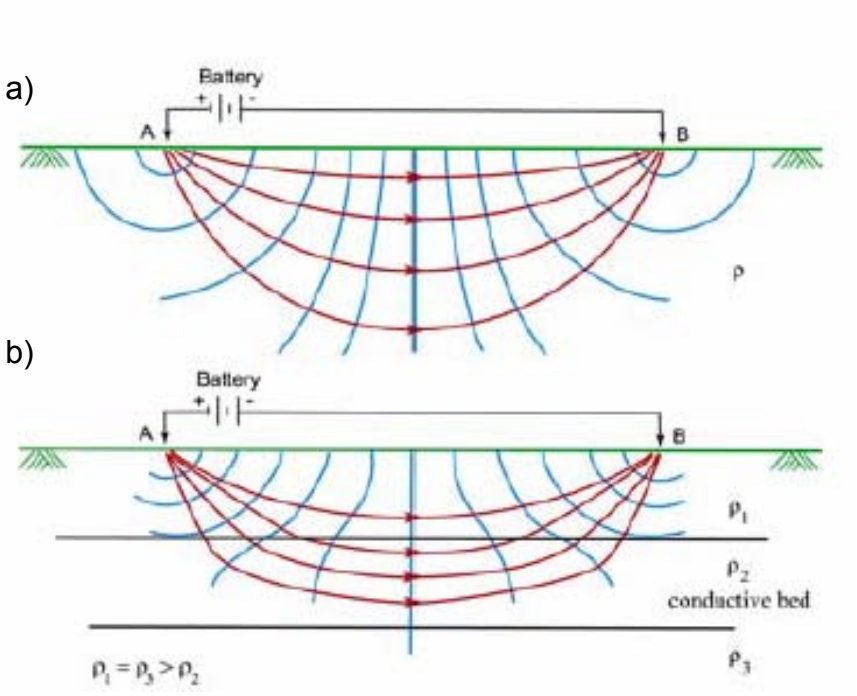

Figure 4-1: Schematic diagram of the distribution of current flow and equipotential lines for different cases of layered conductive and resistive beds: a) Homogeneous soil with uniform distribution. b) A more conductive bed between two resistive beds. The current prefers to flow in the conductive bed. Consequently, the equipotential lines become distorted at the ground surface. The result is a smaller effective depth and a lower measured apparent resistivity (after DAMIATA, 2001).

The choice of array depends on the interest of the researcher concerning the outcome of a particular measurement. In this study, following arrays were applied:

- Schlumberger vertical electrical sounding (VES),
- Wenner switch and
- Dipol-Dipol switch.

In the following these three methods are described briefly.

1-D resistivity surveys and inversion

With the Schlumberger (VES), the centre point of the electrode array remains fixed, while the spacing between the electrodes is increased during the measurement to obtain more information about deeper sections of the subsurface. Due to this arrangement, only vertical changes in resistivity can be measured.

Therefore a subsurface consisting of horizontal layers is the basic assumption used to interpret the measurements. However, in nature lateral changes of resistivity are commonly found (LOKE, 2000). Such a lateral inhomogeneity might lead to the interpretation of a change with depth in the subsurface resistivity. Thus, the measured data needs to be interpreted very carefully.

However, this method provides good penetration depth and is suitable to detect horizontal structures such as for example groundwater table and bedrock for example.

2-D resistivity surveys and inversion

The limitation of the 1-D resistivity survey is that it does not take lateral changes into account. This can be overcome by a two-dimensional measurement. The Wenner and Dipole-Dipole array are common used 2-D electrode arrays.

To give an idea of a typical 2-D setup Figure 4-2 shows a Wenner array survey.

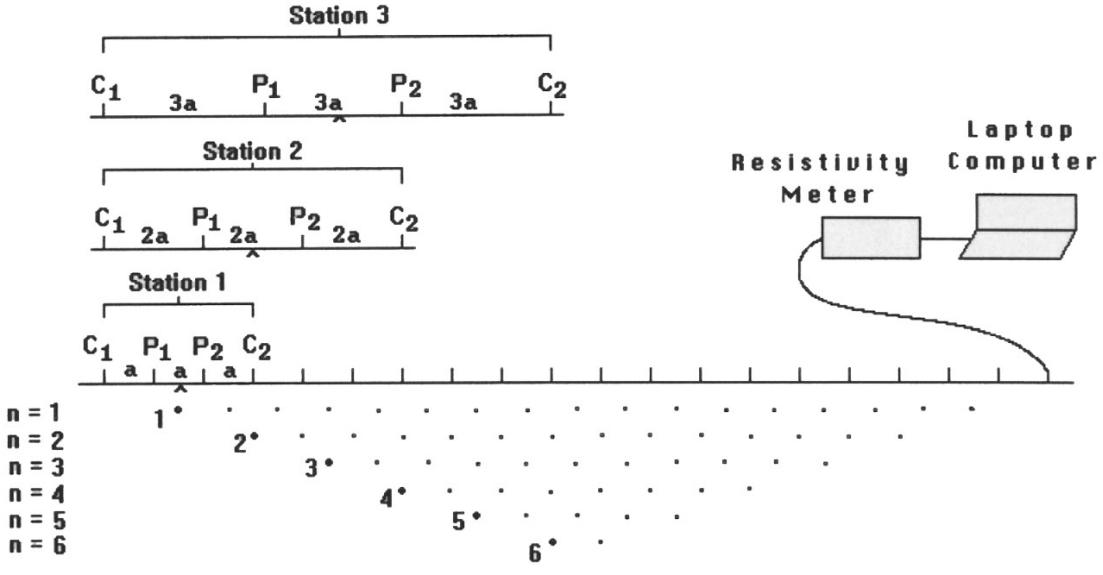

Figure 4-2: Sequence of measurements used to build up a pseudosection (LOKE, 2000).

A number (in this case 20) of electrodes with a constant spacing are installed along a straight line connected to a multi-core cable. Attached to the multi-core cable is an electronic switching unit that, depending on the type of array, chooses the sequence of measurement.

The Wenner array's geometrical concept is shown in Figure 4-2. The distance "a" remains equal between all four electrodes (current electrodes and potential electrodes) throughout the measurement. This is the limiting factor on possible switches based on 20 electrodes. In case of the Dipole-dipole array (Figure 4-3) the distance between the current electrode pair and the potential electrode pair is not fixed to the distance of "a" but can have a multiple "n" of "a". Resultant there are more combinations switching between the 24 strung electrodes.

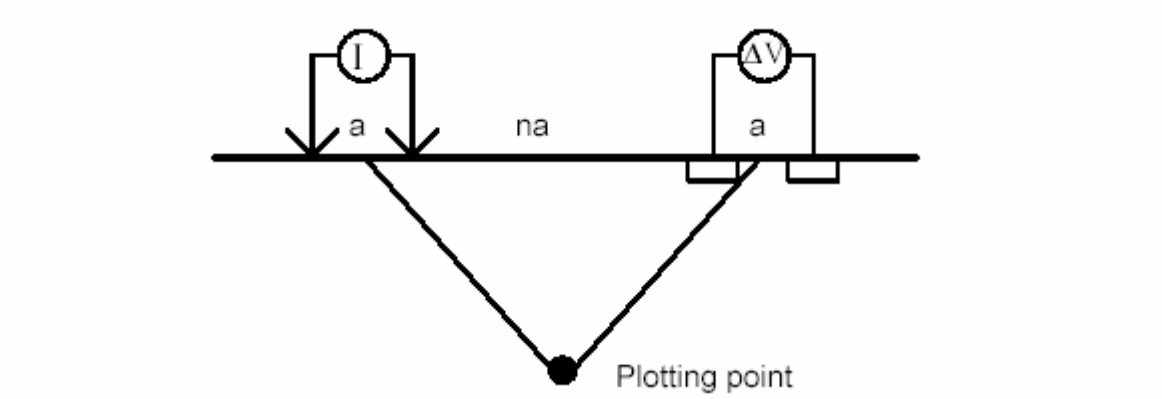

Figure 4-3: Geometry of the dipole-dipole array. The depth of sounding mainly depends on the distance na, as distance a is fixed throughout a 2D survey (CARDIMONA 2002).

As a result of this different geometrical concept:

- Deeper penetration depth is received with Wenner, although due to the pyramid structure of the plotting points the information about the deep subsurface is less reliable (LOKE, 2000). The dipole-dipole array also looses consistence with depth, but each depth level is mapped according to multiple measurements.
- Due to the increased distance between the current and potential electrode in the Dipole-Dipole array the received signal is weaker compared to Wenner thus the signal to noise ratio is smaller which causes higher deviation. For a noisy area, the Wenner array is the better choice.
- Dipole-Dipole provides a good horizontal resolution and better data coverage, whereas Wenner is more suitable if good vertical resolution is required (LOKE, 2000).
- Wenner array allows the calculation of changes of resistivity with time (LOKE, 2000).

4.2.2.4 Tomography interpretation

The interpretation of the VES was carried out with the free available programme IPI2win supplied by the Moscow state University (SHEVNIN & MODIN, 2003). IPI2win is software for 1-D automatic and manual interpretation of VES curves.

The analysis of the measured resistivity collected with Syscal Kid 24 (for technical data see Appendix A 3) was performed by a commercial inversion-software-program. In this study, the software RES2dinv was used.
In the previous section (Figure 4-1), it was illustrates that penetration depth is changing due to the inhomogeneity of the subsurface. This makes interpretation of resistivity data difficult, because without the knowledge about the depth of different materials, it is not possible to calculate the resistivity of the materials and without the knowledge of the specific resistivity of the different materials, no depth can be assigned to the different layers. To solve this problem the use of inversion-software program is necessary to calculate out of a subsurface picture with “pseudo” depth and “pseudo” resistivities a “true” image of the subsurface. Therefore, a top down approach is used. With the assumption that the upper layer consists of only one resistivity a “true“ depth is calculated. Based on this information the second and the following layer are calculated. In this manner, a model of the subsurface is generated which shows which resistivity response fits best to the measured resistivities. The quality of the fit is represented by the root mean squared (RMS). However, even good fits do not guaranty an accurate picture of the subsurface structure.
Essential for the correct interpretation is to keep in mind how the image of the subsurface is created. Errors develop for example due to the 3-dimensional nature of resistivity data, which are transformed to point data and again interpolated to two-dimensional images. As well the assumption that resistivity does not change perpendicular to the measurements profile has to be considered. Otherwise, neighbouring structures can be found on the 2-D picture of the profile while in reality they are located next to it. Due to the small resolution of ERT and averaging, a small subject with different resistivities will influence resistivity value for a much bigger region.
MEYER DE STADELHOFEN (1994) therefore remarks that only several measurements and knowledge about the geological situation enables a clear interpretation of the measurements.

4.3 Determination of Aquifer Parameters

As mentioned in chapter 3.1 there are many possibilities to determine the van Genuchten parameters. In general undisturbed soil samples are used to measure the saturated and residual water content and the soil retention curve (LORENTZ 2001, DÖRNER & HORN, 2004). With the water retention curve, the van Genuchten parameters

(α, n and K_s) can be derived from RETC v 6.0 (VAN GENUCHTEN ET AL., 1991). With laboratory testing, it is also possible to measure the degree of anisotropy, which should be taken into consideration at steep slopes (DÖRNER & HORN, 2004)
Due to the amount and size of coarse material at the test site (WENNINGER, 2002); it would not have been possible to take an undisturbed soil sample. Although, small soil sample is not representative for a soil with mainly coarse material.
The most sensitive parameter to model water flow is the saturated / unsaturated hydraulic conductivity (K_s). To determine this parameter two common used methods were applied which are explained in the following section.

4.3.1 Double ring infiltration experiment

The aim of an infiltration test is to determine the rate of infiltration and to estimate the coefficient of the hydraulic conductivity. The rate of infiltration is defined as the amount of water per surface area and time unit that penetrates the soil.
The double ring infiltrometer is a simple instrument consisting of two steel rings with different diameters. As vertically infiltrated water runs to the sides, the outer ring of the infiltrometer serves as a separation. The measurements exclusively take place in the inner ring through which the water virtually runs vertical. Therefore, the water level in the two rings needs to be identical.
The coefficient of hydraulic conductivity can be estimated with following equation (SCHACHTSCHABEL ET AL., 2002):

$$K_S = \frac{Q_V}{t * A_r} \qquad \textbf{4-3}$$

K_S	=	coefficient of hydraulic conductivity [mm/s]
t	=	time of infiltration [s]
A	=	area of the inner ring [m^2]
Q_V	=	amount of infiltrated water [m^3]

4.3.2 Pumping test

One has to differentiate between pumping tests with stationary and instationary flow conditions. To receive stationary flow conditions a constant water withdrawal is applied until an equilibrium condition between water withdrawal and groundwater afflux is achieved. In practice, this condition is hard to accomplish because groundwater is subject to time varying influences such as groundwater recharge and groundwater

runoff. Therefore, short-term pumping tests with no hydrostatic equilibrium and consequent instationary flow conditions are a common technique.
Within this study, the coefficient of hydraulic conductivity was measured directly in the groundwater station. The advantage of the method is a marginal technical and temporal effort. The disadvantage is that merely information about a small, punctual part of the aquifer is gained (RICHTER & LILLICH, 1975) and thus the calculated coefficient of hydraulic conductivity is up to one decimal power smaller. The reason might be disturbed flow conditions along the traversing length. HÖLTING (1996) argues that only short parts of the aquifer are investigated and resistivity of the filtration device might be noticeable. SCHEYLT & HENGEHAPT (2001) even found a discrepancy of 1,5 decimal power between the stationary and instationary method. Thus, according to the basing flow conditions, a different interpretation is necessary.

Stationary flow conditions:

It is possible to determine K_S out of the amount of water withdrawal for an unconfined aquifer with following equation (HÖLTING 1996),

$$K_S = \frac{Q}{h_m * s} \qquad \textbf{4-4}$$

, with Q = pumping capacity [m³/s]
s = absolute value of draw down in the depletion curve [m],
h_m = h+s/2, with h = draw down of water level above well bottom [m].

Estimation for the transmissivity is given by:

$$T_r = \frac{1{,}22 * Q}{s} \qquad \textbf{4-5}$$

, with T_r = transmissivity [m^2/s],
Q = pumping capacity [m³/s],
s = drawdown in the well [m].

Instationary flow conditions:

By application of this method, water is temporary removed from the groundwater observation well and subsequently the rise of the groundwater table is measured.

Thereby the water table h_1 is measured at the end of pumping and later after the rise h_2. If (L/r) > 8 the following equation to determine the K_S -parameter is valid:

$$K_S = \frac{r^2}{2L(t_2 - t_1)} * 5{,}3 \lg * \left(\frac{L}{r}\right) * \lg * \left(\frac{h_1}{h_2}\right) \qquad \textbf{4-6}$$

, where ***L*** **=** Length of the well filter [m]
r **=** radius of the well filter [m]
h_1,h_2 **=** water table [m] to the time t_1, t_2.

4.4 Conclusion

The experimental work can be separated into three different parts:

- further inquiry of hydrometry data,
- additional exploration of the subsurface,
- determination of soil hydraulic parameters.

Firstly, on 07/07/04, a deeper groundwater well was implemented with a filter device in 5 m depth. Data for the new and old groundwater stations are measured with capacitance rods for three ensuring month. Soil moisture probes in different depth were installed to measure the extend of local infiltration and to provide calibration data for the unsaturated zone. Three times surface / groundwater water samples were collected, with the objective to differentiate and characterise the waters components on the test site. Secondly, with soil probes from the drilling core and additional geoelectric soundings and profiling the subsurface was further explored. Finally, with pumping test and double ring infiltration experiments aquifer parameters were determined.

The applied methods serve on the one hand to identity the dominant flow mechanisms at the test site and on the other hand for parameterisation of the soil water model.

5 Results - Experimental work

Especially for physically based models the quality of model results depend on a substantial degree on input parameters and model conceptualization.
Within this chapter, the obtained data is presented and interpreted with the objective of to understand runoff generation processes at the test site and to develop a conceptual model of the processes connecting subsurface stormflow at the hillslope / floodplain with surface water.
Figure 5-1 shows the locations of the conducted measurements namely ERT profiles, 1-D vertical electrical sounding, double ring infiltration experiments and soil moisture measurements.

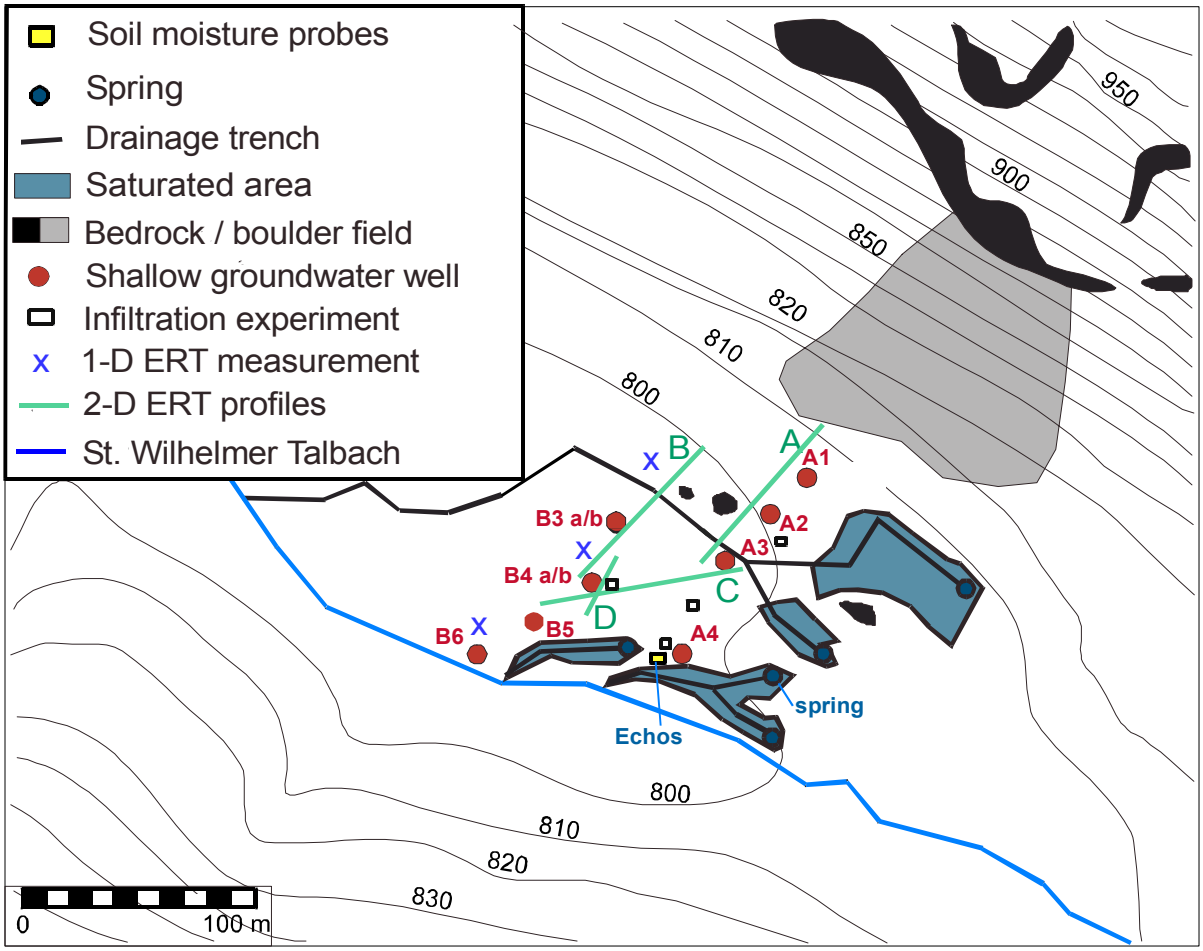

Figure 5-1: Location of conducted measurements.

5.1 Hydrometric and hydrochemistry data

5.1.1 Stream and groundwater data

The hydrographs of stream water level, its electrical conductivity and the piezometric heads of seven groundwater-monitoring wells are displayed in Figure 5-2.

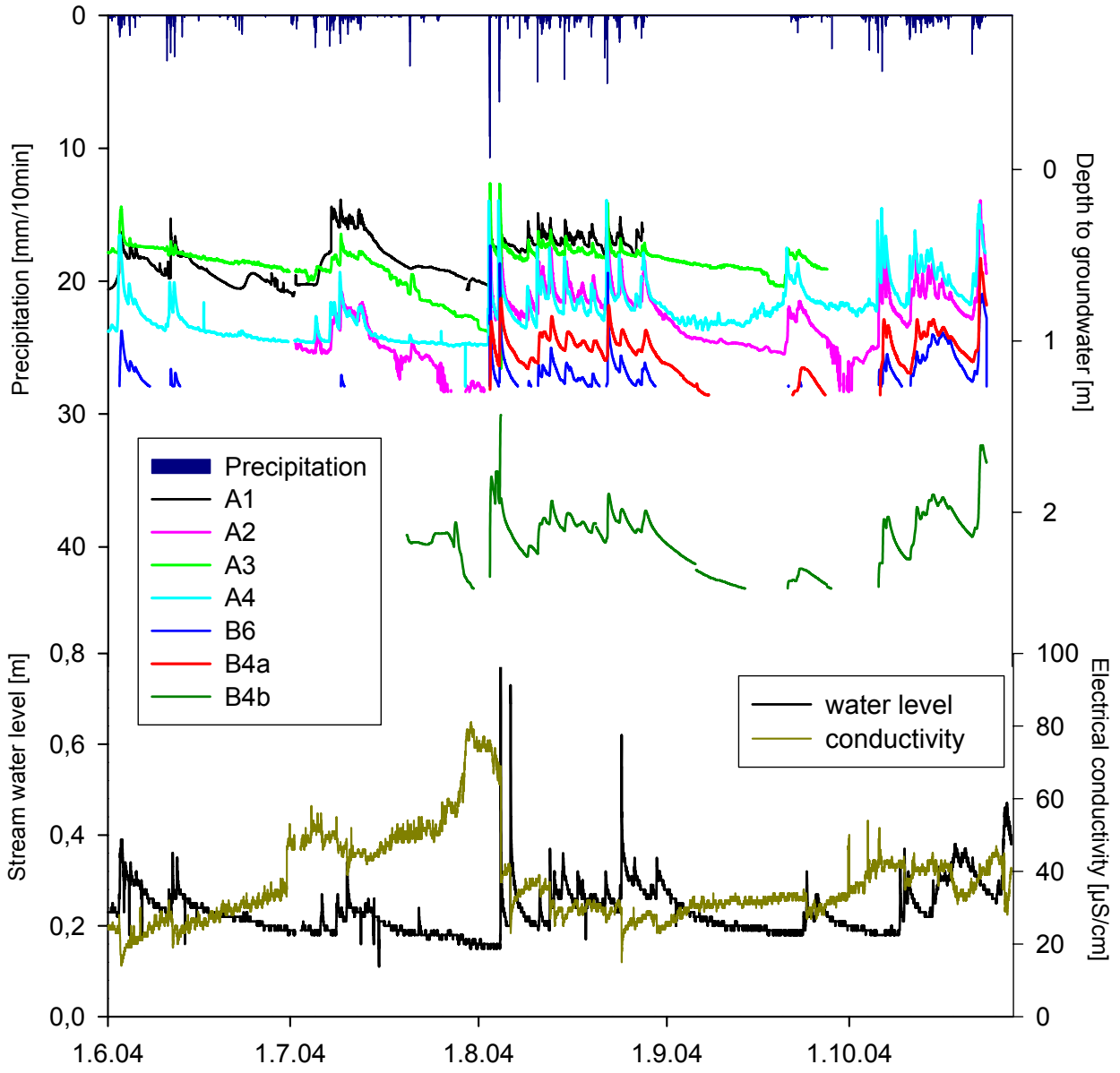

Figure 5-2: Recorded stream data and piezometric heads of the groundwater wells.

The general reactions of the stream water level and the piezometric heads are rapid and pronounced. The missing piezometric data result either from water sampling or from exceedance of the measurement range (one meter) of the capacity rods. The wells fell often dry when persistent dry weather conditions occur.

The water level of the Talbach and the measured electrical conductivity are negatively correlated. The continuous measurements of electrical conductivity accomplished by the multiple-functions probe has a deflection of 10 µS/cm less compared to reference measurements. The relation between the water level rises compared to the rises of piezometric head varies due to rainfall characteristic. During the storm event on the sixth of August with the highest intensities within the observed period water level

increases by 53 cm in about 50 min while the piezometric heads increases by 52 cm three hours later. However, for events with lower rainfall intensity the rises of the piezometric heads in the groundwater wells are approximately two to three times higher (see KOCH, 2004). The response time of the Talbach to precipitation is in general shorter than in the groundwater monitoring wells.

The groundwater well A1 is located closest to the hillslope in vicinity to a saturated area. Here the recorded piezometric heads are closest to the surface. A1 and A3 show slower recession in dry weather periods than the other groundwater wells. In the beginning of October A2 shows distinct reactions although no precipitation occurred. The reaction of the measured groundwater level is not persistent between the different monitoring wells. In addition, the response to precipitation is variable from event to event. While SCHEIDLER (2002) obtained most distinct reactions at A1 and smooth behaviour of B6 (within the period 01/05/02 to 01/0/02), KOCH (2004) obtained it the other way round (within the period 21/11/03 to 19/04/04.)

The knowledge of the flow direction is crucial for the application of a two-dimensional model. With the exact elevation and position of the monitoring wells, it was possible to create the isopiestic surface of groundwater in order to determine flow direction and whether the flow direction depends on weather conditions. For several different hydrologic conditions, the isotropic surface only shows small variations. In Figure 5-3, the isopiestic lines of a storm event on 30/11/01 (blue lines) and groundwater level at dry weather, conditions on 06/07/01 (red lines) are displayed. The direction of groundwater flow is perpendicular to the isopiestic lines.

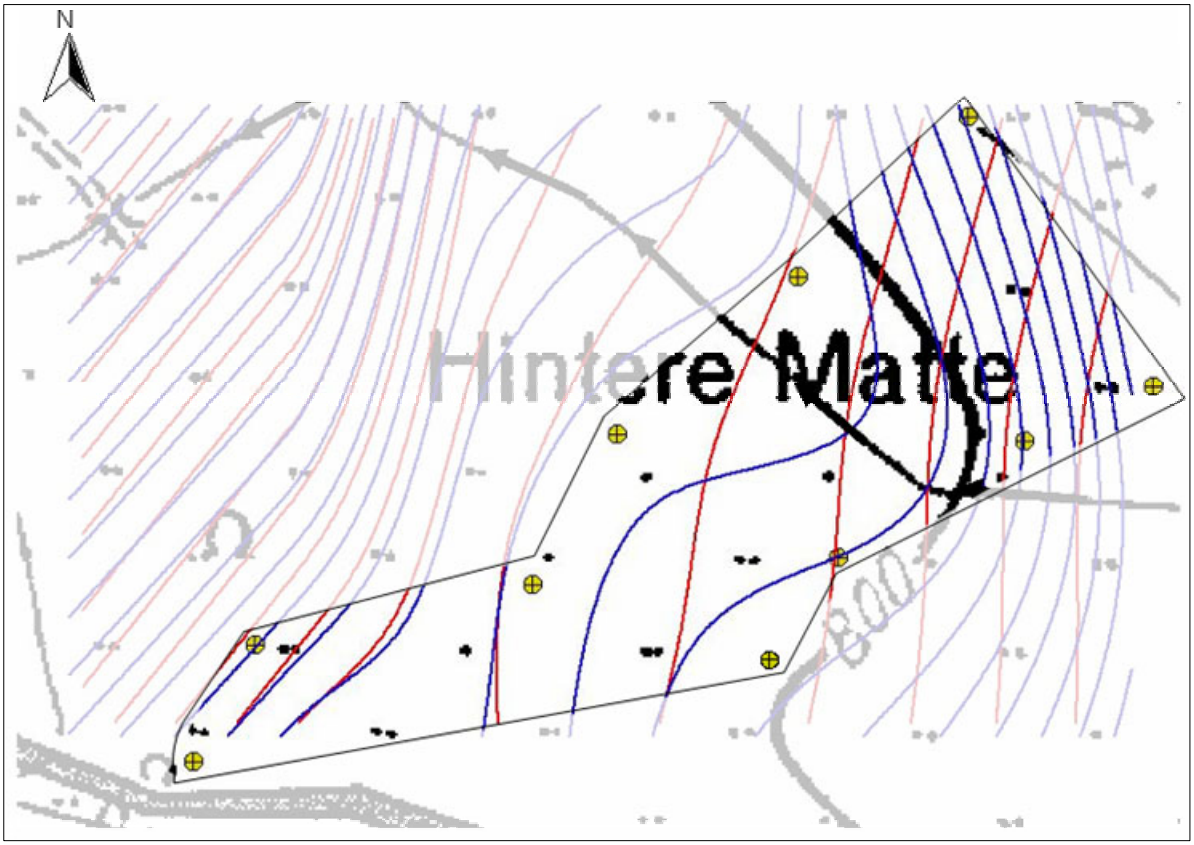

Figure 5-3: Isopiestic lines of shallow groundwater for a storm event (blue lines) and dry weather conditions (red lines).

The main flow direction does not point not from the hillslope to the stream, but parallel to the stream. This main direction persists, although during storm events partitions of groundwater branch off towards the drainage trench.

On the 07/07/04, two additional groundwater-monitoring wells were implemented close to B4a and B3b with a depth of 5 m and 4 m, each with a perforated casing of one-meter length at the bottom end (see chapter 4.1.1). Although the new boreholes (B4b, B3b) are located in close vicinity (34 cm and 190 cm) to the prior shallow ones (B4a and B3a) they showed different piezometric heads throughout the entire observation time.
The water level at B4b is about 1 m below B4a and B3b 30 cm below B3a. Because the conduit of the new implemented monitoring well B3b broke in two meter depth after drilling, the recorded data was not analysed any further.
A detailed description of groundwater variations observed in shallow groundwater stations is being provided by WENNINGER (2002) and SCHEIDLER (2002). In the following section, the focus shall be set on the comparison of dynamics of the shallow and the deep groundwater well observed at the groundwater wells B4a and B4b.
Figure 5-4 shows the well hydrograph of shallow groundwater (monitored in B4a) and deep groundwater (monitored in B4b) and the difference of the two water levels for a period of one week. The entire time series for all groundwater stations are displayed in Figure 5-2.

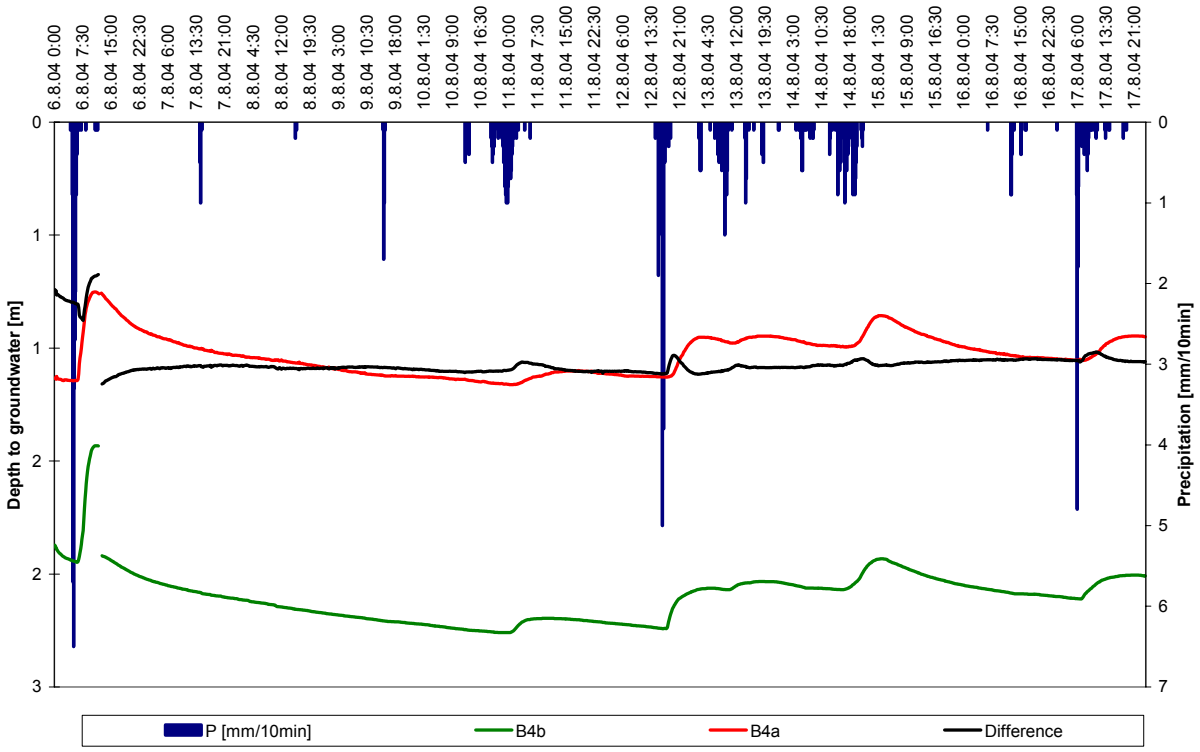

Figure 5-4: Comparison of the dynamic of piezometric heads measured in the shallow and deep groundwater observation wells (B4a, B4b).

The well hydrograph of the deep groundwater station B4b is characterised by an even stronger dynamic than the monitoring station B4a of the shallow groundwater. In addition, response time in the underlying main groundwater is faster in 25 of 47 events. The different response times are visualised by differences of the measured water levels. A rise of the difference curve indicates a faster response of the deep groundwater while a decrease prior to the event shows a faster reaction of the shallow groundwater. Whereas 17 events with marginal precipitation intensity (< 0,09 mm/10 min) and precipitation amount (< 4 mm) caused no reaction of the groundwater levels. During dry weather conditions a constant difference between the two water tables persists. On only two events, the reaction of B4a was faster. During the first event on 04/08/04 only 0,1 mm/10 min caused a rise in both monitoring wells, whereas in general an event of this size causes no reaction. The second event was the storm event on 06/08/04, which is displayed in Figure 5-4 . The missing data at the peak resulted form the extraction of a groundwater sample (see chapter 4.1.3). The faster reaction of B4b is also reflected by the mean response time for all events. The mean response time for the shallow B4a groundwater station is 402 min while for the deeper B4b it is 312 min. If the reactions in the two groundwater wells are induced by infiltration, for B4a a flow velocity (calculated with the distance from the surface to the filter) of 1,8 m/d results. At B4b a flow velocity of 18,5 m/d would be necessary to achieve the obtained response time.

In order to analyse the different reactions of the two hydrographs and their connection to rainfall characteristics a correlation matrix is used. Three precipitation characteristics are correlated with the height of the rise and the response time of the two well hydrographs (Table 5-1).

Table 5-1: Correlation matrix of precipitation and groundwater hydrograph characteristics.

	P-duration	P [mm]	P-intensity	Response time B4a	Response time B4b	Rise B4a	Rise B4b
P-duration	1	0,1	0,05	0,59	0,4	0,02	0,07
P [mm]		1	0,57	0,01	0,02	0,79	0,67
P-intensity			1	0,04	0,02	0,59	0,54
Response time B4a				1	0,87	0,05	0,09
Response time B4b					1	0,07	0,09
Rise B4a						1	0,91

Rise B4b							1

Basis for this statistic are 49 events, which showed clearly distinguishable reactions.
The reactions in B4a are stronger related to precipitation characteristics. It is remarkable that the rises correlate with the precipitation amount and intensity, but not with its duration while response time is only related to duration. The rise and response time of B4a and B4b are strongly correlated with each other, while response time and the height of the rise show no connection.

5.1.2 Soil moisture data

As mentioned in chapter 4.1.2 a soil specific calibration was carried out for the upper 60 cm and for the material below to 90 cm. During the calibration, two problems arose:

- The measurement produces a failure of up to 20 % if stones are located close to the ECH_2O probe.
- As soon as the adhesive soil moisture content is exceeded, water starts to drain and accumulates on the horizontal probe. Therefore, all water contents above this limiting value produce almost the same measurement output.

With the received calibration curves (given in A 4), soil water contents become negative. This is explained by the high amount of coarse material at the test site location (Figure 5-5) of the ECH_2Os and lower packing density.

The problem to assign the measured signal of the calibration to the field measurements could be overcome with an infiltration experiment above the ECH_2O probes at the test site to achieve a constant plateau of the soil moisture (see A 5). The measured signal for the plateau water content was assigned to the calibration measurement for saturated water conditions. The gradient of the calibration curve was maintained with changed absolute values of water contents. Hence, the absolute values of water contents should be regarded very carefully. The capacitive measurement method is better suited to observe water content changes, although the fact that water accumulates on the horizontal probe should be considered.

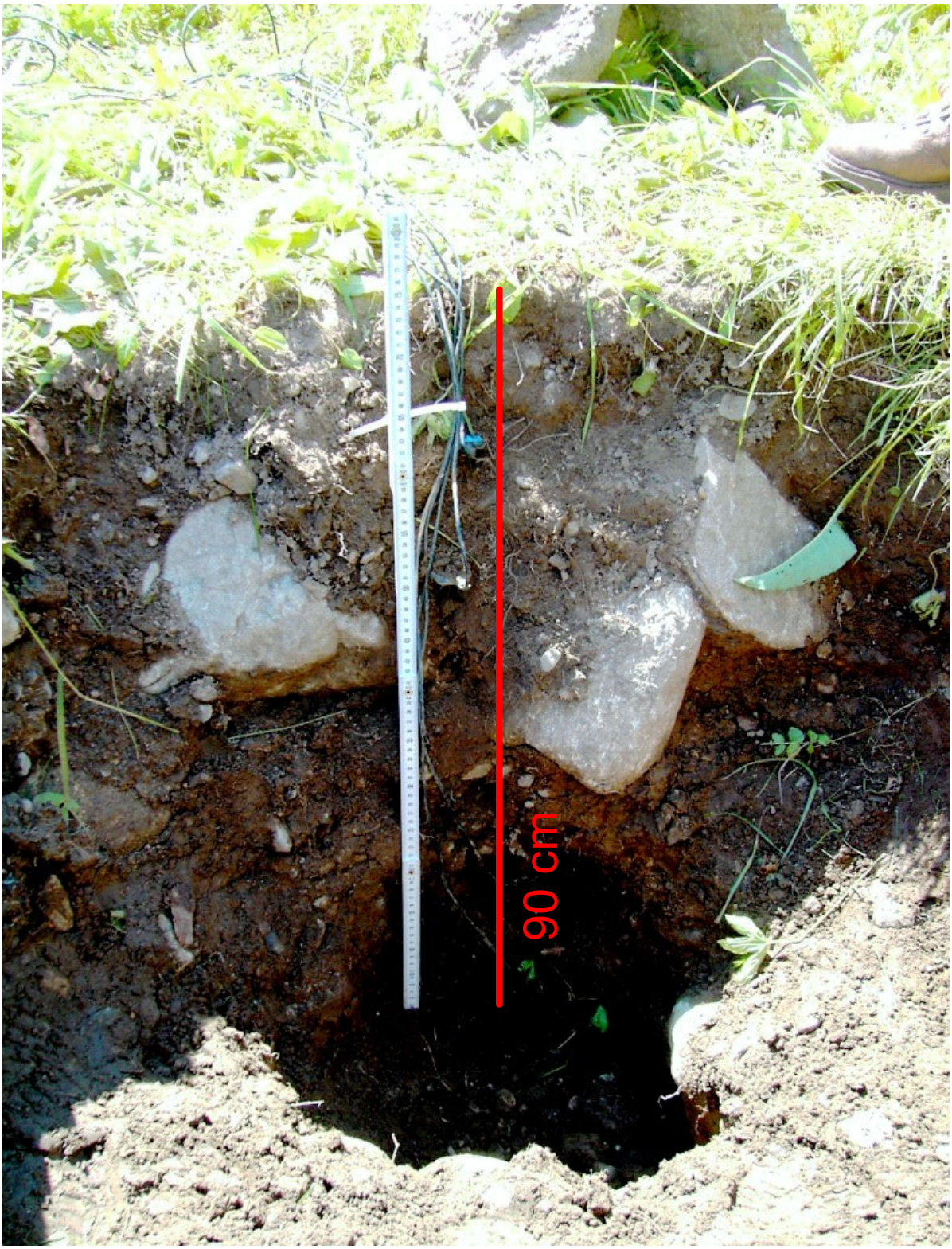

Figure 5-5: Soil profile at the location of the soil moisture probes.

In Figure 5-6, the time series for four ECH$_2$O probes in different depths (13 cm, 23 cm, 62 cm, and 86 cm) below surface is displayed. The probe at the depth of 38 cm produced nonsensical results and thus is not plotted.

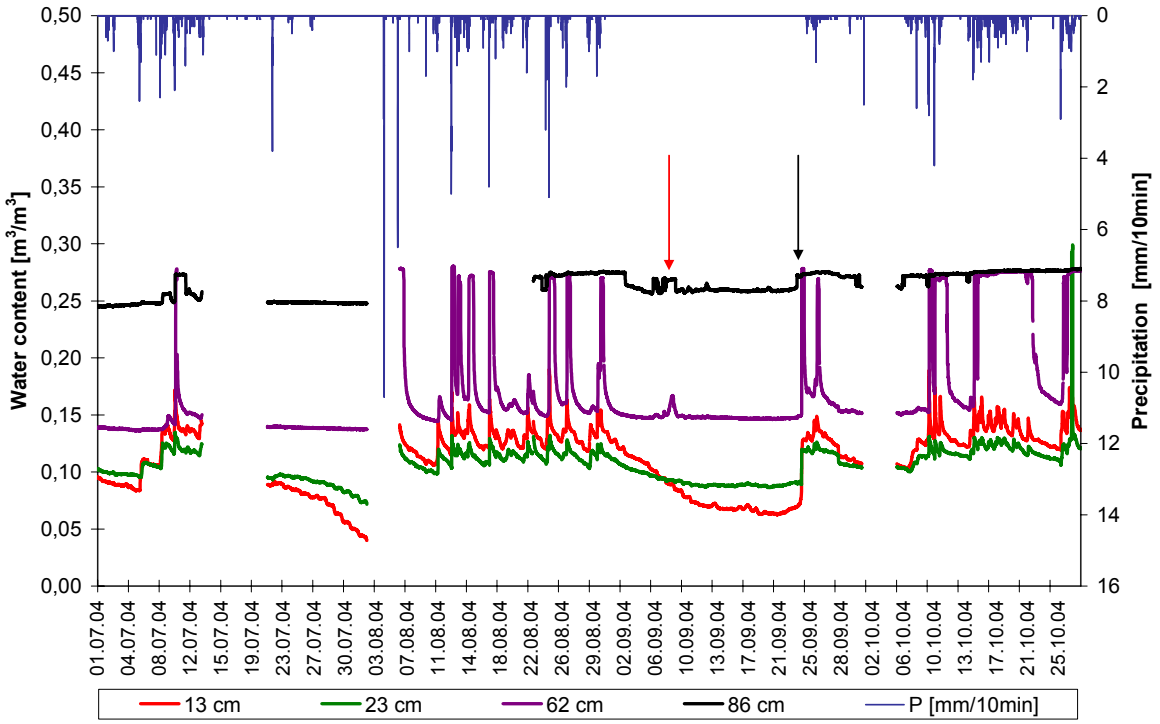

Figure 5-6: Soil moisture data in four depths for the entire observation period.

The ECH_2O probe in 86 cm depth remains on a high level of water content for the entire observation period. Precipitation events only create a marginal increase (3 %) of soil water content. At the beginning of October, the dynamic becomes more constant.
The probe in 62 cm depth is marked by flashy reactions with constant values at the peak. The phases of constant high water content are very short in summer and become increasingly longer in autumn.

The probes closest to the surface in 13 cm and 23 cm show minor water contents that do not reach a constant maximum value within the observed period (except for one event displayed in Figure 5-7).Along with dry weather conditions the probe in 13 cm depth shows faster recession than the probe in 23 cm depth. In general, the probe in 23 cm depth is characterised by a smoother behaviour.
From 31/08/04 to 24/09/04, there is no rainfall but on 21/09/04 (black dart), all probes show a peak. On 08/09/04 (red dart), the two deep ECH_2O probes recorded an increase while the ones at the surface did not.
The probes showed a clear response to 48 rainfall events. The recorded precipitation of the climate station Katzensteig was accounted as one event, if there was no interruption exceeding four hours.

Regarding the time series of the water content measurements more precisely, inconsistent reactions can be observed (see Figure 5-7).

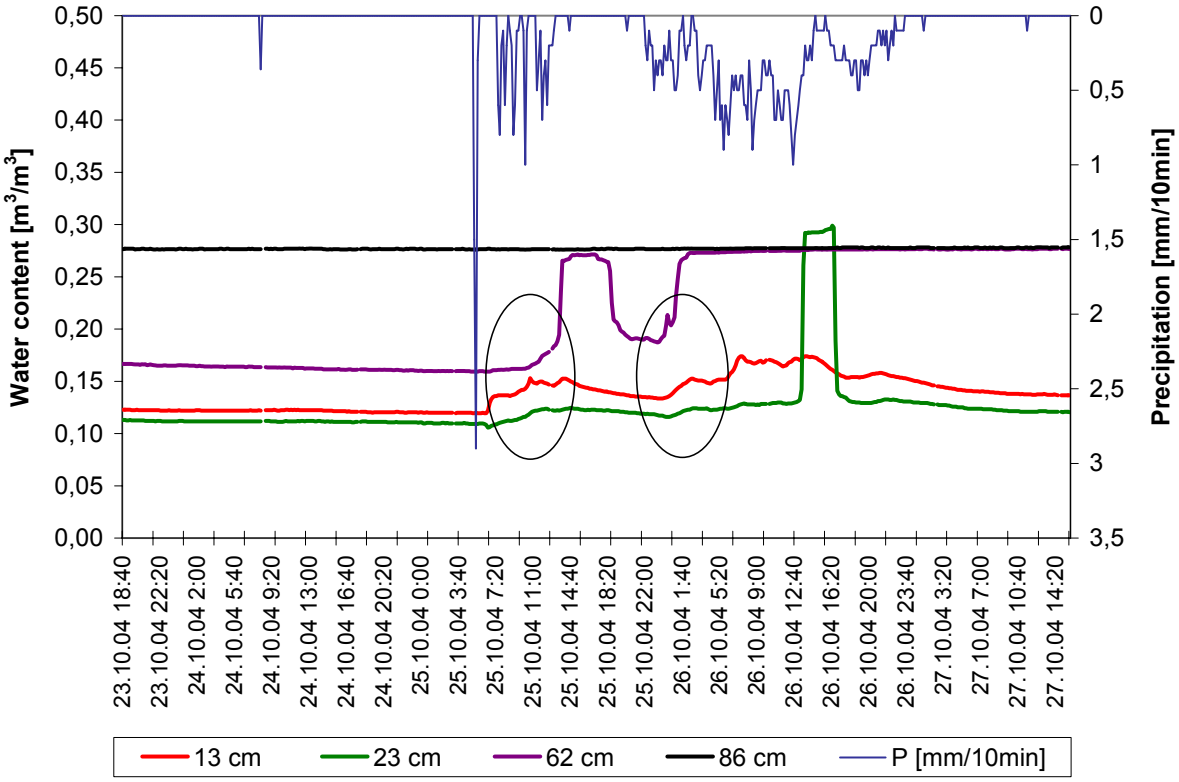

Figure 5-7: Graphic display of varying response time of soil moisture probes in different depth.

At the beginning of the event on 25/10/04 the surface near probes, show an increase in water content prior the probe in 86 cm depth, while during the following rainfall the deeper probe rises earlier than the overlying ones. For the whole observation period, this phenomenon could be observed for 11 events. Thereby it is remarkable that a distinct antecedent moisture condition seems to be the precondition for this reaction. Small precipitation events (< 2 mm) following dry conditions caused no reactions. For events with a clear response, the mean response time (from the beginning of the rainfall until the beginning of the rise) was calculated for the four probes:

- 215 min for the probe in 13 cm depth
- 302 min for the probe in 23 cm depth
- 280 min for the probe in 62 cm depth
- 263 min for the probe in 86 cm depth

The probe located closest to the surface has the fastest mean response time, followed by the deepest. The probes located in-between show a slower response time.

5.1.3 Hydrochemistry data

During the ground- and surface water sampling, conductivity and temperature was additionally measured. These two parameters are utilised to characterise and differentiate the waters occurring on the test site. However, temperature is a parameter that probably is more affected by the actual location than by the origin of the water itself and therefore has to be interpreted with care. A better tracer to distinguish the origin of different water components is silicate but due to a high analytical error and less samples the temperature is displayed instead (see Figure 5-8).

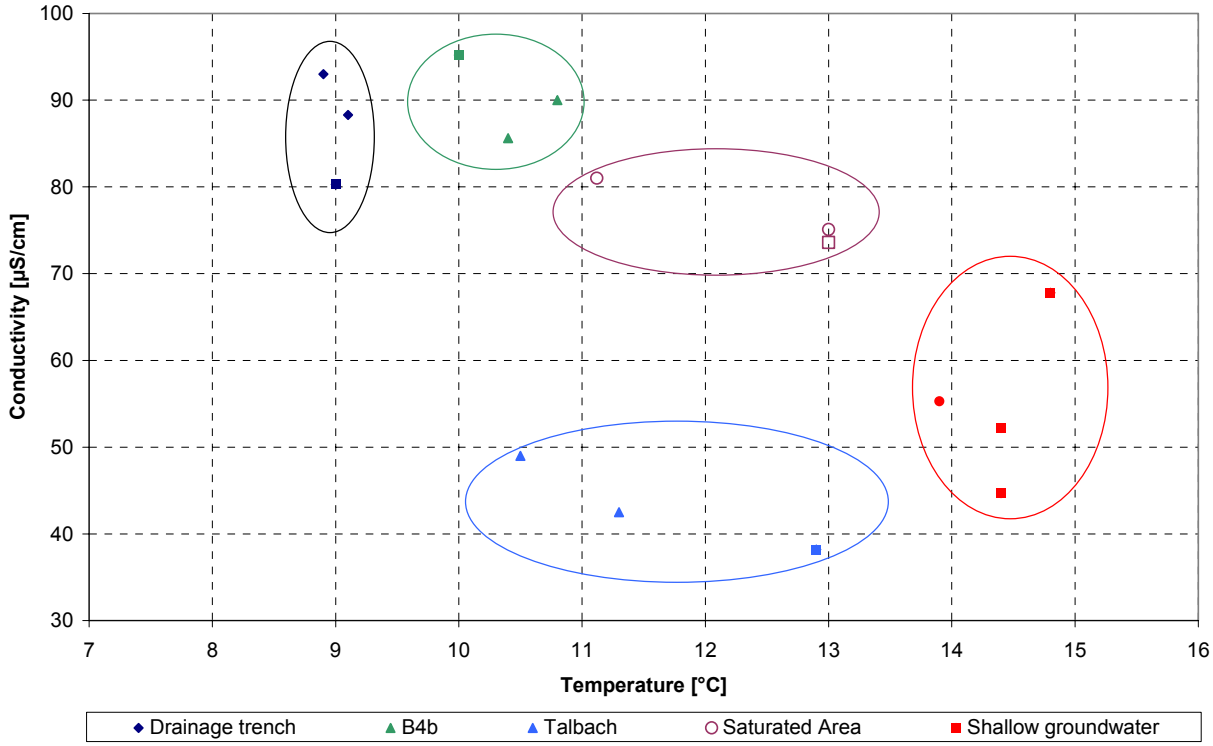

Figure 5-8: Differentiation of surface and subsurface waters by the parameters electrical conductivity and water temperature.

The dots in Figure 5-8 symbolise the samples collected on different dates. Same locations are marked with identical colours. The samples were extracted from the drainage trench, the main groundwater monitoring hole B4b, Talbach, saturated area and from three shallow groundwater stations B4a, B6 and A3. The samples of the shallow groundwater form a consistent group with high temperatures and conductivities (from 45 µS/cm to 68 µS/cm). On the other side of the chart, the drainage trench is located with its consistent low temperature and high conductivity (above 80 µS/cm).
The other samples are located in-between, with the exception of lowest conductivities measured at the St. Wilhelmer Talbach.
The samples of B4b show closest similarity to the drainage trench with only slightly higher temperature values.

The samples of the deep groundwater station can be clearly separated from samples of the shallow groundwater station 3,5 m above. The samples from the saturated area have lower conductivity and higher temperatures than the deep groundwater. The plot of conductivity versus silicate concentration shows similar tendencies (see A 6 in the Appendix).
Water samples were taken on the peak of the storm event on 06/08/04. These samples are marked with a big square.
Although sampling is far away from being representative and differences might occur as a result of accidental variations, the observed differences of the event samples compared to the dry weather samples are mentioned briefly:

- slightly less conductivity at the drainage trench,
- higher similarity of B4b and drainage trench,
- no change at the saturated area,
- higher similarity between Talbach and shallow groundwater,
- higher temperatures of shallow groundwater samples.

The concentration of the major ions is displayed in Figure 5-9. The event samples are coloured in red.

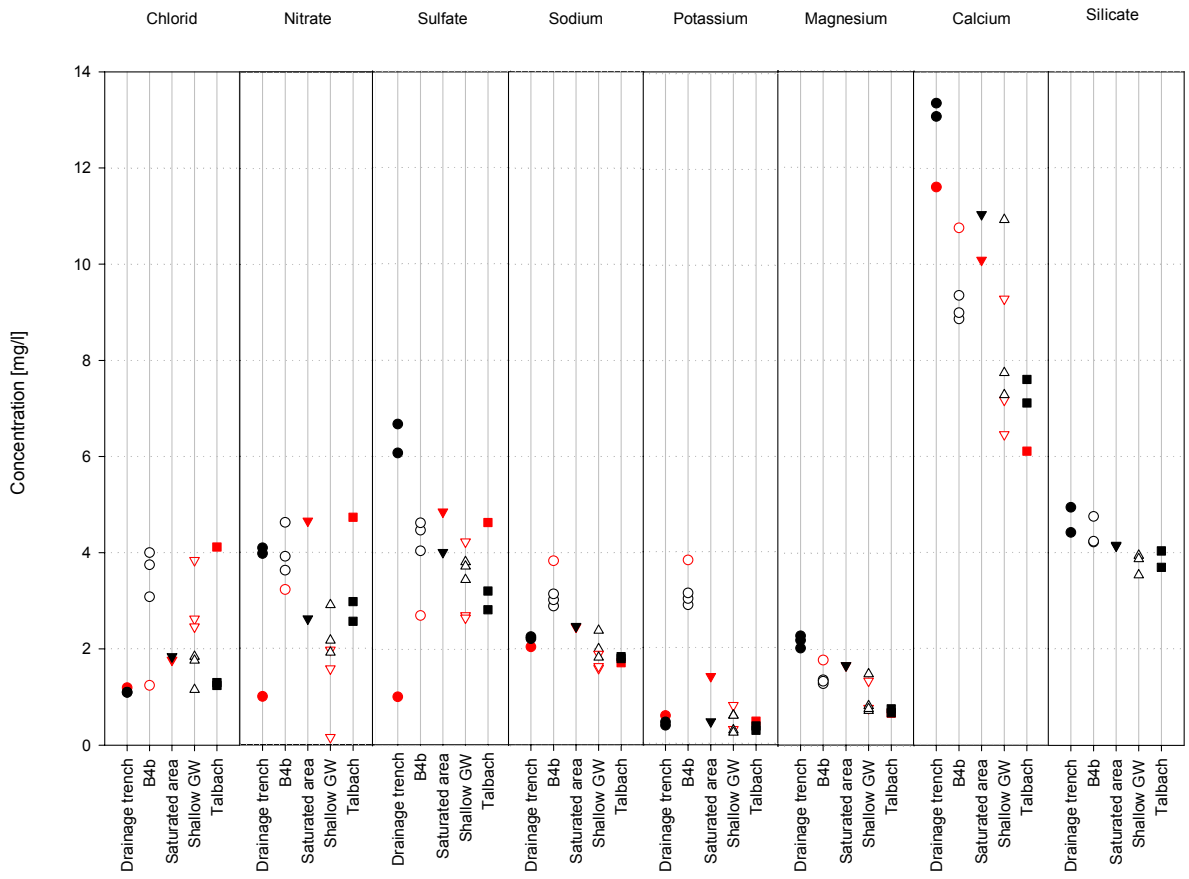

Figure 5-9: Graphic display of major ions for sampled locations.

During dry conditions, the chloride concentrations in B4b are outstandingly high: that change during the event where concentration decreases. The shallow groundwater and Talbach chloride concentrations increase during the event.
The drainage trench and the deep groundwater are marked by higher nitrate values than the other sampling locations. During the event nitrate shows inconsistent reactions.
During dry conditions sulphate concentrations decrease from the highest values at the drainage trench followed by B4b, saturated area and shallow groundwater towards lowest in the Talbach. It is remarkable that sulphate concentrations significantly decrease in the drainage trench during the event.
Exclusive of B4b with higher values, sodium and potassium values are located in the same range with no significant variations during the storm event.
Sulphate concentrations, just like magnesium and silicate show a stepwise decrease of concentrations (from drainage trench to B4b, saturated area, shallow groundwater and finally with lowest values the Talbach). The concentrations of event samples do not show a significantly different behaviour. There are no event samples of silicate. Higher concentrations of calcium can be found at the drainage trench. Except for B4b, all event samples have minor concentrations compared to dry weather conditions. During the event calcium concentration at B4b increases towards concentrations observed at the drainage trench.
To abstract ion concentrations of B4b are often outstanding but with the closest similarity to the water composition of the drainage trench. In addition, shallow groundwater and Talbach show similar ion concentrations. The ion concentrations of the saturated area are mainly in-between these two groups.

5.1.4 Discussion

The negative correlation between the electrical conductivity and the water level of the St. Wilhelmer Talbach indicate a dilution effect that probably results from direct precipitation onto stream surface or from another runoff component with low electrical conductivity. However, hydrograph separations between event and pre-event water of the river Brugga indicated that pre-event water provides an important proportion to the storm hydrograph (UHLENBROOK, 1999).
The varying relation of stream and groundwater rises is probably caused by varying runoff coefficients. Summer storm events with high intensities create more overland flow and less groundwater recharge. Consequently, the rises of the water level and the piezometric heads have the same magnitude. Events with lower intensity cause a higher rise of piezometric heads, due to heightened recharge rates and soil porosity.
The isopiestic surface for several events showed that the flow direction is almost perpendicular to the Talbach. This flow direction was also confirmed by a tracer experiment conducted by SCHEIDLER (2002).

In July, two deeper groundwater-monitoring holes were installed. The piezometric heads of the new groundwater wells lay below the shallow ones, which leads to the assumption that the shallow groundwater stations are measuring the variations of a perched groundwater table. The existence of a perched groundwater table (s) above a main groundwater body is commonly found (WARD & ROBINSON, 2000). However, the observed dynamic of the underlying groundwater at the test site is extraordinary. Except for two events at the beginning of the measurement period, response of the deeper groundwater is always faster. Precipitation characteristics and catchments conditions give no reasonable explanation for these two “exceptional” reactions. The reason might be a silitation of the deeper groundwater filter because both reactions were observed ensuring the drilling. During dry weather, one would assume that the deep groundwater shows minor recession due to percolating water from the perched water table but instead both hydrographs have similar recessions.

In general, the groundwater hydrograph below a perched groundwater table is characterised by smoother and slower reactions (e.g. LORENZ, 2001 see A 8), due to a longer passage of infiltrated precipitation through soil matrix. With help of Figure 5-10, different concepts shall be discussed to explain the faster reactions in the deeper groundwater body.

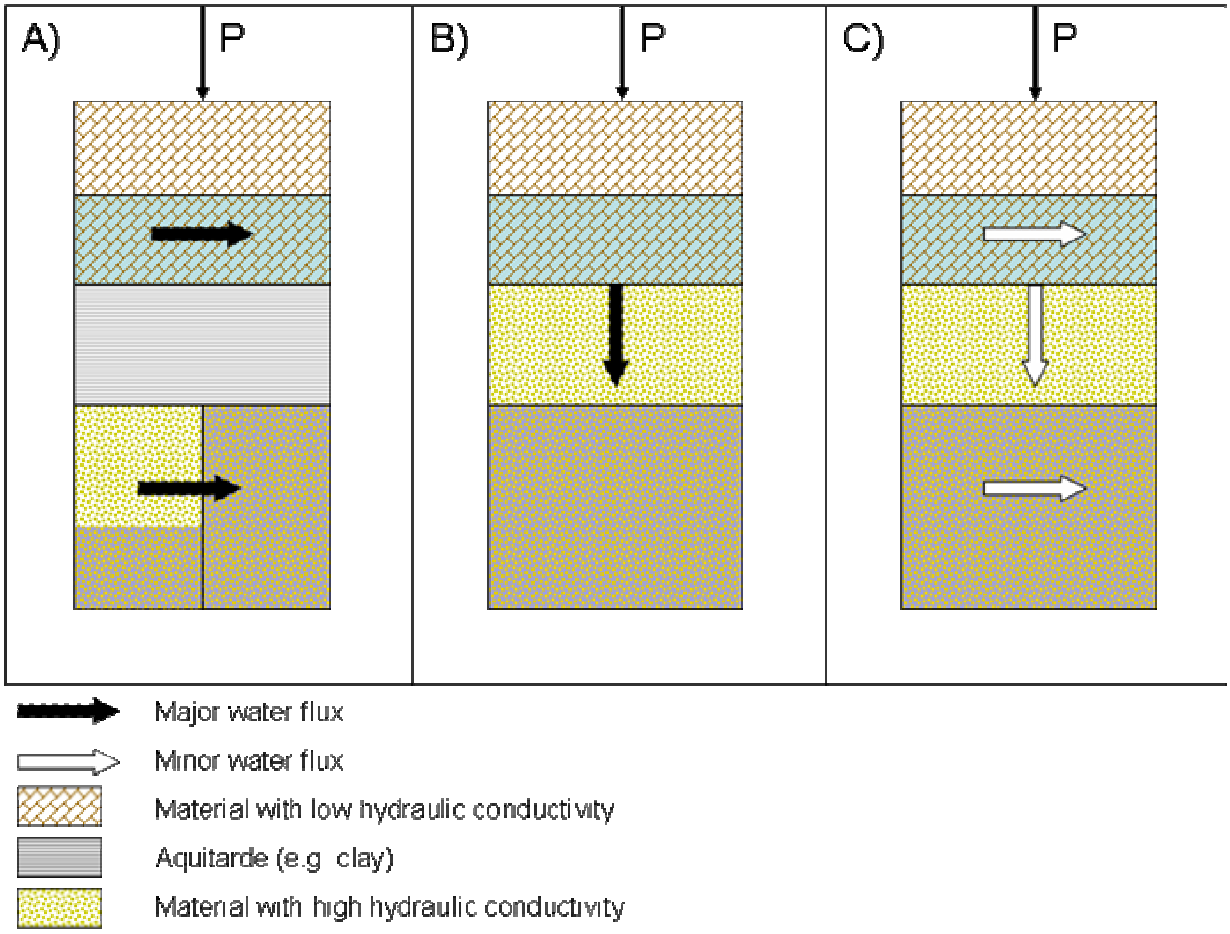

Figure 5-10: Visualisation of plausible hydrological concepts of subsurface water fluxes.

- A) The two water tables are divided by an aquitard. The water table of the perched groundwater is highly determined by lateral fluxes with a minor importance of local infiltration. The deeper groundwater might be confined or unconfined. For unconfined conditions higher hydraulic conductivity and less pore space would be necessary to cause the more pronounced reactions by lateral flow. A pressure wave induced by an area with fast groundwater recharge could induce pronounced changes in the piezometric head of a confined aquifer.
- B) The main flow direction is downwards. The existence of the perched groundwater table is only possible due to a layer with minor hydraulic conductivity overlying a layer with good hydraulic conductivity. Water percolates form the upper to the lower groundwater table. While the perched water table loses water by draining to the deep groundwater body, the water starts to pile up and it produces a higher increase and faster response.
- C) The last concept is a compromise of the previous two. Minor and slower vertical drainage fluxes from the perched water table add up with faster lateral fluxes.

B4a is higher correlated to precipitation characteristics than B4b. This is probably explained by a higher infiltration component. Nevertheless, the two hydrographs show high correlation with each other. This indicates that variations are provoked by the same impulse.

Against previous assumptions, the flow direction of the perched groundwater is not from the hillslope towards the stream but parallel to the stream. The flow direction of the deep groundwater is unknown. There is a difference of one meter between the water level measured in the broken conduit of B3b and B4b which would be five times the gradient towards the stream as measured in the perched groundwater stations.

One intend of soil moisture measurements was to prove to which extend water infiltrates through the unsaturated zone.

The probe in 86 cm depth was in almost saturated condition within the entire observation period. The probe in 62 cm depth was temporary reached by the water table during rainfall events. While periods of saturation are short in summer, they become increasingly longer in October due to the replenishment of soil moisture storage. The two upper probes are located in the unsaturated zone. Maximum water contents are limited by drainage with exception of the event on 25/10/04 when the water table even rises to a high of 23 cm below surface. During the installation of soil moisture probes roots were evident in the upper 15 cm. Root water uptake and evaporation might be a reasonable explanation for distinct recessions of the probe in 13 cm depth. Variations of the second probe are much smoother due to a longer passage of infiltrated

water through the soil and less influence of evapotranspiration. Nevertheless, local influence of a boulder cannot be excluded.
The fact that up welling groundwater is faster than infiltrating water due to humid preconditions might be explained by preferential flow. The moist preconditions are either necessary to shorten the distance of the water table to the probe or preferential pathways only become active with less matric suction. The theory of preferential flow is confirmed by the observation of numerous mole warrens on the test site (biotic macropores). An evidence for lateral fluxes might be the rise in the two lower soil moisture probes on 08/09/04 (red dart in Figure 5-7). This was the only event where no reaction in upper probes could be detected. This leads to the assumption that no precipitation directly fell onto the surface above the probes. Responsible for the response of the deeper probes is preferential flow (probably from the nearby (2 m) saturated area were water flow path converge.
MCDONNELL (1990) observed a similar phenomenon on a hillslope test site in New Zealand. Tensiometer measurements were conducted in different depth (see A 9). Reactions of the tensiometer depend on event characteristic while for events < 50 mm were sufficient to reach into greater depth during a large magnitude (58 mm) rainfall event matric potential in the lower soil horizons (> 75 cm) responded almost instantaneously to infiltrating rain. MCDONNELL (1990) reasoned that this response was caused by presence of macropores. Vertical bypassing of water to greater depth allowed saturation while the wetting front was still moving downward through the upper soil.
Within this work, it was not possible to quantify the relevance of preferential flow to the shallow groundwater table. Therefore, longer observation period with a detailed statistical analysis and further field experimentation is needed to achieve quantification.

Within the period of 31/08/04 to 24/09/04 probable rainfall at the climate station Katzensteig was not recorded because runoff, soil moisture and groundwater measurements showed clear reactions (black dart in Figure 5-7).

The water of the drainage trench originates directly from the bedrock at the accumulation zone (Figure 2-5) and has persistent low temperatures and high conductivity; therefore, the water is probably representative for the composition of the deep groundwater origin from fractured bedrock. High temperatures and low conductivity of the perched groundwater let suppose that this water is mainly influenced by precipitation. The conductivity measurements of the Talbach are lower than any other measured at the test site. The reasons for this might be a different characteristic of the rest of the Talbach catchment or evidence of a less mineralized runoff component. Assumed that the water of the drainage trench is similar to deep groundwater and the perched groundwater is represents mainly precipitation-influenced

water, the waters of the saturated area, Talbach and B4b are mixtures of these two to different fractions.
Deductive, water of B4b seems to be slightly influenced by the drainage of perched groundwater. The saturated area seems to be fed from both perched and deep groundwater. The vicinity of water to surface might however increase the temperatures so that deep groundwater is probably predominant. The Talbach has the closest similarity to the perched groundwater during the event. During dry weather conditions water characteristics tend more towards deep groundwater. B4b and the saturated area do not show a significant change during the event. The temperatures of event samples at the perched groundwater, Talbach and drainage trench are slightly higher due to a stronger influence of warmer summer precipitation while in dry periods the deep groundwater component becomes more important.

The previous drilling probably influences the major ions concentration measured in the deep groundwater-monitoring hole. Nevertheless, silicate values clearly confirm the results of temperature and conductivity measurement and are well suited to mark different runoff components. In addition, sulphate, calcium and magnesium did mark surface and groundwater significantly different.

Summarising the results of the conducted measurements scenario C is the most plausible because hydrochemistry of the shallow and deep groundwater well are significantly different due to marginal influence of precipitation water in B4b. The responses of the piezometric heads to precipitation are very similar what argues for that variations are caused by the same impulse.

5.2 Subsurface structure

5.2.1 Results of soil probing

During the drilling of the two deep groundwater stations, every 20 cm soil samples were extracted from the drilling core. The soil texture was determined with the feel method (AG BODEN, 1996). The gained information during the drilling is schematically displayed in Figure 5-11.
In the first column, the distribution of wet soil (as it was found in both drilling core and the soil samples) is shown.
From 1 m to 2,2 m below surface and below 3,8 m wet conditions occurred while the soil in-between is dry. The second column shows the location of shallow and deep groundwater monitoring well and a schematic diagram of the main identified soil types.

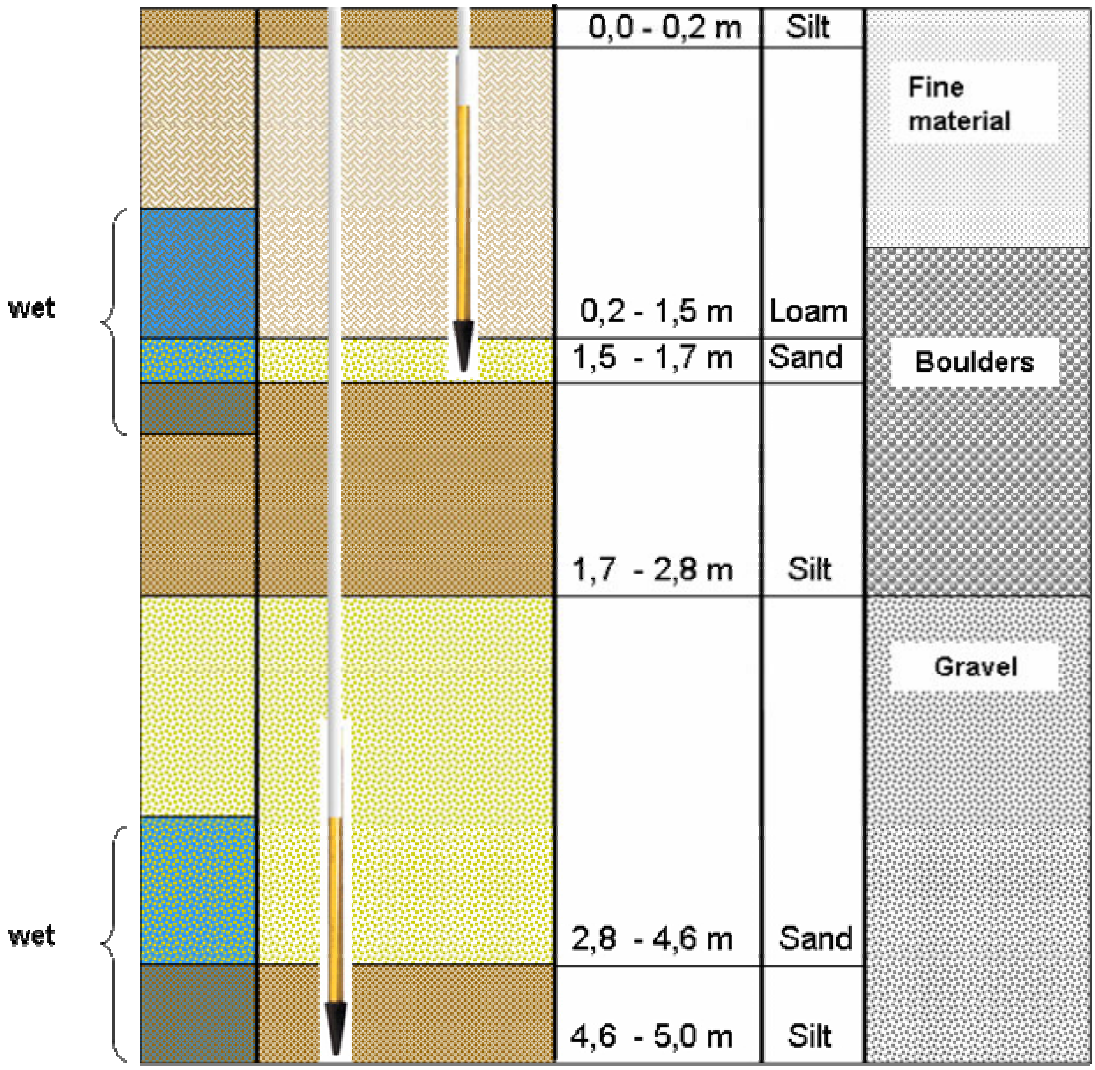

Figure 5-11: Schematic display of subsurface structure for the shallow and deep groundwater monitoring wells B4a and B4b.

The upper 0,2 m are silty riddled with roots followed by a 1,3 m thick loamy horizon. A thin but clearly definable layer of sand occurs in 1,5 m to 1,7 m depth. Another layer with a broad range of grain sizes that is best assigned as silt follows. This material is intermittent by a sandy layer but continuous in a depth of 4,6 m.
The third column describes the structure of the subsurface, as it was observed during the drilling. The first meter is determined by fine material followed by a layer of more than 1,5 m with a high content of coarse material, which caused problems while drilling. In greater depth, drilling became easier and collected soil samples contained a high amount of gravel.

5.2.2 Results of electrical resistivity tomography (ERT)

From the electrical resistivity tomography carried out by KOCH (2004), a detailed three-dimensional picture of subsurface structure arises. Nevertheless, additional measurements were conducted especially parallel to the flow direction of shallow

groundwater. The information about the spatial distribution of different materials measured at the chosen transects should be assigned to a finite element grid in HYDRUS-2D.

The location of the ERT transects is displayed in Figure 5-1. The transect A and C have been chosen along the flow direction. The measurement was done with 5 m spacing with Wenner as well as with dipole-dipole array.

Figure 5-12 show that three main zones of resistivity can be derived for transect A.

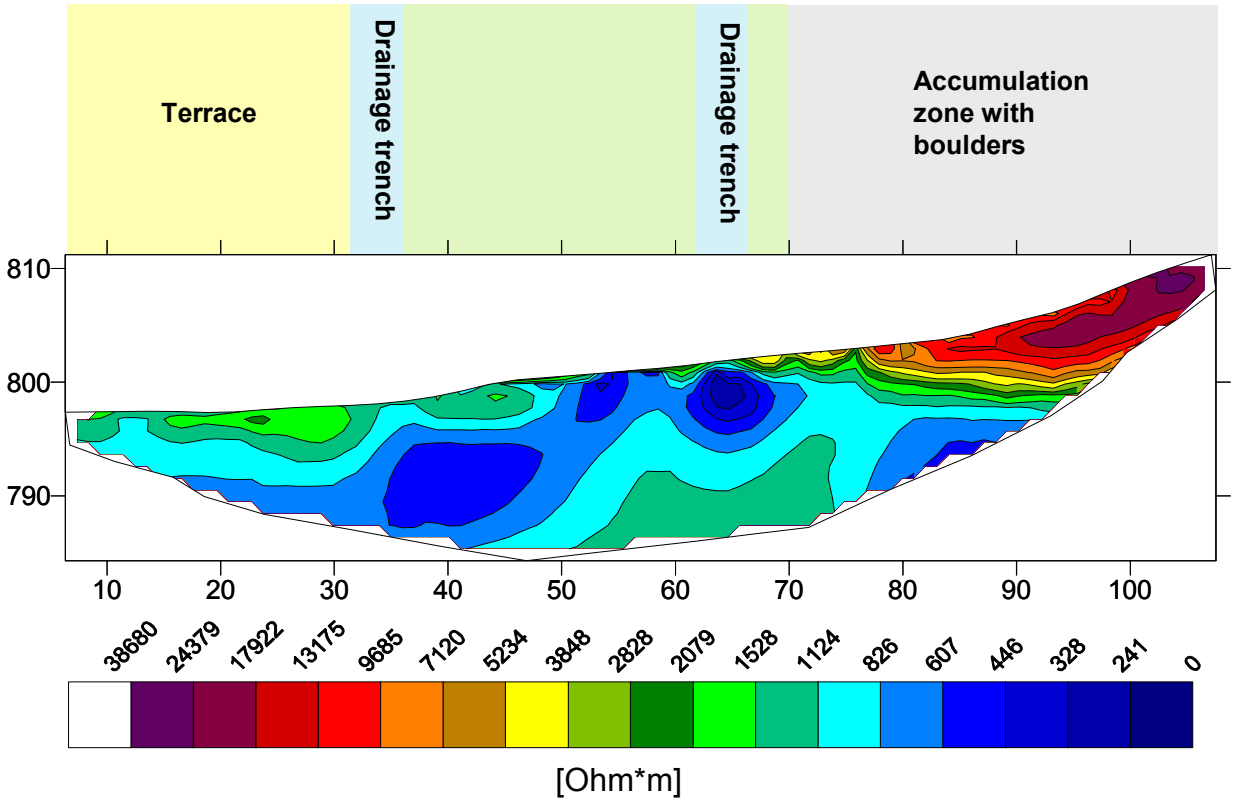

Figure 5-12: ERT Transect A (Wenner | 5 m spacing | 24 electrodes | RMS error 3,4 % | 27.07.04) with surface facts.

A zone of resistivity > 10.000 Ωm is located at the hillslope (zone I). At the bottom end of this zone resistivity changes drastically to values between 400-1200 Ωm (zone II). This zone is almost spread over the entire transect except of the domain around the middle terrace where the third layer with resistivity > 1800 Ωm is overlying (zone III). This layer is also found in greater depth below A1.

Transect C cuts through the floodplain and crosses the middle terrace (Figure 5-13).

The picture of the subsurface structure is more homogeneous. Along the middle terrace the layer of low resistivity (zone II) is covered by the layer with resistivity >1800 Ωm (zone III). In contrast to the hillslope profile, there is no evidence for zone III in greater depth. Zone I is not existent in this profile.

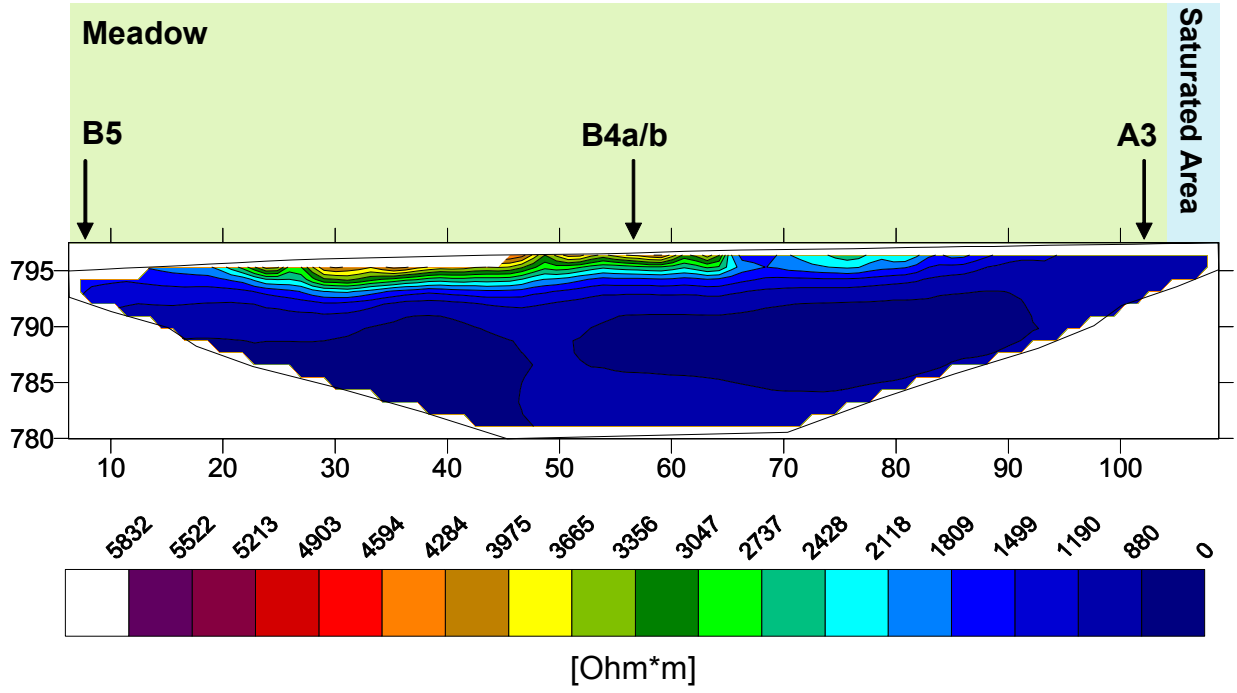

Figure 5-13: ERT Transect C (Wenner | 5 m spacing | 24 electrodes | RMS error 2,9 % | 27.07.04) with surface facts.

To improve the resolution of the surface near structures a measurement with smaller spacing was conducted in close vicinity (2 m) to the groundwater station B4a/b (Figure 5-14).

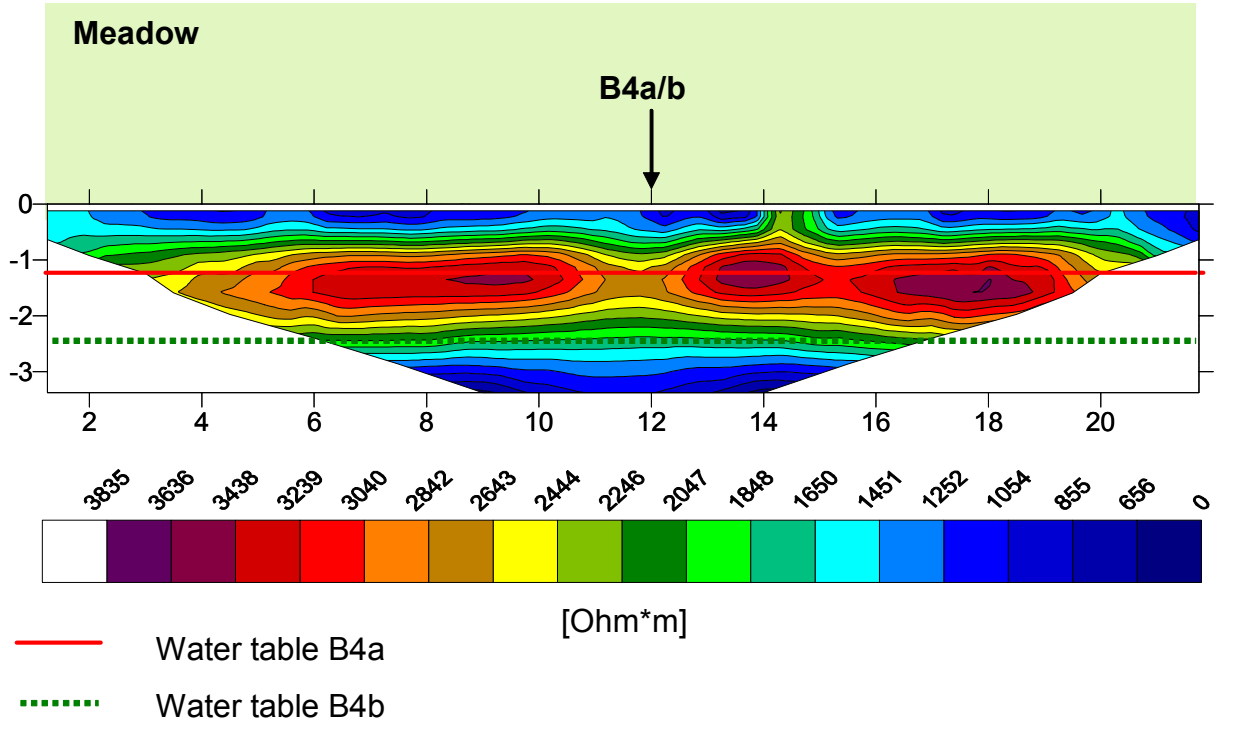

Figure 5-14: ERT Transect D (Wenner | 1 m spacing | 24 electrodes | RMS error 2,4 % | 08.09.04) with surface facts.

This profile allows the detection of another horizontal zone (IV) with resistivities between 1000 -1400 Ωm at the surface (above zone III). The horizontal lines through the profile indicate the measured water tables in the groundwater wells B4a (red line) and B4b (green dotted line). The extension of the intermittent zone and the higher resistivities of zone III agree quite well.

In order to investigate whether the zone III of higher resistivity is a barrier to water fluxes and to determine the influence of soil moisture on resistivity measurement an infiltration experiment was done.

With the double ring infiltrometer, water from the drainage trench was infiltrated for 30 min with a hydraulic head of 1 cm. The profile was measured before and directly afterwards. The percentage change in resistivity calculated by the inversion software is displayed in Figure 5-15.

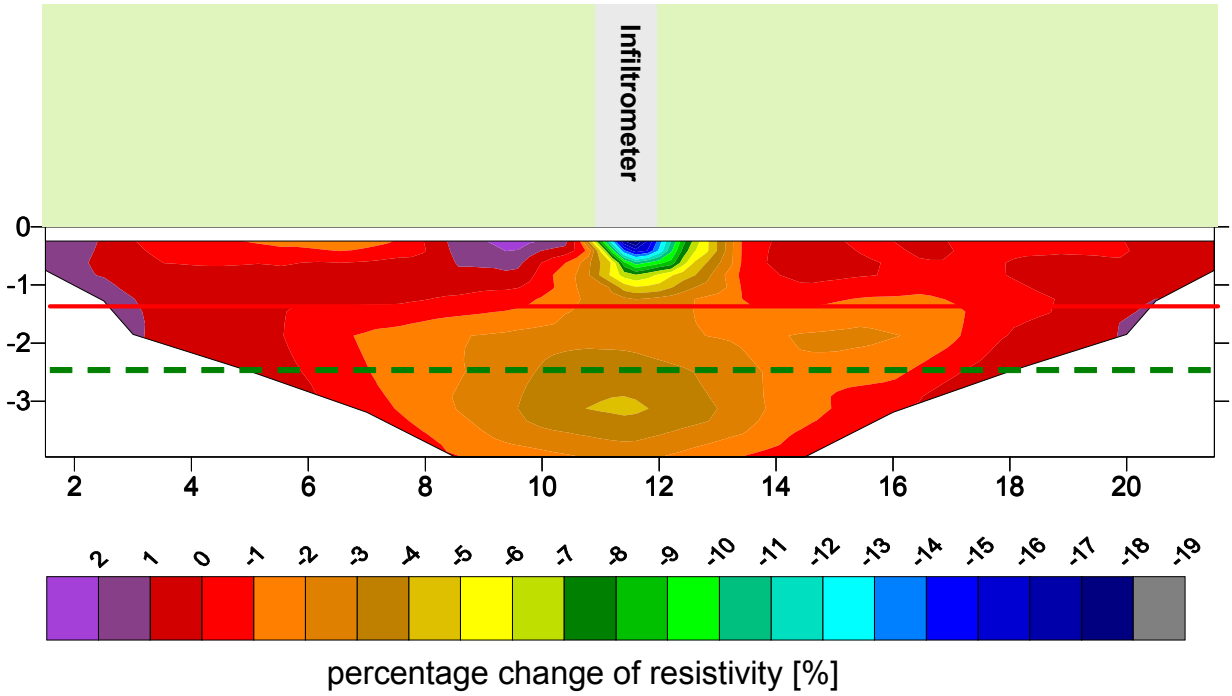

Figure 5-15: ERT Transect D (Time-lapse model of perceptual resistivity change calculated with the simultaneous inversion method).

Up to a depth of one meter, changes in resistivity of up to 18 % can be observed. At the depth of the perched groundwater table, (red line) changes become less (3-5 %) but extent over a larger area. Increases in resistivity of about 2 % give an account of the error range of the measurement. The infiltration experiment induced a rise of 14,6 cm in the perched groundwater well but in the deep groundwater well no reaction could be observed. The water arrived in the observation well after 12 min. During the experiment, it was remarkable that the infiltration capacity increased after 20 min.

Because the two-dimensional ERT profiles did not show clear evidence of bedrock, three one-dimensional vertical soundings were conducted (location see Figure 5-1).
The measured resistivities for the particular depth are logarithmic displayed (sounding curve) in Figure 5-16. To reproduce the measured sounding curve 3 horizons were manually fitted. The first horizon has a thickness of only one 1cm with very low resistivities (200 Ωm), the second horizon reaches into a depth of 0,44 m and shows extraordinary high resistivities (20000 Ωm). The third layer has a thickness of 27 m and is characterised by low resistivities (850 Ωm).

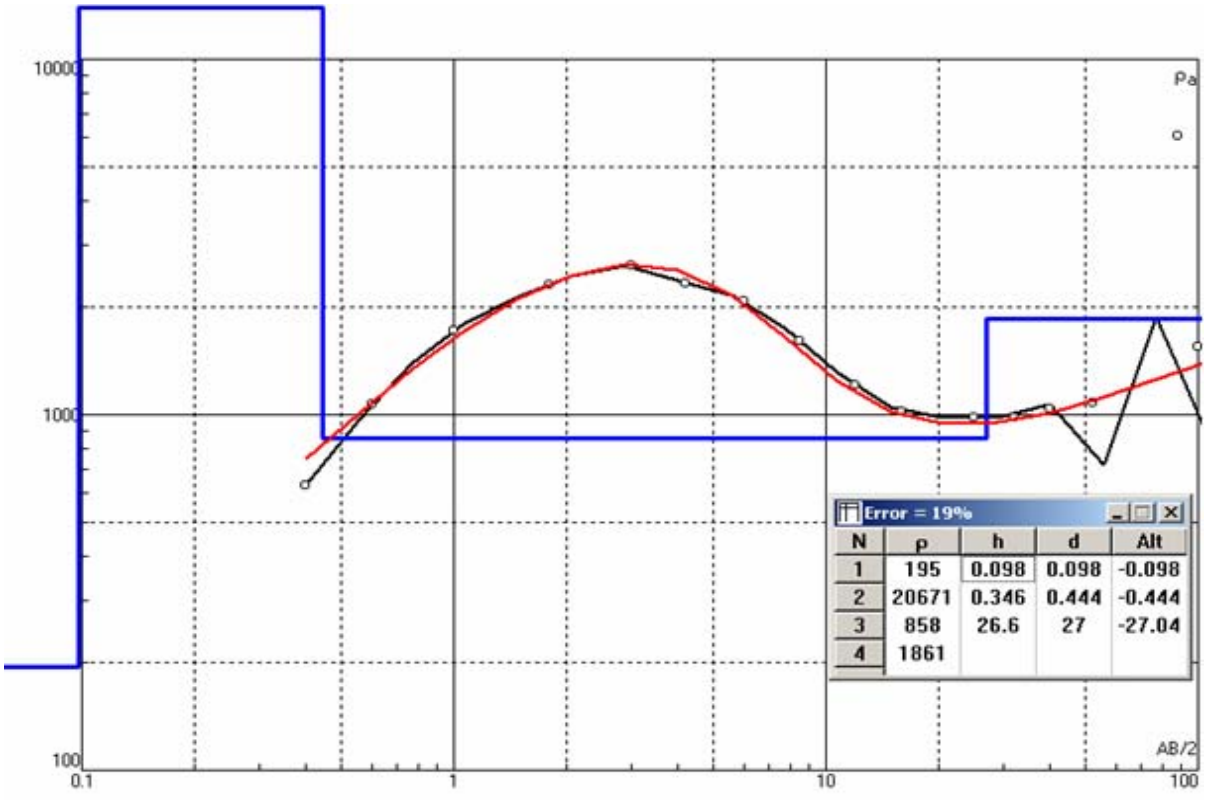

Figure 5-16: VES at the toe of the hillslope conducted on the 07/07/04 (Error:19 %, ρ= resistivity, h = thickness of a layer, d = depth of the layer).

As measurements in greater depth had standard deviations of up to 30 %, the 1-D profiling was repeated at the same locations.
The second measurement showed no agreement to the prior investigations (Figure 5-17).
Although current has to pass longer distances in the subsurface when electrodes are further apart resistivity decreases with depth from 0,5 m downwards.

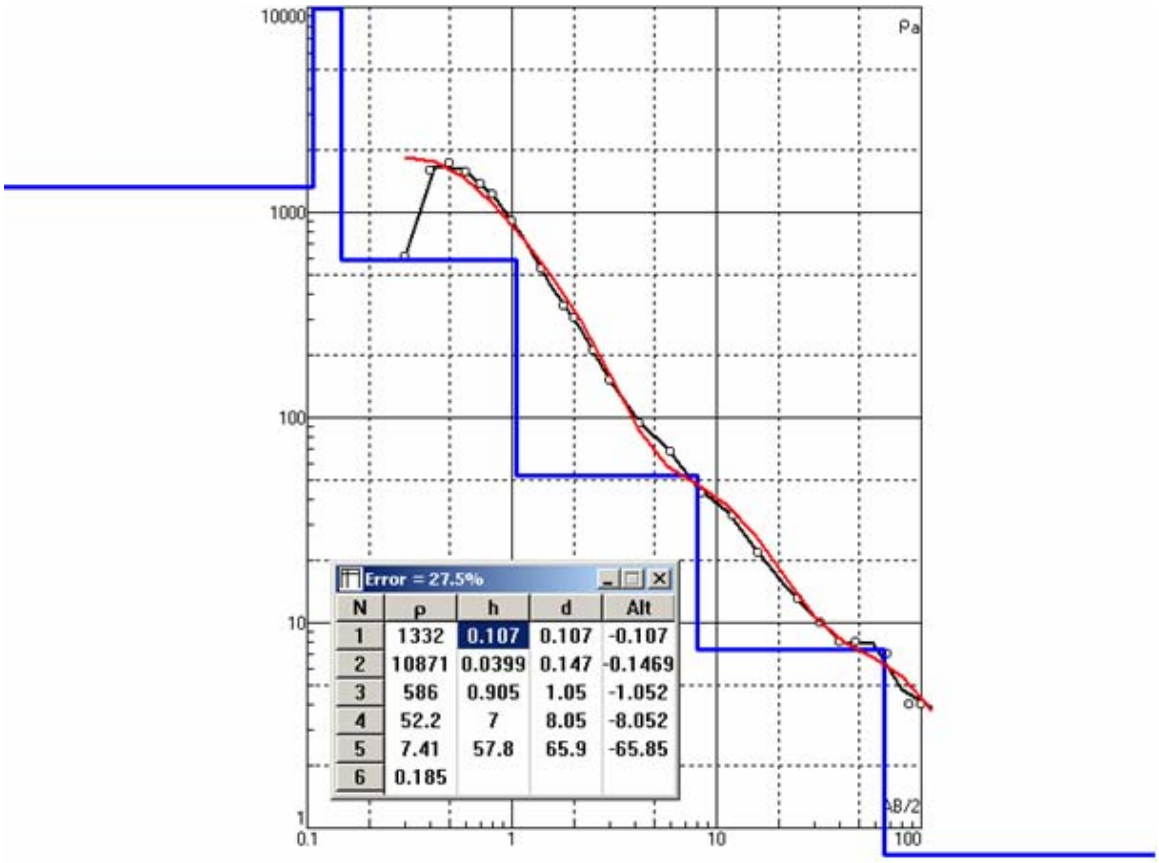

Figure 5-17: VES at the toe of the hillslope conducted on the 27/07/04 (Error:27,5 %, ρ= resistivity, h = thickness of a layer, d = depth of the layer).

Even so, the errors for all measurement points were rather small the resistivities show no agreement to a 2-D measurement (Transect B in the Appendix A 7) conducted at the same location and date. Also, no comparable results could be found in literature.

5.2.3 Discussion

The information gained from the drilling profile support the existence of a perched groundwater table, although the samples are highly influenced by the drilling process (compaction and more fine material). The investigation of the soil probes could not prove the existence of a clearly water impermeable layer but the silty layer might be responsible for the pile up of water.

The three clearly definable zones detected in the transect A and C correspond with the measurements of KOCH (2004). The high resistivities of zone I only occur at the boulder field with its air-filled gaps. In Figure 5-12, zone II reaches up to the surface at the location of the drainage trench spring and again in Figure 5-13 beside the terrace. In agreement with the measurement displayed in Figure 5-14, this zone can be assigned to the deep groundwater body. The existence of zone II is most distinct at the middle terrace. Nevertheless, against previous assumptions and the inverse model output this layer does not reach the surface. By reducing the spacing of the electrodes it was possible to visualize another layer of lower resistivities above zone IV, because with

decreased spacing information of upper regions becomes more precise (see chapter 4.2.2.3). This layer could be assigned to the perched groundwater. Therefore, the zone II is either a layer of different material e.g. the silty layer of the drilling profile or simply unsaturated. The resistivity values for zone II range between 2300 - 2850 Ωm. To receive more information about these three layers and their effect on the water flow the infiltration experiment are examined more detailed. The program RES2Dinv smoothes the measured values by averaging over the spacing resolution. The calculated point values from the inversion software for the two points (I1, I2) of geoelectric profile that lay below the double ring infiltrometer are displayed for different depth in Table 5-2.

Table 5-2: Resistivity point values for the location below the infiltrometer.

Depth [m]	I1 Dry [Ωm]	I2 Wet [Ωm]	I1 Dry [Ωm]	I2 Wet [Ωm]	I1 Change [%]	I2 Change [%]
-0,13	1445	1092	1269	896	-24,43	-29,39
-0,38	1492	1221	1305	979	-18,16	-24,98
-0,64	1894	1712	1706	1442	-9,61	-15,47
-0,93	2463	2376	2303	2136	-3,53	-7,25
-1,24	2829	2771	2726	2621	-2,05	-3,85
-1,59	2750	2661	2699	1593	-3,24	-40,98
-1,98	2330	2226	2307	2195	-4,46	-4,85
-2,4	1822	1744	1809	1722	-4,28	-4,81
-2,87	1392	1363	1392	1334	-2,08	-4,17
-3,38	1084	1111	1084	1111	2,49	2,49

The zone with higher resistivity is coloured in red letters. If presumed that zone II is an impermeable layer of high resistivity the values of resistivity would not change by inducing water from the soil surface. However, at location B a decrease of 40% can be observed due to wet conditions. This supports the assumption that zone II has different resistivity because of different soil moisture content. Another conclusion might be that water flows through this zone on preferential pathways.

For the top layer (values marked with blue letters) the decisive role of soil moisture content for resistivity measurement is reflected. Resistivity decreases to one third with saturation.

From one meter depth onwards, the water spreads sideways. The reasons for this might be better hydraulic conductivities due to higher values of the saturated hydraulic conductivity or a general increase of hydraulic conductivity. The infiltrated water penetrates also already saturated areas probably because of the lower temperature of

the infiltrating water from the drainage trench that due to higher conductivity causes a decrease of measured resistivities.

Within the work of KOCH (2004) a time-lapse measurements during a storm event was conducted. The result was an increase in resistivity in about 2,5 m depth, which could not be interpreted (given in A 10). With the new gained knowledge about the location of deep groundwater and the electrical conductivity of its water, it was possible to estimate the amount of precipitation arriving in the deep aquifer. Therefore, Archie's law was used (equation 4-1) assuming that materials are saturated and with calibration of the effective porosity. The conductivity of the deep groundwater was set to 90 µS/cm (as measured in B4b) while for the electrical conductivity of the precipitation the conductivity measured in the Talbach was used (45 µS/cm). A proportion of 5 % precipitation influencing the deep groundwater was estimated. In the zone II of high resistivity no significant resistivity changes were observed.

The nonsensical result for the VES cannot be explained by different moisture conditions, as the second measurement was conducted during dry weather conditions. The most plausible explanation is that the basing assumption of lateral homogeneity (see chapter 0) is not valid at the test site and the lateral resistivity changes are interpreted as horizontal changes.

5.3 Aquifer parameterization

5.3.1 Results of infiltration experiments

To estimate the coefficients of hydraulic conductivity of the surface layers, three double ring infiltration experiments were carried out; on the terrace, close to the soil moisture probes and nearby A2 (see Figure 5-1). The measured infiltration rates with time for the terrace and beside it are displayed in Figure 5-18.

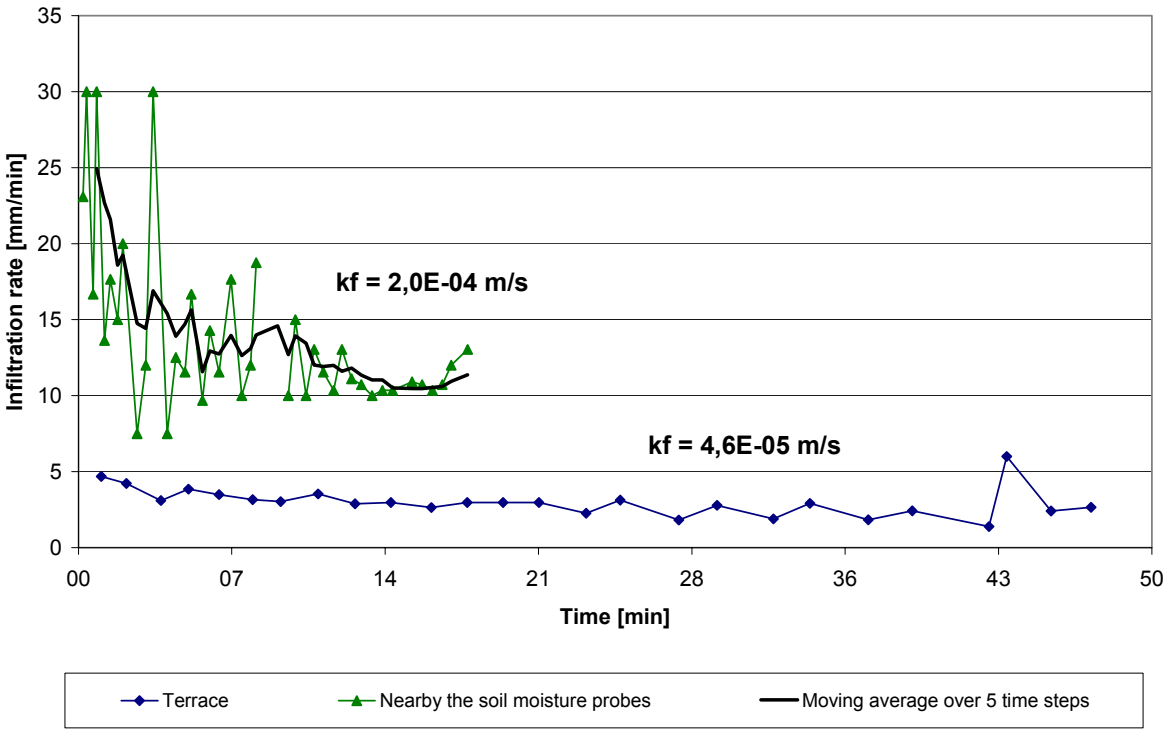

Figure 5-18: Infiltration curves conducted on the terrace and nearby the soil moisture probes at the border to the saturated area.

The calculation of the Darcy coefficient was done according to equation 4-3. The infiltration rates on the terrace shows a smooth behaviour with a marginal decrease of infiltration rates in the first 3 min. After 40 min, one extraordinary value occurs, but the following values drop back to previous low rates again.

The infiltration rates observed near the soil moisture probes show an entire different character. The most obvious feature is the flashy behaviour of the infiltration rate from one time step to another. The applied moving average of five time steps show that infiltration rates exponentially decrease with time. Nevertheless, throughout the infiltration experiment infiltration rates lay at least three times above the ones at the terrace. The higher infiltration capacity is also reflected by the coefficient of hydraulic conductivity, which is about five times higher. The obtained infiltration rates at A2 have a similar behaviour and an identical coefficient of hydraulic conductivity therefore the curve is not separately displayed in Figure 5-18.

5.3.2 Results of pumping tests

Pumping tests are a common tool to determine aquifer parameters and therefore were conducted at most monitoring wells. The received values for the hydraulic conductivities are displayed in Table 5-3.

Table 5-3: Determined coefficients of hydraulic conductivity by pumping tests.

Groundwater well	average values for K_S [m/s] - instationary flow conditions	average values for K_S [m/s] - stationary flow conditions
B1	3,5E-07	-
B3a	1,3E-06	1,7E-05
B3b	2,8E-08	-
B4a	5,6E-06	-
B4b	2,3E-05	-
B5	2,9E-07	-
A1	1,1E-07	-
A2	4,5E-07	-
A3	5,3E-07	-
A4	3,1E-07	-

The obtained coefficient of hydraulic conductivity ranges over four orders of magnitude. The repetition of the measurements gave reproducible results. The pumping test with stationary flow conditions, which is about one magnitude below instationary test, is an exception. In contrast to the infiltration experiments, the K_S -values of groundwater wells on the terrace are larger.

The transmissivity of the shallow groundwater (estimated according to equation 4-5) has a value of 1,6 E-05 [m/s]. At the deep well B4b, the highest K_S -value was obtained in contrast the other deep well B3b that has the lowest value. The low value and the characteristic of the water rise (compared to the other well e.g. A1 see Figure 5-19) confirm the loss of the filter device. In general, the hydraulic conductivities of the B groundwater stations are one magnitude bigger than at the A wells.

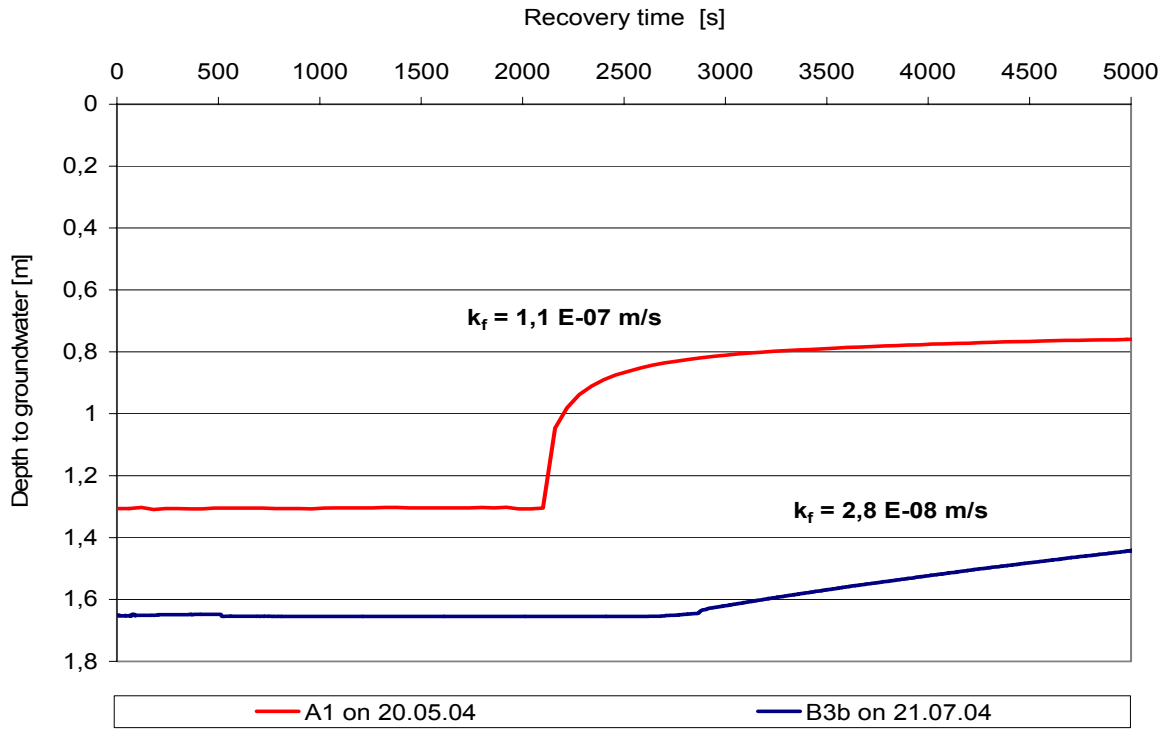

Figure 5-19: Recovery of the groundwater well A1 compared to the defect B3b.

5.3.3 Discussion

The double ring infiltration experiment could clearly point out the heterogenic infiltration capacities of the soil surface materials. The infiltration rates reflect the character of soil composition. On the terrace surface near layers are composed of fine silty and loamy soil types where water moves slower due to higher matric suction. In contrast, sandier with stones riddled profiles beside the terrace cause flashy changes in infiltration rates and a higher velocity of water infiltrating fluxes.

The distribution of the hydraulic conductivities obtained with pumping test show no reasonable distribution for shallow groundwater. However, coefficients of hydraulic conductivity of shallow groundwater are one magnitude smaller than of the deep groundwater. The value determined for stationary water fluxes is one magnitude larger and therefore approves that the resistivity of the filter device has a significant influence on values obtained with the instationary method (see chapter 4.3.2). The stationary method was successfully applied only at one groundwater well because pumping rates could not be adjusted. It can be assumed that real values of hydraulic conductivity are about one magnitude above. Thus, the hydraulic conductivity of the shallow groundwater with values between 10^{-5} - 10^{-6} [m/s] can be signified as permeable to weak permeable and according to HÖLTING (1996) is typical for silty sand. From this values follow that local influence of infiltrating water is possible. The deep groundwater

with values of 10^{-4} [m/s] is strong permeable and the coefficient of hydraulic conductivity is typical for sand.
The communication of the monitoring well with the aquifer is obviously disturbed due to the resistivity of the filter device and soil compaction. While changes in pressure heads transferred directly, exchanges of water chemistry probably precede slower. Therefore and because of erosion of the conduit, (see chapter 5.1.4) it is crucial that prior to water sampling older water is extracted by pumping.
Continuous measurement of temperature or conductivity in groundwater wells might show great errors.

5.4 Conclusion

After the drilling of the two deeper groundwater observation wells the presumption (raised from the ERT measurements of KOCH (2004), that the shallow groundwater stations do no reach the main aquifer was confirmed.
Throughout the entire observation period, the piezometric heads of the deep monitoring well were one meter below the water table measured in the shallow well, located 30 cm next to it. The existence of perched groundwater above the main groundwater body is commonly observed (WARD & ROBINSON, 2000). It is remarkable that the hydrograph of the deeper groundwater shows faster and stronger reactions to rainfall than the overlying perched groundwater, while groundwater recharge induced by local infiltration processes would let suppose the opposite (as e.g. observed by LORENTZ, 2001).
Capacitive soil moisture measurements could prove that not all arises in the perched aquifer can be explained by a well-defined wetting front moving down the soil profile. Instead, during wet soil moisture conditions water flows on preferential pathways to reach the saturated zone of the shallow groundwater table.
With hydrochemistry data, it was possible to prove that perched and deep groundwater have a significant different water composition. The perched groundwater is probably influenced to a high extend by rainfall while the water of the deep groundwater well has more similarity with the deep groundwater measured at the drainage trench.
The analysis of the soil samples did not clearly show the evidence of a water impermeable layer separating the perched from the deep groundwater.
With ERT, it was possible to visualise the two groundwater tables with a layer of higher resistivity separating the two. A conducted infiltration experiment verified that this layer is probably not entire impermeable.
With infiltration- and pumping experiments and determined values of hydraulic conductivity, it was shown that variations of the perched water table might be explained by infiltration processes. The Darcy coefficient at the deep groundwater well is at least one magnitude larger than at the shallow well.

The reason for the pronounced dynamic of piezometric heads measured in 5 m depth below the perched water table could not be finally explained by the conducted experimental work. Several concepts are possible:

- vertical fluxes with a earlier pile up in the deeper groundwater,
- minor lateral fluxes with earlier response time add up with infiltrating water,
- the dynamic of both water levels is determined by lateral fluxes,
- Piston flow displacement induced by fast infiltration (e.g. at the boulder field or area with a direct connection to the deep groundwater) that is found on the terrace.

With the physical based soil water model, HYDRUS the plausibility of these conceptual models shall be tested.

6 Model application

The gained knowledge of subsurface structure and parameters should be implemented into the soil moisture model HYDRUS in order to prove to which extend runoff processes at the test site can be explained by physical laws describing the movement of water in porous media.
Groundwater data measured with the same method during three former studies is available, but influenced by intensive groundwater sampling or snowfall. As mentioned in chapter 3, HYDRUS-2D has no snowmelt routine; therefore, this data could not be used for model calibration. In addition, after the drilling of the deeper groundwater well the focus of model application was to simultaneously simulate the dynamics of deep and shallow groundwater.
In order to shorten run time all meteorological data was used as time variable boundary condition with an hourly resolution instead of 10 min. Model output was not affected. Whereas a daily time step clearly smoothed the simulated variations because the processes causing the reactions of groundwater happening in shorter time intervals.

6.1 HYDRUS - 1D

In a first step, HYDRUS-1D is used to estimate initial parameters for the two-dimensional hillslope profile, due to shorter calculation times and to prove the plausibility a model concept with vertical water fluxes (scenario B in chapter 5.1.4).

6.1.1 Modelling of soil moisture content

The correct description of processes happening in the unsaturated zone is essential for the determination of groundwater recharge. Hence, the observed soil water contents were simulated.
A schematically display of the parameterisation of the soil profile is given below (Figure 6-1).
A block of 1m depth was defined with a grid resolution of 0,5 cm. Observation points are inserted in 13 cm, 23 cm, 62 cm and 86 cm according to the location of the ECH_2O probes. The upper boundary condition is set as an “Atmospheric” boundary condition, which allows precipitation and actual evapotranspiration. At the lower boundary, a free drainage condition is assumed to allow infiltrated precipitation to leave the profile.

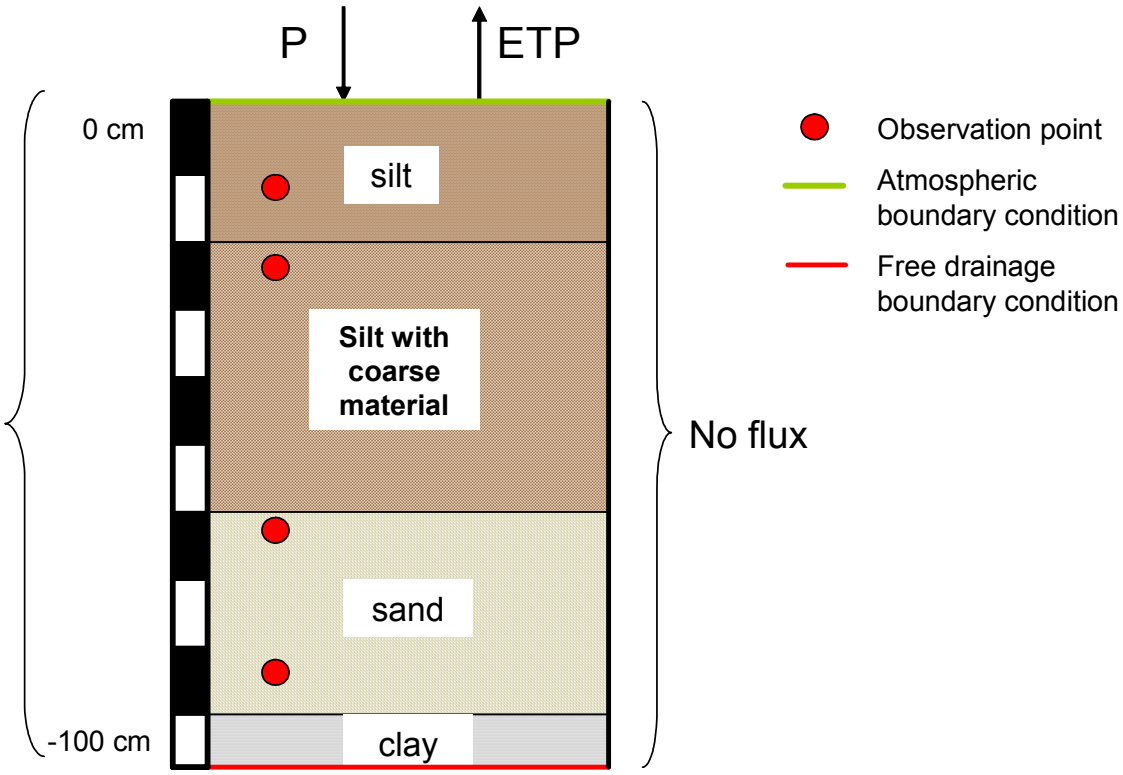

Figure 6-1: Schematically display of the applied concept for modelling of soil water contents.

According to personal observation during the implementation of the ECH_2O probes, a subdivision into three materials was chosen. The upper 20 cm consist of silty material; below 20 cm, fine material still is silty but the amount of coarse material (stones and gravel) increases. In 60 cm depth begins a sandy horizon. Initial values for silty and sandy materials were determined using the percentage proportions of textural classes (soil probing WENNINGER, 2002) to predict the van Genuchten parameter with the neural network database of HYDRUS-2D. For residual and saturated water contents, initial values were set according to the measured values during the calibration procedure of the soil moisture probes.

With the chosen structure, it was not possible to back up a water table in the sandy horizon because water drained unhindered through the sandy bottom layer. Therefore, an artificial layer with soil hydraulic parameters of clay was integrated at the lowest 10 cm to provoke the development of a water table.

The results for the probes in 13cm and 86 cm depth are displayed in Figure 6-2.

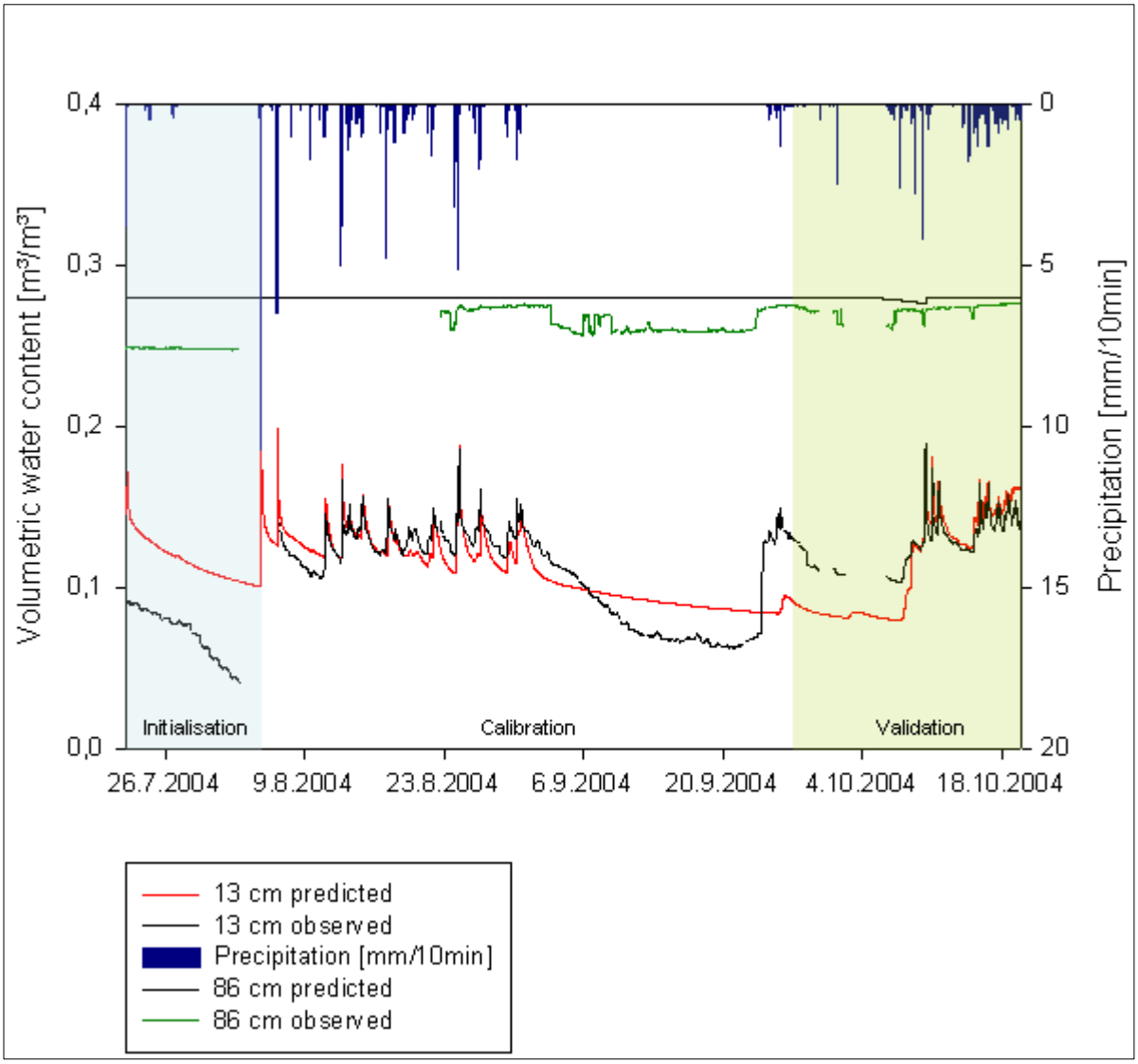

Figure 6-2: Predicted versus observed water contents for soil moisture probes in 13 cm and 86 cm depth.

Within the first two weeks, the model was initialized (highlighted in blue). For the following 70 days, the model calibration was carried out. The last 20 days served as model validation period (highlighted in green).

The probe in 86 cm depth is located in almost saturated conditions with marginal variations (3 %) of water content due to precipitation. The simulated values or the probe is constant except for the beginning of October when a marginal decrease is visible.

The surface near probe in 13 cm depth is positioned in the unsaturated zone, where infiltrated water is rapidly transferred into deeper layers and distinct recessions occur because of evapotranspiration. The simulated water contents for this probe show good agreement with the observed values during peaks and persistent wet conditions. The predicted water contents show stronger discrepancy to the observed values during recession of water contents. While recessions of short duration are underestimated, water contents during the long persistent dry period in September are overestimated.

Clearly distinguishable is also the discrepancy for the event on 23/10/04, due to missing precipitation data.

Multiple runs with different parameters could either show good agreement between simulated and observed water content for recession periods or for the peaks.

A display of the predicted and observed water contents for the probe in 23 cm depth can be found in the Appendix A 11. Simulated and observed water contents of the second probe are both characterized by smoother behaviour. In particular, the simulation results for the probe in 62 cm below surface that shows rapid changes between unsaturated and saturated conditions are interesting (given in Figure 6-3).

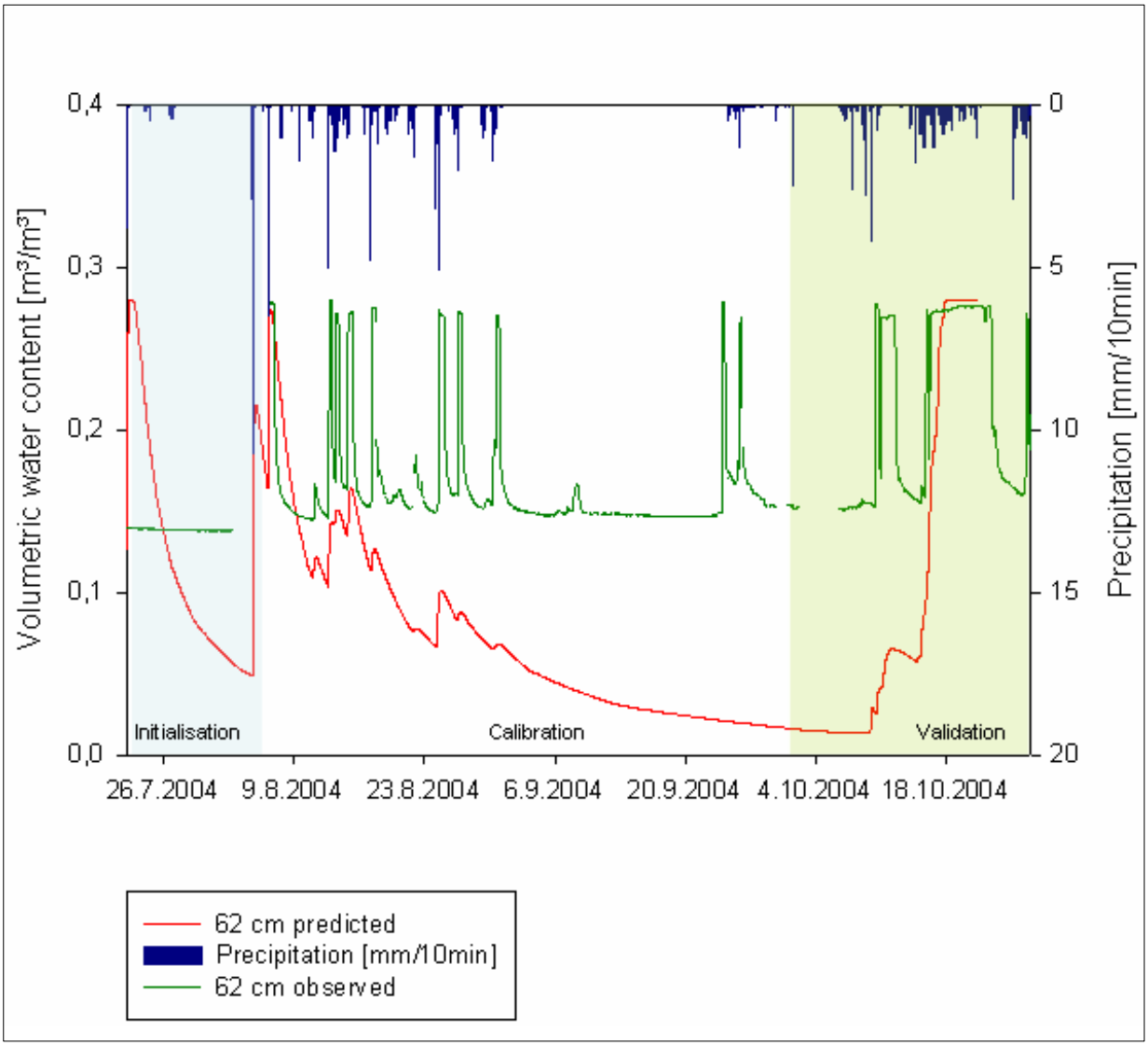

Figure 6-3: Predicted versus observed water contents for soil moisture probe in 62 cm depth.

The observed water contents show faster reactions than the surface near probes if distinct antecedent moisture condition occur and rapid changes between saturated and unsaturated conditions can be observed. The simulated water contents show a change from unsaturated to saturated conditions only due to strong precipitation events.

Reason for this might be the in general smoother reactions of the simulated water contents as well as too strong recessions. A faster reaction of the probe than the surface probes could not be simulated.
Simulations with a less impermeable layer at the bottom end of the profile resulted in endured period of saturation with short unsaturated conditions, the smooth character of the simulated responses maintained.

6.1.2 Modelling of pressure heads

Because the 1-D modelling of the pressure heads should provide initial parameters for the two-dimensional model design with four / three materials, a simplified approach with three materials was chosen (Figure 6-4).

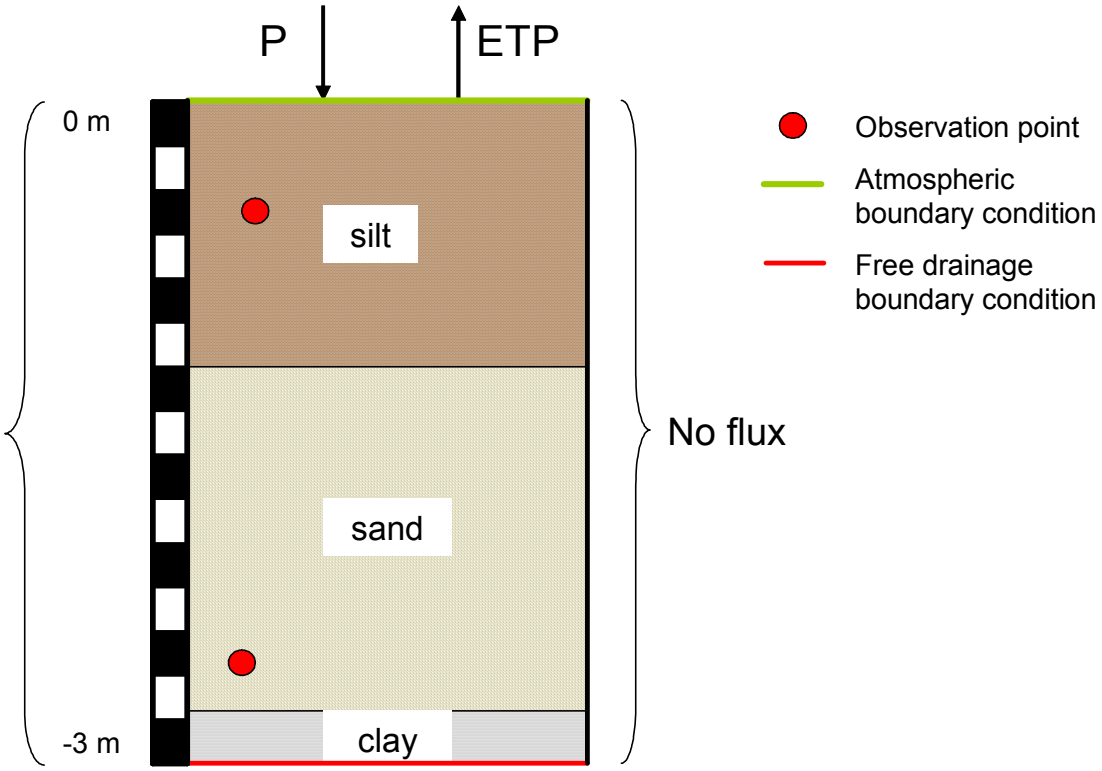

Figure 6-4: Schematically display of the applied concept for modelling of perched and deep groundwater pressure heads.

The model domain is one-dimensional, extending from the soil surface to a depth of 3 m with a spatial resolution of 0,01 m. Observation points that provide both water content and pressure heads are positioned in 0,5 m and 2,5 m depth. This position was chosen because it is the height where variations of the two water tables take place.
At the beginning of a simulation, the lower part of the profile is water saturated and the pressure head at the bottom node is specified at the height of the measured water column. From the water table to the soil surface, the profile is supposed to be at hydraulic equilibrium. At the upper boundary, atmospheric conditions were imposed.

Hourly potential evapotranspiration rates (TURC) were calculated based on data from the nearby weather station and specified together with hourly measured rainfall as a time variable boundary condition.
The upper 1,5 m consist of loamy material ; below 1,5 m the sandy layer of the main aquifer starts. To imitate the back up of water on bedrock at the bottom end a layer of clay with hydraulic conductivity of bedrock was implemented. Initial van Genuchten parameters for loamy and sandy materials were estimated on the chosen soil textural class based on the publication in WRR by CARSEL & PARRISH (1988). The values for the hydraulic conductivity are set according to the determined values of pumping and infiltration test (see chapter 5.3).
In Table 5-1, the initial values with the applied calibration range and the final parameters for the two materials are listed.

Table 6-1: Van Genuchten parameters for the loamy surface and sandy aquifer material.

Van Genuchten Parameters	Q_r	Q_s	α	n	Ks	l
Loam Initial	0,078	0,43	3,6	1,56	0,25	0,5
Loam Min	0,03	0,15	2	1,2	0,25	0,1
Loam Max	0,1	0,43	20	3	20	1
Loam Final	0,1	0,18	15	2,4	20	0,1
Sand Initial	0,045	0,43	14,5	2,68	7,13	0,5
Sand Min	0,01	0,1	2	1,5	5	0,1
Sand Max	0,08	0,43	25	3	100	1
Sand Final	0,03	0,12	3	2,5	80	0,2

The final residual water contents for the loamy layer are high what probably reflects the fact that in reality the surface layer receives groundwater. In contrast, saturated water contents for both layers are quite small. Reasons for this might be the large amount of course material and the coexistence of coarse and fine material what leads to minimal porosity (SCHACHTSCHABEL ET AL., 2002). The parameters α and n define the shape of the water retention curve. α is the reciprocal of the air-entry value. Coarse-grained soils have a low air-entry value and high α whereas fine textured soils have a lower α. The parameter n controls the slope of the water retention curve and reflects the particle size distribution. For coarse textured soils values of n are typically high causing higher extraction of water from coarse-textured soils. The parameter range for the saturated hydraulic conductivity is very broad reflecting the observed heterogeneity measured with the pumping tests. The final values lay closely to the upper limits.

During the calibration procedure, insensitive parameters were omitted from the optimisation list in order to reduce correlations between other optimised parameters. With respect to the heterogenic soil composition at the test site, the differences to the literature values that were estimated for the homogeny soils are reasonable.
The results for model simulation versus observed values for perched and deep groundwater are given below (Figure 6-5).

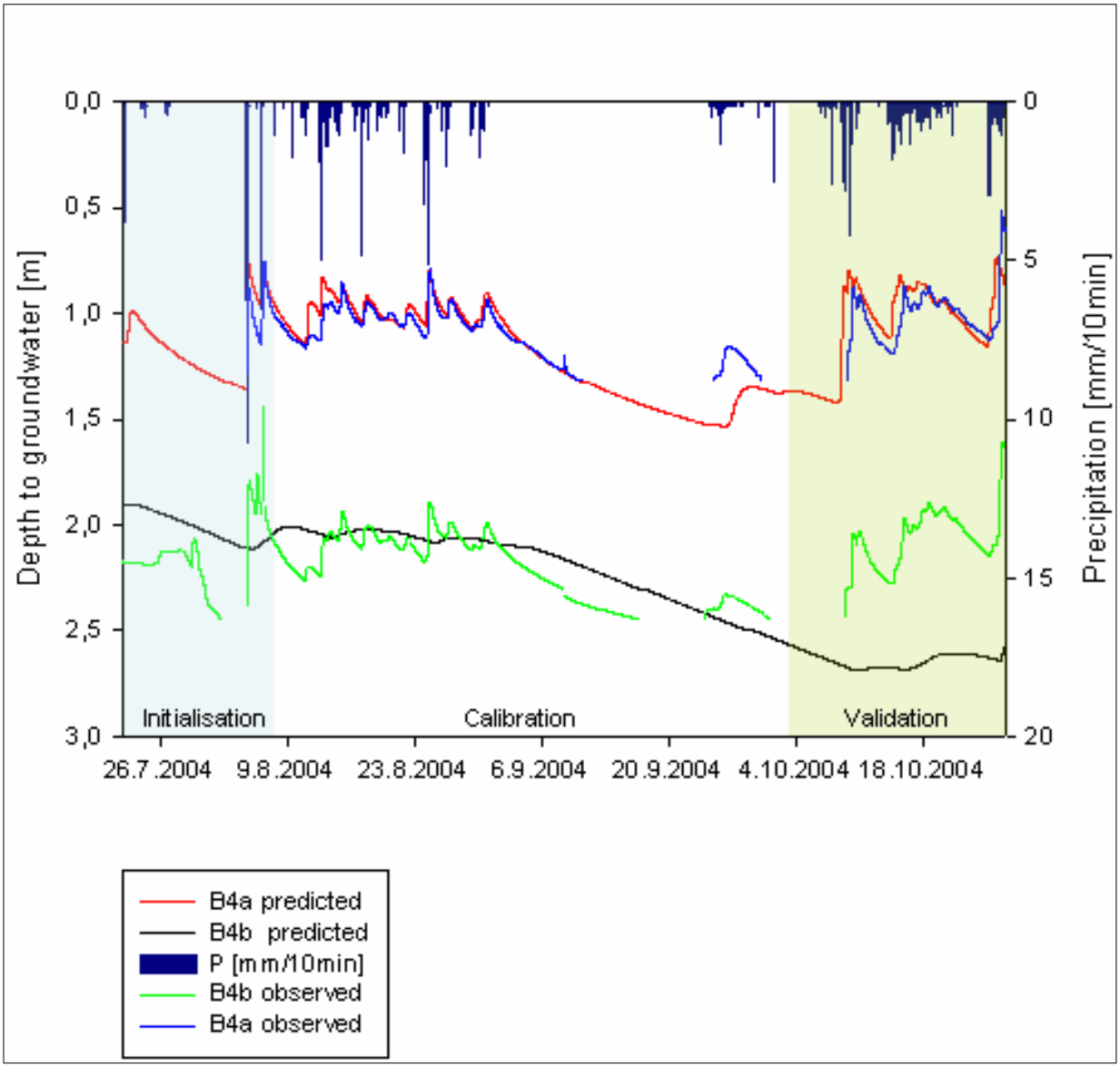

Figure 6-5: Simulated piezometric heads for the shallow and deep groundwater well.

The observed period for piezometric heads of the deep groundwater comprise three month. The missing values result either from low groundwater levels that lie beyond the measuring range of the capacity rods or water sampling. Within the first two weeks, the model was initialized (highlighted in blue). For the following 70 days, the model calibration was carried out. The last 30 days served as model validation period (highlighted in green).

With determined soil hydraulic parameters and the introduced conceptualisation, it was possible to provoke the development of a perched and a deep groundwater table. The elevation of both water tables could be accurately reproduced.

The simulation for the perched groundwater table shows good correspondence with measured groundwater levels. For the calibration period, the coefficient of determination between simulated and observed time series is r^2 = 0,74. During the calibration, there are two events where deviations of observed and predicted values occur:

- On 10/08/04 when two simulated peaks at the beginning of the event are higher than the observed.
- On the end of September when the simulated peak is small and delayed due to uncertainties of precipitation measurement.

For the validation period, the simulated peaks occurred slightly before the measured rises of water level while shape and size are similar. The coefficient of determination for this period is with r^2 = 0,63 slightly lower.

Simulations for the observation point in 2,5 m depth could not reproduce the observed dynamic as the coefficients of determination for the calibration (r^2 = 0,52) and validation (r^2 = 0,56) reflect.

The simulated reactions of deep groundwater to precipitation are retarded and very smooth compared with the measured dynamic.

Several other runs with different parameters were conducted and proved that:

- A difference of one magnitude in hydraulic conductivity is sufficient to allow the development of a perched water table.
- A model approach with an impermeable layer located (according to the ERT measurement) in between the groundwater tables does prevent variations in the deep groundwater body.
- In addition, several runs with unrealistic parameters (e.g. very small pore space due to compaction) could provoke neither distinct variations nor an earlier rise of deeper groundwater (due to ponding on bedrock).
- When drainage from the upper to the lower groundwater table was increased in order to receive pronounced reactions of deep groundwater, the existence of perched groundwater was impeded.

6.1.3 Discussion

In general, model results for the simulation of the capacitive soil moisture measurement are unsatisfactory. This can be ascribed to several reasons:

- Local influence of stones on the capacitive measurement
- Accumulation of water on the flat top of the parallel to the surface orientated probe (as mentioned in chapter 4.1.2).

- Inability of the unsaturated soil model (van Genuchten) to describe the hydraulic properties of soil material composed of both silt with a diameter of 0,002 - 0,06 mm (HÖLTING, 1996) and stones with a size 0,5 m (see Figure 5-5). Probably the implementation of a scaling factor would help to describe the spatial variability of the unsaturated soil hydraulic properties in the flow domain. HYDRUS-2D provides such a technique based on the similar media concept introduced by MILLER & MILLER (1956). However, the exercises to derive this scaling factor would have gone beyond the scope of this work.
- The basing flow equation of HYDRUS-1D /2D does not account for preferential flow.

The simulated water contents for the two surface near probes, could simulate the peaks but not the recessions. In addition, the predicted recessions did show an inconsistent behaviour with an underestimation of water contents during short periods and an overestimation for persistent dry conditions. The short-term underestimation of water contents might be due to accumulation of infiltrating water on the horizontal probe, while the overestimation at the enduring dry period in September is possibly explained by smaller simulated values for actual evapotranspiration (due to limitations of water supply) than the rates that actually occurred. That supports the assumption that the properties of the fine-grained fraction are not well reproduced by the chosen parameters.

The probe positioned at the border between saturated and unsaturated zone showed fast changes between these conditions, which could not be simulated mainly because of two reasons:

- The observed values maintained on a constant high water content, although the residual water content for the soil material is lower. A reasonable explanation might be capillary rise from the water table below. Simulated results could not reproduce the constant higher water contents instead recessions to residual water contents occurred. This is another indication that the hydraulic properties of the fine material could not be parameterised properly.
- The fast reactions of the water table are partially caused by preferential flow (chapter 5.1.2), what of course could not be reproduced. One of the main reasons why water in natural soils does not always move in the manner predicted by Darcy's equation is that, in certain circumstances, water movement may be dominated by flow through a few large openings or voids rather than the bulk flow through the microstructural interstices of the soil matrix.

The one-dimensional model approach for the simulation of pressure heads give good results for perched groundwater. In contrast to the location of the soil moisture probes,

the surface near material (upper meter) at B4a/b consists of fine material without stones. This might be a main reason for better simulation results. The underestimation of the event at the end of September occurred because of measurement errors of precipitation. The calibration was carried out for the summer month while the validation was done for autumn. Therefore, the slightly faster arrival and overestimation of predicted peaks probably have their cause in seasonality e.g., evapotranspiration values calculated with the TURC equation (3-8) might be too small in autumn. The consideration of variable transpiration due to crop growing status is probably negligible with the focus on flood events but is decisive for issues like irrigation or groundwater recharge etc.

The necessity to implement an semi-permeable layer at the bottom end of the soil moisture conceptualisation leads to the conclusion that at least partially there is a less conductive layer below the perched groundwater table.

The simulation of deep groundwater showed smooth and retarded response to precipitation as water filtrates through a soil block of 2,5 m. The distinct and rapid reactions could not be simulated. Nevertheless, the initial estimate for the soil hydraulic parameters enables the simulation of a perched water level. Both simulated water tables were positioned in the same altitude as observed during the measurement period.

With the model application, it was possible to prove, that observed variations for shallow groundwater mainly occur because of local infiltration. On the other hand, failure of good model simulations for deep groundwater indicates that vertical processes are not responsible for the dynamic behaviour of observed piezometric heads in the deep groundwater well B4b.

6.2 HYDRUS - 2D

The fluctuations of the deep groundwater level cannot be reproduced just by vertical infiltration processes. Thus, a two-dimensional vertical finite element grid of the test site is generated to allow lateral flow path within the porous media. Because the model was mainly used as a hypothesis testing tool the results are presented qualitatively. In addition, because of the numeric instability of automatic calibration procedure only minor manual calibration was applied.

6.2.1 Modelling of the test site transect

As the model domain is two-dimensional, it is necessary to choose a profile where only marginal water fluxes perpendicular to the profile occur. Therefore, the transect was defined parallel to the flow direction. To determine the flow direction the isopiestic surface was created for ten shallow groundwater stations for different events (chapter

5.1.1). With only one measurement point for the deep groundwater, its flow field could not be determined.

To define the spatial dimensions of the outer boundary as well as the distribution of different soil materials serve beside direct measurement mainly the ERT profiles. As described in chapter 5.2.2 four resistivity zones were determined whereas it is not clarified whether zone II represents an unsaturated layer or a different impermeable material. Hence, both possibilities are tested. The ERT subsurface structure is assigned to the finite element mesh. A schematically display of the material distribution (for the approach without an impermeable layer) is displayed in the Appendix A 12.

Crucial for the model application is the setting of reasonable boundary conditions. A schematically display of the two dimensional profile with its boundary conditions and the observation points is given below (Figure 6-6).

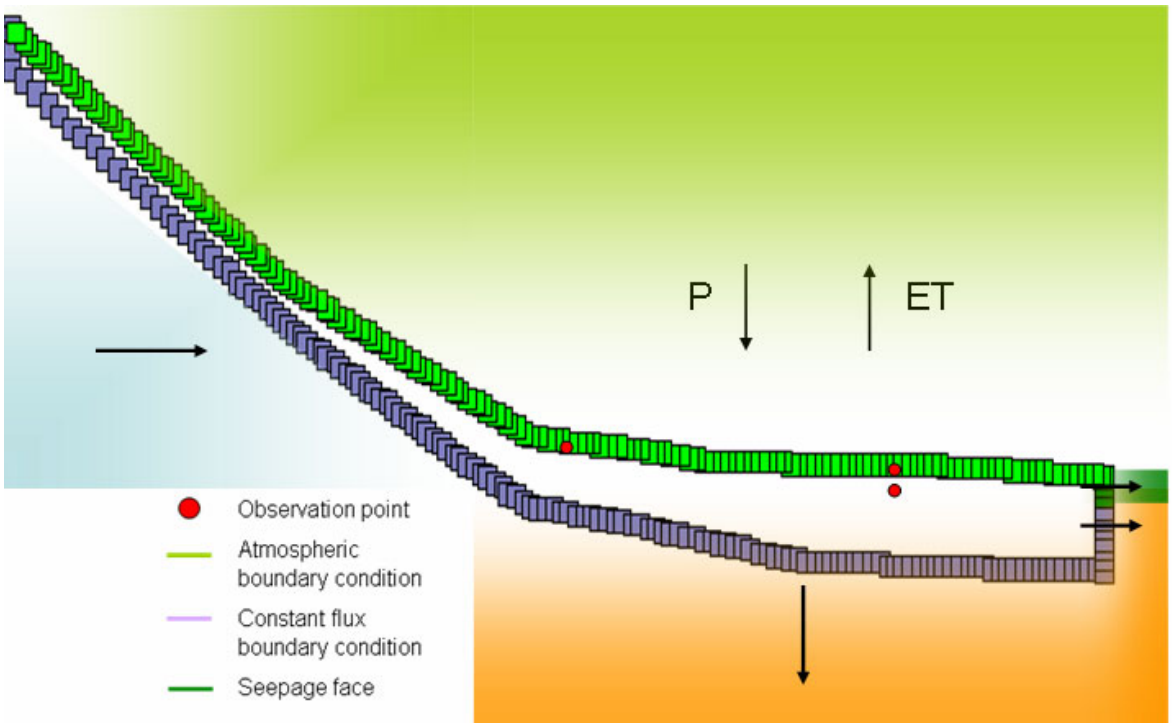

Figure 6-6: Schematically display of the vertical profile of the test site.

Every square on the outer boundary represents a node of the finite element grid. The light green spares indicate an atmospheric boundary condition with precipitation as influx and actual evapotranspiration as out flux. The dark green boundary towards the stream is a seepage face that allows water to leave the profile according to the actual potential gradient and soil specific hydraulic parameters. Because these boundary conditions assumes unhindered outflow, it could not be assigned to the entire vertical side, or otherwise the profile would have drained completely. In reality, water backs up on the fractured crystalline bedrock. To imitate this process a constant flux boundary condition is applied that enables outflow at the bottom and to the side (red area) an inflow towards the hillside (blue area). Due to small porosity of crystalline bedrock

(between 0-10 % according to WARD & ROBINSON, 2000) and small coefficients of hydraulic conductivity between 10^{-5}-10^{-10} m/s (according to STOBER, 1995) the applied fluxes are with 0,009 m/d small.

To observe the predicted pressure heads observation points are positioned in the grid at the location of B4a ad B4b (0,5 m and 2,5 m below surface).
As initial conditions at the hillslope are highly instationary, inducing numeric instability the profile is initialised with low water contents followed by an intense precipitation.
Three respectively four materials need to be parameterised: the main aquifer, the surface layer of the perched groundwater, the boulder field and the intermediate layer between the groundwater tables.

The utilized parameters for the main aquifer material and the surface layer are already discussed in chapter 6.1.2. For these layers parameters were determined by direct measurement and calibration with the 1- D model.
However, parameters for the two other materials are unknown and because the inverse solution for the hillslope profile terminated were calibrated manually.
MEHLHORN ET AL. (1998) amount the hydraulic conductivity to 10^{-2} - 10^{-1} m/s for boulder fields. Problematic is the definition of the other five parameters because the boulder field is a medium were the assumptions of the basing Richard's equation for saturated and unsaturated flow probably is not valid because mainly turbulent gravitational flow without matric suction affects water transport. Nevertheless, hypothetic parameters that describe the water retention curve of the boulder field material were assumed. With low residual and saturated water contents and high values for n and α according to the high content of coarse material. For the profile with the extra material for the intermediate zone, parameters of clay are assigned.

In order to predict the dynamic of the deep groundwater following scenarios are conducted:

- BEVEN (1989) provided the mathematical background for the piston flow effect showing that within the saturated zone, inputs can be translated down slope at kinematic wave velocities, which are much faster than flow velocities predicted by Darcy's law. By an estimated specific storage coefficient S_S of about $1*10^{-1}$ 1/m (for unconfined conditions, according to HÖLTING, 1996), flow velocities of about $2{,}3 \cdot 10^{-4}$ m/s of the deep groundwater well B4b (assuming Darcy's law) will result in wave velocities of approximately 200 m/d. This is the result of the reciprocal value of S_S multiplied by the measured water flow velocity. However, storage coefficients S_S of confined aquifers are even lower ($1*10^{-5}$ 1/m - $1*10^{-3}$ 1/m, according to HÖLTING, 1996) but it could not be proved whether the deep

groundwater is confined. Thus, a scenario with K_S = 200 m/s and a porosity of 0,1 m³/m³ is conducted .Scenarios with smaller porosities than 0,1 m³/m³ in order to imitate confined conditions terminated. The model itself does not have an option to include confined conditions.

- Anisotropy on hillslopes is rather the rule than the exception (WARD & ROBINSON, 2000). Also at the test site, there are hints that anisotropy occurs. (e.g. the detection of the layered structure during the drilling and the existence of perched groundwater itself). DÖRNER & HORN (2004) could quantify an anisotropy vector parallel to the soil surface with laboratory testing of soil samples. The anisotropy of water conductivity depends on the matric potential and is related to the pore continuity. At the investigated hillslope, it was found that conductivity parallel to the surface is about 7 times better as in the perpendicular direction. Considering the anisotropy in the model, their results were improved. For the test site scenario the saturated hydraulic conductivity was assumed 10 times higher in lateral direction.

- Lateral flow might be not exclusively originate from the boulder field, possible faster components might also generate at zones where the intermediate layer (zone II) is not distinct and infiltration capacities are higher e.g. beneath the terrace (according to ERT and infiltration measurements) or at the saturated area. Therefore, a profile was created where the more conductive aquifer material reaches up to the surface beneath the terrace.

- Instead of a constant inflow from the bedrock side, a time varying flux was applied. But since the applied fluxes should not exceed the capacity of the soil which is given by porosity, hydraulic conductivity and actual gradient it was not possible to induce a varying flux that did not cause the termination of the model.

- An impermeable layer between the perched and deep groundwater table was generated with the soil hydraulic properties of clay.

In addition, different combinations of the discussed scenarios are conducted. As mentioned above some scenarios failed due to numeric instability. The best result explaining the dynamic of the deep groundwater well by lateral fluxes is presented below (Figure 6-7).

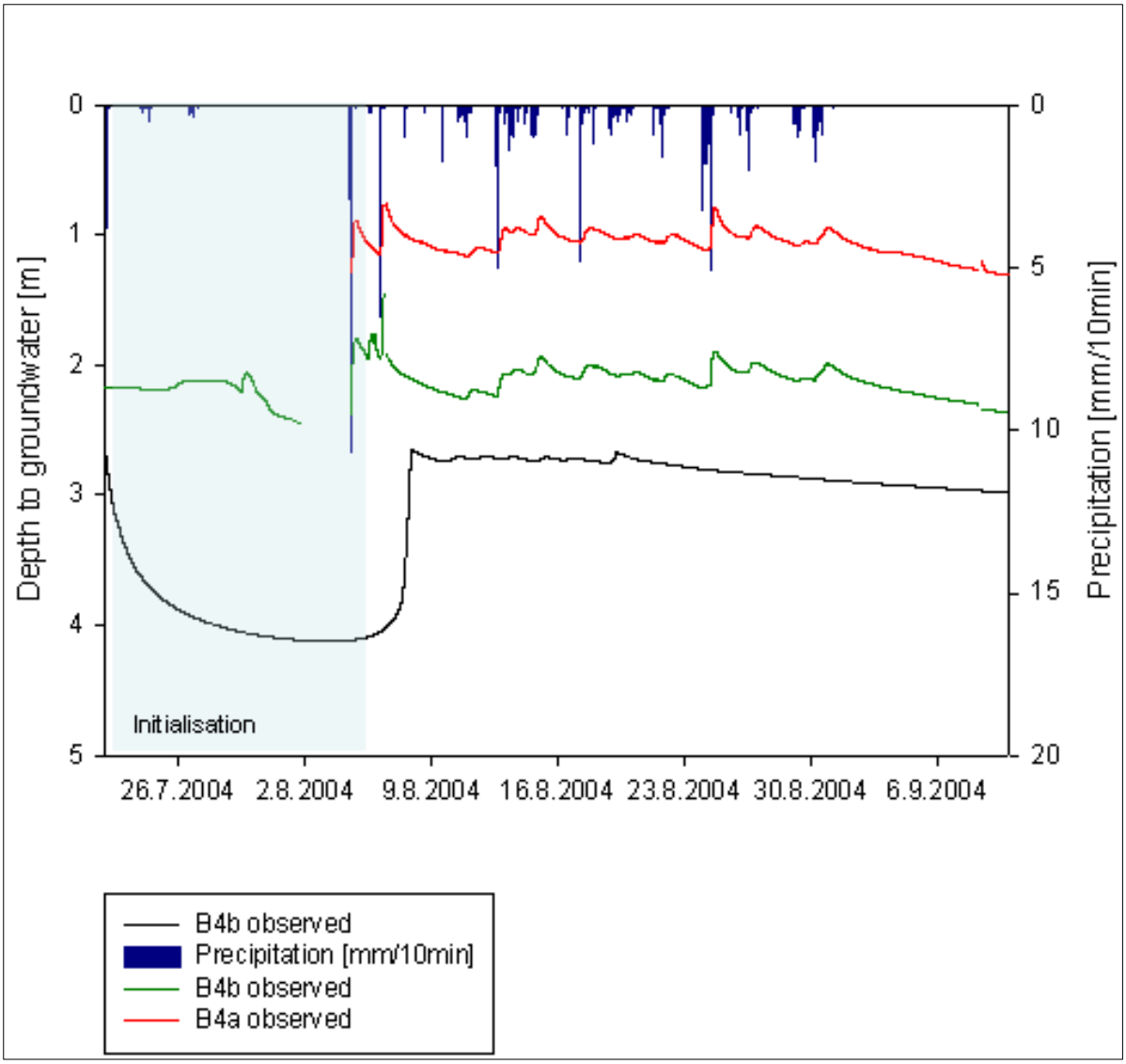

Figure 6-7: Model results for the deep groundwater with assumed values for hydraulic conductivity of 200 m/d parallel to the surface and 20 m/d perpendicular to the surface.

Figure 6-7 model results for the deep groundwater with assumed values for hydraulic conductivity of 200 m/d parallel to the surface, and 20 m/d perpendicular to the surface. After the initialisation of the model the simulated groundwater level is positioned constantly 0,5 m below the observed water level. The predicted peaks arrive with a time-delay of approximately three days. The fluctuations of the deep groundwater level compared to the simulated are about five times larger.

Nevertheless, qualitative examination of the model results could explain some processes at the test site (Figure 6-8).

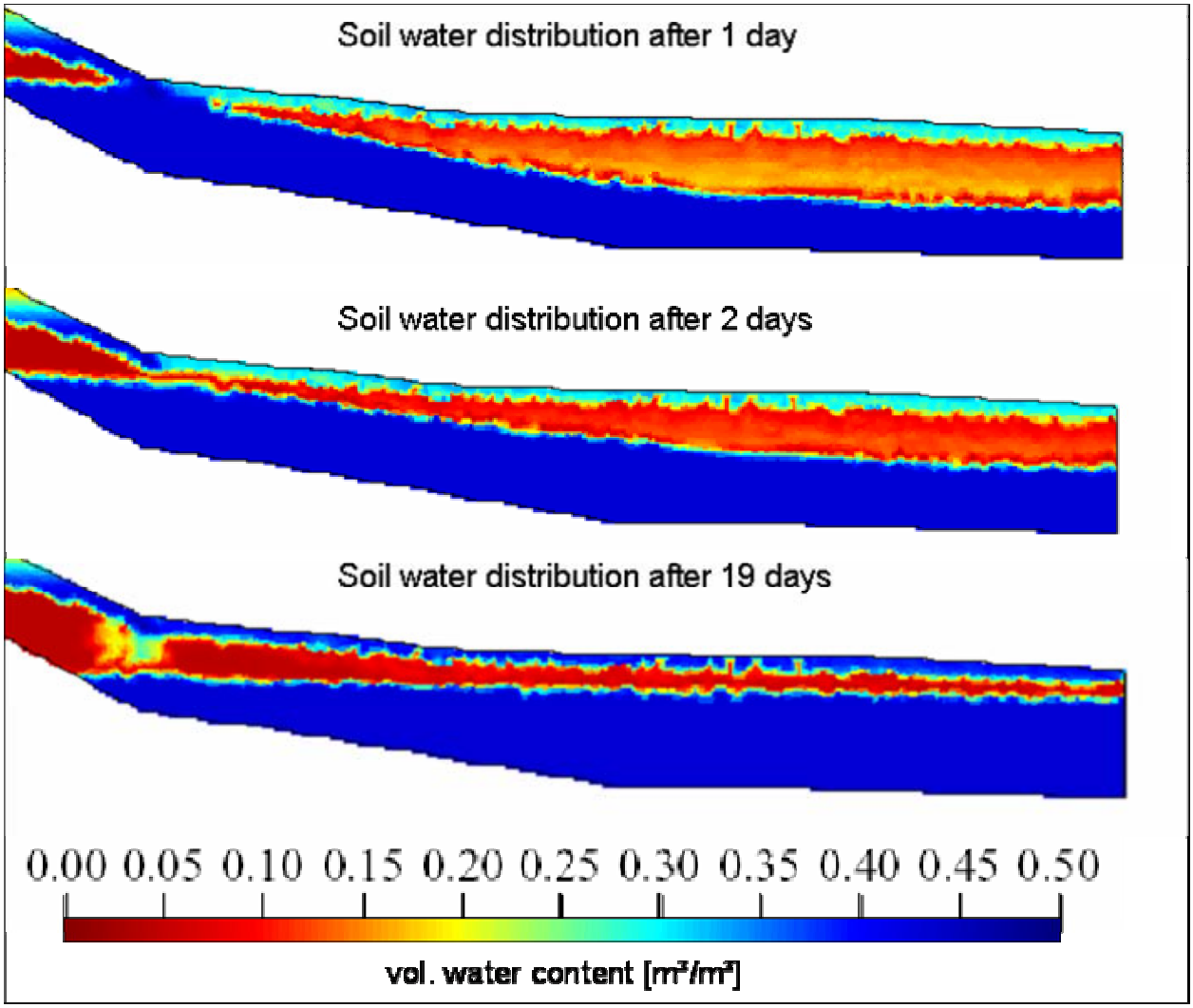

Figure 6-8: Distribution of soil water content at the hillslope profile (with three materials) for three time steps.

The induced precipitation that served to initialise the model created a wave that originates at the hillslope (below the boulder field) and passes within 3 days through the flood plain. At the toe of the boulder field, water accumulates for several days due to the crossover to the less conductive silty surface material. Thereby parts of the water are defected to the surface where it produces constant high soil water contents. At the same location on the test site there is a saturated area and the smallest depth to groundwater occurs (measured at A1). The majority of arriving hillslope water drains to the deep groundwater.

After initialisation of the model the two groundwater levels maintain on there level. Where the dynamic of the perched groundwater is caused by meteorological effects (precipitation and evapotranspiration), the minor fluctuations in the deep groundwater are induced by fast infiltration at the boulder field.

6.2.2 Discussion of model uncertainties

Also with the HYDRUS-2D, it was possible to observe a persistent perched groundwater table. In addition to the 1D-model, the 2D-application could prove that it is possible to create waves origin at the hillslope and passing through the flood plain. However, because of the small gradient and the long passage through the unsaturated porous media the reaction is delayed and smoothed.
The several scenarios carried out for the test site transect could not reproduce the distinct fluctuations that are measured in the deep groundwater well B4b.

Mainly two reasons might be responsible:

- uncertainties of conceptualisation and
- model uncertainties

Major conceptual uncertainties are the assessment of the role of the underlying crystalline bedrock and the unknown flow field of the deep groundwater.

Model uncertainties that arise from constraints in model structure as well as available information on parameters and input data complicate the application of any hydrologic model. CHOW ET AL. (1988) distinguishes three categories of uncertainty in hydrologic modelling:

- Natural uncertainty, which arises from the random variability inherent in hydrologic systems.
- Model uncertainty, which describes how accurately the natural processes are represented by equations in the mathematical model.
- Parameter uncertainties, which are dependent on how accurately the values of model parameters may be determined.

MELCHING (1995) describes a fourth source of model uncertainty:

- Data uncertainties, which include systematic and random errors inherent in the input data.

Natural uncertainties influence all aspects of hydrologic modelling because they affect the input data, model parameters and model structure (MELCHING, 1995). Therefore, natural uncertainty is treated as a part of model, parameter and data uncertainty.
Data uncertainties:
In September a clearly distinguishable discrepancy of simulated and observed values occurred. Thus, the period was regarded in more details and measurements of the soil moisture as well as runoff measurements proved that errors in precipitation gauging are responsible. In general, data uncertainties can be neglected compared to the uncertainties that arise from model and parameter uncertainties.
Parameter uncertainties:

According to spatial dimensions of the test site, it can be assigned to the micro-scale (DYCK & PESCHKE, 1995). The micro-scale is defined as an elemental hydrological unit that can be described with fundamental physical laws and one set of parameters. Nevertheless, it could be shown that the test site is more heterogenic (see chapter 5.3) and the summation of several processes (chapter 6.2.1) is responsible for the system response. For example, the hydraulic conductivity of the surface layer (zone IV) ranges over four magnitudes and was simplified described with only one parameter set. A critical point is also the parameterisation of the boulder field where hypothetical values were assumed. The simulations for soil moisture contents clearly reflected the inability to describe the entire water retention curve of a soil consisting from both very coarse (0,5 m) and fine silty (0,002 mm) material with the van Genuchten parameters.
Uncertainties also arises from the design of the finite element mesh that comprises about 250 m whereas the observed variations are between 0,01 m and 1 m. A compromise of run time and accuracy had to be found. Therefore the mesh density was increased from 2 m to 0,2 m next to the observation points (Figure 6-9).

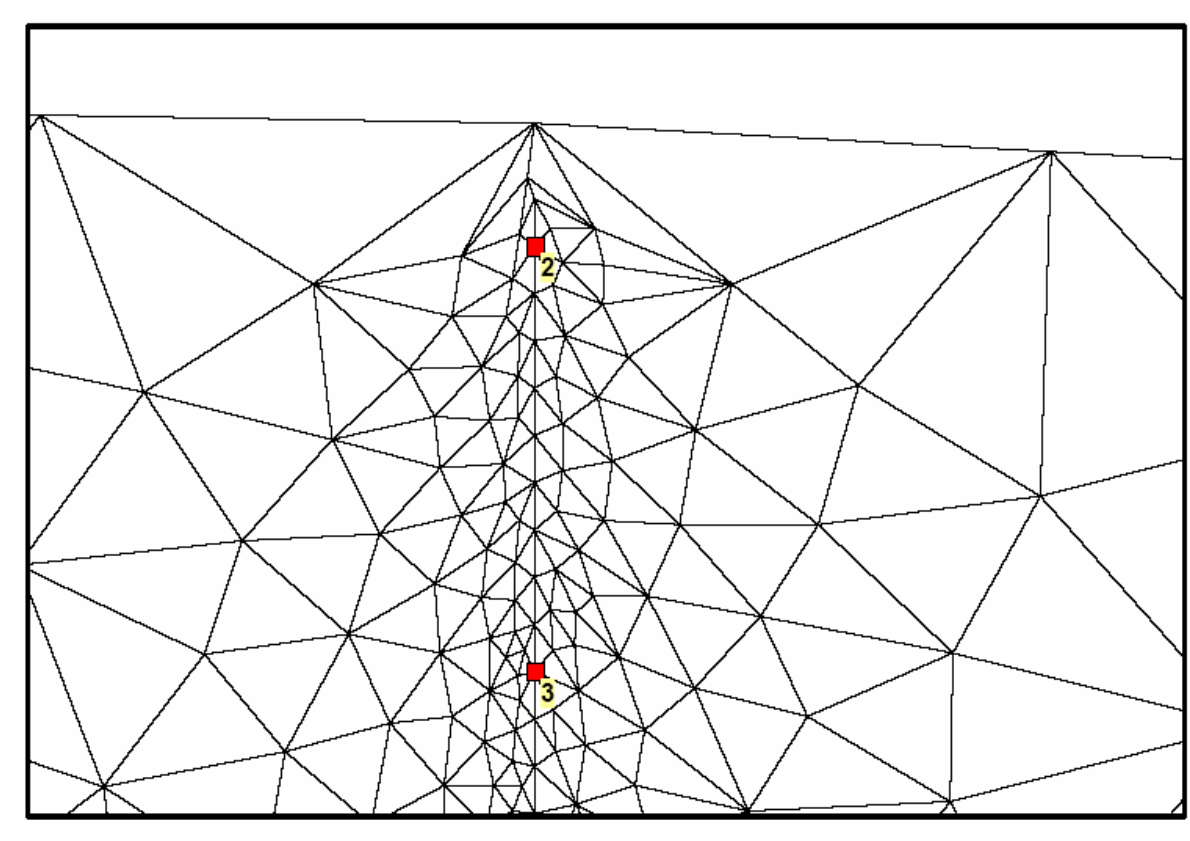

Figure 6-9: Section with higher density of the finite element grid at the location of the groundwater wells B4a and B4b.

Model uncertainties:
The most critical point is probably model structure because the assumption of Darcy flow at the hillslope simplifies natural processes markedly. There are clear evidences of

processes as e.g. lateral macropore flow (e.g. MOSLEY,1982; MCGLYNN ET AL., 2002), pressure wave effects (TORRES ET AL., 1998), transmissivity feedback mechanisms (BISHOP, 1991) and pipe flow (UCHIDA ET AL., 2001) were the assumption of laminar and stationary water movement is not valid.

Limiting for the test site modelling is the lack of a nonequilibrium flow (preferential flow) module for the perched water table and a dual-porosity hydraulic property model (DURNER, 1994) for the underlying crystalline bedrock as applied by HUADE & WILSON (2003) on Mexican bedrock.
There are dual-porosity and dual-permeability models (SIMUNEK ET AL., 2003). Both groups divide the soil into two separate pore domains. While dual-porosity models assume that water in the matrix domain is stagnant, dual-permeability models allow for water flow in both, the macropores and the micro (matrix) pores. Dual-permeability models are frequently used to describe flow and transport in fractured or structured media displaying shrinkage cracks, earthworm channels, root cracks, or heterogeneous soil textures. This extension would probably serve to improve simulation for the soil moisture probes where infiltration of the wetting boundary through the matrix and preferential flow in macropores is evident. In dual-porosity models the water flow is restricted to one flow domain (inter-aggregate pores), while the matrix domain (intra-aggregate pores) retains and stores water, but does not permit convective flow. This mobile-immobile water concept is often used to describe solute transport processes in aggregated porous media (VANDERBORGHT ET AL., 1997).
Crucial for the application at the test site is also the implementation of a kinematic wave approach to simulate water flow in macropores where matric suction is neglectable as probably happens at the boulder field.
Momentary endeavours are made to expand HYDRUS with following new processes:
Nonequilibrium flow and transport (preferential flow):

- dual-porosity approach (mobile-immobile concept)
- dual-permeability approach (two overlapping porous media, one for matrix flow, one for preferential flow) (GERKE & VAN GENUCHTEN, 1993)
- kinematic wave approach for flow in macropores (JARVIS, 1991)
- dual-porosity hydraulic property models (DURNER, 1994)
- Overland flow

It is hard to assess how widespread the observed processes of preferential flow are or to quantify their contribution to runoff generation and groundwater recharge. Therefore, it is necessary to include these processes in model structure in order to determine and quantify their relevance.

6.3 Conclusion

Simulation of soil moisture contents gave clear evidence that rapid fluctuations of the shallow groundwater cannot be explained by passage of infiltrating water through the soil matrix alone. The application for the probes in the unsaturated zone gave better results although the properties of the fine grained material were not reproduced adequately because of the inability of the unsaturated soil model to describe the hydraulic properties of soil material composed of both very fine material (silt) and stones with one set of parameters.
The one-dimensional model approach for the simulation of pressure heads could prove that observed variations for shallow groundwater mainly occur because of infiltration processes. Compared with soil moisture probes the correlation between observed and predicted values is good due to absence of coarse fractions in the upper material at the location of the groundwater well. The initial estimate for the soil hydraulic parameters enables the simulation of a perched water level just because of the discrepancy in hydraulic conductivity. It was found that a difference of one magnitude in hydraulic conductivity between a less permeable layer covering a more permeable is sufficient to create a temporary limited perched water table. Both simulated water tables were positioned in the same altitude as the observed levels.
Increasing the rate of soil drainage in order to increase the dynamic of reactions at the deep observation point was limiting the development of perched groundwater conditions. The simulation of deep groundwater showed smooth and retarded response to precipitation (because water needs to filtrate through a soil block of 2,5 m) which indicates that vertical processes alone are not responsible for the dynamic behaviour of observed piezometric heads in the deep groundwater well B4b.

The 2-D application could prove that it is possible to create waves origin at the hillslope and passing through the flood plain. However, due to the small potential gradient and the long passage through the unsaturated porous media the reaction is delayed and smoothed.
The several scenarios carried out for the test site transect could not reproduce the distinct fluctuations that are measured in the deep groundwater well B4b. Groundwater flow is typically three-dimensional and therefore, a saturated - unsaturated 3-D model would be more appropriate. Nevertheless, HYDRUS-2D allowed to describe qualitatively some observations and to confirm the assumption that accelerated flow occurs at the test site.

7 Hydrological concept

A conceptual model of runoff processes, derived from the observations and model application is schematically presented in Figure 7-1.

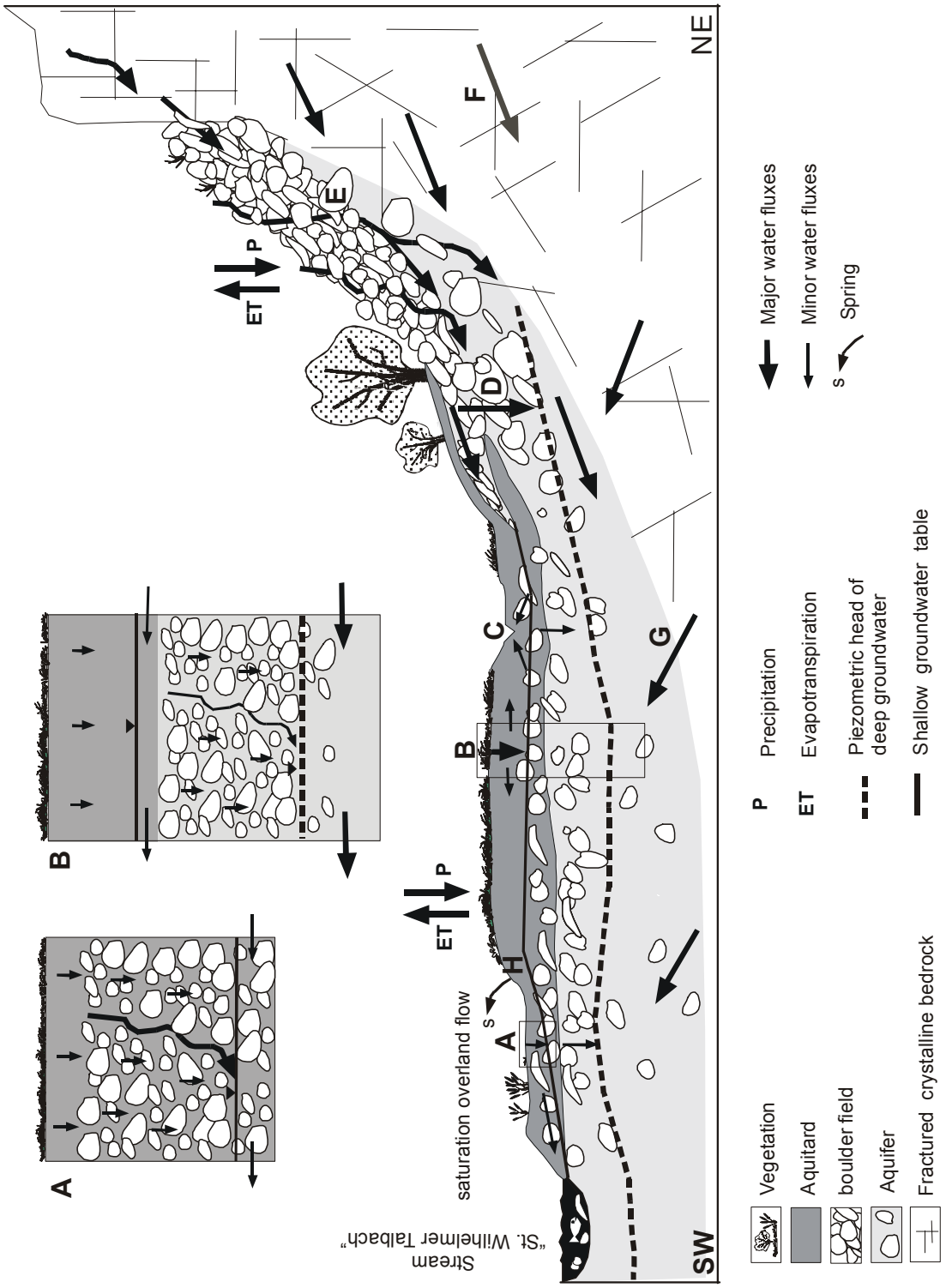

Figure 7-1: Conceptual model of runoff processes at surface / groundwater test site "Hintere Matte" (modified after WENNINGER ET AL., 2004).

The different processes indicated with letters are:

A) Beneath the terrace, closely below the surface, a mixture of coarse material and fine material is evident. The soil composition, beside infiltration allows accelerated preferential flow during wet soil conditions. The variable occurrence of preferential flow depending on antecedent soil moisture status reflects the generally variable nature of macropore flow systems that complicates the finding of appropriate model algorithms (LORENTZ, 2001) In the saturated zone lateral fluxes (perhaps from the nearby saturated area) probably also affect the dynamic of the shallow groundwater table.

B) A perched water table of long persistence is evident at the test site. Its existence is enabled either by an impermeable soil layer or by the measured differences of the hydraulic conductivity between the surface and aquifer material. The fluctuations of the perched water table on the terrace are mainly caused by local infiltration processes. Whereas the rapid and even faster increase of deep groundwater elevation after commencement of rainfall cannot be explained by vertical processes alone. Water is probably transferred to this groundwater body from the hillslope where the boulder field allows faster infiltration than surface material on the terrace but also beneath the terrace, accelerated infiltration might be possible. The fluctuations of the deep groundwater was not be explained by assuming Darcy flow. Whether the transport takes place by piston flow displacement or by gravitational flow in a defined soil pipe system could not be verified within this study. The latter however seems more plausible due to the detection of subsurface pipes by KOCH (2004).

C) The drainage trench receives its water from a bedrock spring at the toe of the hillslope. This water is characterised by high electrical conductivity and low temperatures throughout the year. During storm events, shallow groundwater is exfiltrating into the drainage trench while in dry weather conditions marginal amounts of drainage trench water infiltrate.

D) At the toe of the boulder field, the water fluxes are deflected both to the surface where it feeds a saturated area and to the deep groundwater. At the border between the boulder field and surface material (with less hydraulic conductivity), water accumulates at the downhill end of the boulder field for several days.

E) Rapid lateral flow occurs inside the boulder field. The hydraulic properties of the boulder field are probably not adequately represented by the assumption of the Richard’s equation. The impulses of fast throughflow from the hillslope probably induce the observed groundwater dynamic at floodplain.

F) Deep groundwater from the bedrock converges at the valley bottom and feeds beside the main aquifer surface waters (e.g. the drainage trench, saturated area). The properties and relevance of this underlying system is hard to access due to the fractured character of the crystalline bedrock.

G) The flow direction of shallow groundwater is not from the hillslope toward the stream but almost parallel to the stream. Because ERT measurement did not show distinct connections between the deep aquifer and the Talbach, the aquifer fluxes are probably also directed towards the valley entrance with only local linkages to the Talbach.

H) Hydrochemistry analysis clearly proved that beside water from the perched groundwater table also deep groundwater influences the saturated area. In the same way, there might also be local pathways for surface and shallow groundwater to the deep groundwater. There is evidence (hydrochemistry) of local weak points between the separation of perched and deep groundwater however, these are probably too small for direct visualisation with ERT. Nevertheless, KOCH (2004) detected pipe like subsurface structures of greater dimensions (3 m to 5 m) parallel to the Talbach.

Figure 7-1 provides an overview of the different processes measured at the test site. With focus on flood-event their importance and contribution to rapid hydrograph reactions in the stream needs to be discussed.
Early attempts to explain quickflow mainly by HORTON (1933, 1945) and HEWLETT (1961) almost exclusively concentrated on the overland flow path. Later work proved that throughflow (chapter 1.2) and even groundwater flow (SKLASH & FARVOLDEN, 1979; O'BRIEN, 1977; ZALTSBERG, 1987) also play an important role for fast runoff components. The subdivision into overland-, through- and groundwater flow is mainly defined by subsurface structure and material.
A shallow perched groundwater table is evident at the test site. Its existence is either possible due to an impermeable layer or the rate of vertical percolation is reduced because usually hydraulic gradient is reduced as the flow path of the percolating water lengthens WARD & ROBINSON (2000). This perched water table plays a decisive role for the runoff generation at the test site because it leads to faster surface saturation and saturation overland flow. The shallow groundwater and saturated areas are drained by a dense network of drainage channels (developed due to shallow groundwater) that transport the water from the shallow groundwater and saturation overland flow to the Talbach.
In addition, lateral movement due to the layered character of the soil with movement in biotic macropores and macrofissures that allow preferential flow to the saturated zone may be responsible for rapid throughflow during storm events, when the relevance of

laminar movement in the soil matrix gets less. At riparian zones of saturation, the transport to the stream is probably also diffuse. The saturated areas occur at zones of flow convergence. Typical zones of flow convergence at the test site are the riparian zone and slope concavity where, assuming uniform hydraulic conductivity, water will enter from upslope areas more rapidly than it can leave downslope due to a smaller hydraulic gradient.

Usually a saturated soil layer reduces the rate of groundwater recharge because water is laterally transferred to the stream. This statement is supported by hydrochemistry and geoelectric measurements at the location of B4b that show only marginal influence of perched groundwater in the main aquifer. Additionally, model results indicated that with increased vertical percolation the existence of perched groundwater is limited. Another indication is that during recession in the shallow groundwater the deep groundwater is not gaining water from percolation.

Nevertheless, the groundwater has a faster and more pronounced response to rainfall which shows evidence of a rapid component that is transferred though the flood plain. Thereby it is still unsure how these impulses reach the groundwater table that fast and how the water is transported. Most probable is a turbulent transport because model results assuming laminar flow conditions failed to reproduce the distinct dynamic reactions to rainfall.

Possible mechanisms for fast reactions are piston flow displacement or flow in pipes of larger dimensions (formed by hydraulic and hydrological processes according to JONES, 1981) as the biotic voids that by some hydrologists are regarded as pseudo-pipes.

The high velocity of conducted macropore subsurface flow suggests that the arriving water will be event-water; whereas it was proved that, the influence of event-water in the deep groundwater is marginal. However, macropore flow and occurrence of pre-event water might not be a disagreement as tracer experiments in a variety of environments confirm that pre-event water dominates the storm hydrograph even in areas where the existence of macropores is well-established (SKLASH ET AL., 1986; PEARCE ET AL., 1986 and MCDONNELL, 1990). Figure 7-2 shows a conceptual model purposed by MCDONNELL (1990) that explain that macropore flow and the occurrence of pre-event water are compatible. Although the reactions of macropores in general are very inconsistent, depending on the water status of the soil structure system.

The multiple ERT measurements showed evidence of such a pipe network that is directed towards the valley entrance and that does not show a direct linkage to the stream as assumed in the idea of the steam bank concept where exchange between groundwater and stream water in both direction is possible depending on the actual flow gradient. Inside these structures, the flow is directed straight down the valley and probably stays under the surface until a natural barrier is reached.

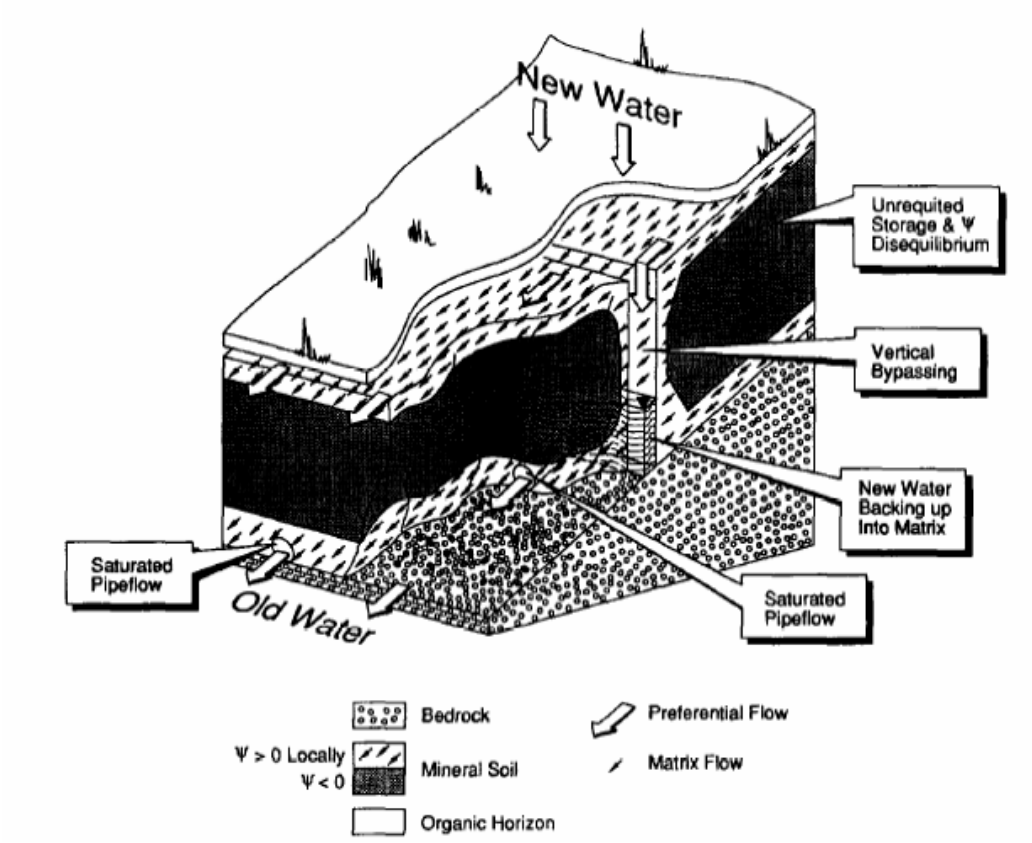

Figure 7-2: A conceptual model of runoff production combining the idea of unrequited storage with disequilibrium in producing preferential flow of fully mixed (old) water (MCDONNELL, 1990).

As the hydraulic conductivity of the main aquifer is better than within the surface layer of throughflow, it is likely that the relevance of groundwater for rapid components of the storm hydrograph is more important.

KOCH (2004) purposed the idea that the perched stream above the main groundwater body and the possible existence of a subsurface drainage system are a more efficient water transport system than the stream itself. While this statement needs further quantification of the single components, it was clearly verified that the groundwater body at the test site play an important role for the generation of fast runoff components.

Whereas the importance of rapid groundwater components in flat terrains due to groundwater ridge is well known, the general idea of processes in steep sloping terrain of the headwater is that throughflow dominates subsurface runoff. While percolation to the groundwater is delayed as water in depth moves slowly, the outflow of groundwater into the stream channel may be only responsible for the long-term component of total runoff.

At the test site, one can find a constellation where as well saturation overland flow throughflow and especially groundwater may contribute to stormflow.

8 Concluding remarks and outlook

In this section the potential of the applied methods and the main results are discussed and finally, suggestions for additional investigations are proposed.

The concrete objective of this study was to implement the knowledge of the three previous conducted diploma theses in the soil water model HYDRUS in order to simulate water and solute transport of the groundwater for several weeks with the focus on flood events.

In the third month of this study, the drilling of the two deeper groundwater observation wells confirmed the presumption (raised from the ERT measurements of KOCH (2004), that the shallow groundwater stations do no reach the main aquifer.

This new development indicates the limitations of the previous conceptualisation and necessity of additional experimental work. Due to the new situation, it seemed sensible to shift the former emphasis of mainly model application more towards extended experimental investigations.

The most remarkable observation during this study was that the existence of perched groundwater does not impede fast reactions of deeper groundwater. The deep groundwater probably has a great contribution to fast reactions of flood hydrographs due to better hydraulic conductivity of the main groundwater body.

The hydrochemistry analysis allowed a classification of the different waters components on the test site. Also, it was found that erosion in conduit material of the well increases electrical conductivity (that is approximately 60 µS/cm for the shallow groundwater) by up to 300 percent. Therefore, extensive pumping is necessary before a representative sample can be collected. Especially in summer, this is problematic when the shallow groundwater wells sometimes run dry.

As the passage through the unsaturated zone is decisive for subsurface flow, soil moisture probes were installed for calibration of the unsaturated zone. During the installation and analysis of the soil moisture data the main problem of the model application on the test site became obvious. Due to the high content of coarse material water flows on preferential path.

In order to estimate the soil hydraulic properties infiltration and pumping tests were conducted. An important perception was that the filter device and / or the compacted soil in close vicinity to the groundwater well noticeable reduce the transmissibility, which leads to a delayed exchange of hydrochemistry, while changes of piezometric heads are transferred unhindered. This makes the interpretation of time series of temperature and electrical conductivity measured inside the groundwater well difficult. During the groundwater sampling, the aspects of erosion and delayed exchange have to be considered to prevent significant errors.

ERT measurement showed that the perched groundwater is evident all over the test site but with probably weak points at the saturated area. It could be shown that the combination of a drilling with ERT is necessary for proper interpretation. In general, ERT proved a powerful tool that allows to regionalise the point information of the drilling to the test site. The derived resistivities for the different layers probably provide good reference values for other parts of the catchment with comparable geology. It remains unknown if an impermeable layer is responsible for the existence of the perched groundwater table but it seems plausible as the Talbach also seems to be perched (KOCH, 2004).
The model was used as a hypothesis-testing tool. It was possible to prove that the dynamic of the shallow groundwater mainly is explained by local infiltration processes while the dynamic of the deep groundwater cannot be explained by vertical water movement. Fast throughflow at the boulder field might induce the dynamic observed in the deep groundwater. Constraints in model structure as well as in the available information on parameters and input data complicate the application of any hydrologic model. Although there are still model uncertainties the application of HYDRUS-2D verified that water does not move in the manner predicted by Richard's equation. Water movement may be dominated by flow through macropores rather than bulk flow through the microstructural interstices of soil matrix.

Nevertheless, although the hydrological perception of the research site advanced greatly new questions also emerged:

- How are the two water tables separated / connected?
- Is the deep groundwater body confined?
- From where do the fast variations of the deep groundwater originate?
- It this impulse transferred by piston flow or by a macropore system?
- In which way is the deep groundwater linked to the stream?

The remarkable situation at the test site justifies further investigations, e.g. the installation of additional deep groundwater station (s) which would provide information about the gradient (three-dimensional flow field) of the deep groundwater which is necessary to asses the connection to the stream on one side and for model application on the other side. However, the drilling is very problematic because of the high content of coarse material. The soil samples of the drilling core should be analysed more precisely than with feel probe in order to identify possible impermeable layers. Additional groundwater wells would also allow the conduction of tracer experiments in the deep groundwater simultaneously sampled and observed with ERT. The combination of ERT and tracer methods provides several attractive possibilities.

Beside further drilling it would also be reasonable to extend the observation period for the B4a/b and the soil moisture probes to allow further statistical analysis and to observe the behaviour of the groundwater for the different statuses of subsurface storages.
The sampling of deep groundwater with higher temporal resolution during an event in order to estimate the fractions of event and pre-event water would also be interesting. This might provide additional information about the development of the distinct fluctuations in the deep groundwater and whether this process might be responsible for the fraction of pre-event water measured during flood events at the Brugga basin outlet.
Nevertheless, this sampling is only useful if sufficient pumping is applied due to the complications mentioned above.
As the electrical conductivity and the temperature of water components influenced by event water and deep groundwater are significantly different, a temperature and conductivity profile of the St. Wilhelmer Talbach could probably verify the local character of effluent groundwater. The zones where a connection between deep groundwater and stream exists might be further investigated with ERT.
Endeavours of SIMUNEK ET AL. (2003) to incorporate nonequilibrium flow into HYDRUS-2D and the application of the new code could perhaps allow quantifying the relevance of the single runoff components.

This study could greatly improve the understanding of the processes occurring on the test site and clearly highlight the importance of rapid groundwater components.
The most remarkable observation during this study was that the occurrence of perched groundwater does not prohibit fast reactions of deeper groundwater.
It was also verified that models basing on the Darcy flow equation would underestimate flood events. In addition, the lack of models to account for preferential flow water may also have consequences for other hydrological purposes:

- The bypass of water and reduced wetting of the matrix will be decisive for irrigation questions and
- estimation of groundwater recharge.
- Since macropore flow does not pass the natural filter of the soil matrix it might be a problem for groundwater contamination due to leaching from nitrates and other constituents from agricultural land.

The results of this study indicate the need for a two-domain concept to be incorporated into simulation models that would help to improve predictions concerning different hydrological purposes as well as a quantification of these accelerated flow components.

It was showed that it is necessary to combine experimental work and model application in order to reciprocally complement one another.

The several applied methodologies improved the understanding of runoff generation process at the hillslope test site and identified the importance of groundwater components for generation of stormflow hydrographs.

References

AG BODEN (1996). *Bodenkundliche Kartieranleitung*, 4. Edition, Publisher Bundesanstalt für Geowissenschaften und Rohstoffe und den Geologischen Landesämtern in der Bundesrepublik Deutschland, Hannover.

ALLEN ET AL (1998). *Crop evapotranspiration - Guidelines for computing crop water requirements*, Food and Agriculture Organisation of United Nations; Irrigation and drainage paper 56, Rome, ISBN 92-5-104219-5.

ANDERSON, M. G. & T. P. BURT (1990). *Process Studies in Hillslope Hydrology,* Wiley, Chichester, UK. 539 pp.

BATTLE-AGUILAR, J., Y. COQUET, P. TUCHOLKA, P. VACHIER (2004). *Axisymetrical water infiltration in soil imaged by non-invasive electrical resistivimetry*, Geophysical Research Abstracts, Vol. 6, 01343 (unpublished), http://www.cosis.net/abstracts/EGU04/01343/EGU04-J-01343.pdf, [Access date: 02/01/05].

BAUMGARTNER, A. & H. J. LIEBSCHER (1996). *Allgemeine Hydrologie – quantitative Hydrologie*, 2. Edition, Gebrüder Borntraeger, Berlin.

BEVEN, K. J. (1989). *Interflow In Unsaturated Flow in Hydrological Modelling*, Morel-Seytoux H. J. (ed). Kluwer Academic Publishers: Dordrecht, Boston, London.

BISHOP, K. (1991). *Episodic increases in stream acidity, catchment flow pathways and hydrograph separation*, PhD thesis, University of Cambridge, Cambridge, UK.

BONELL, M. (1998). *Selected challenges in runoff generation research in forests from the hillslope to headwater drainage basin scale*, Journal of American Water Resources Association 34(4): 765-785.

BERCKHEMER, H. (1997). *Grundlagen der Geophysik*, Wissenschaftliche Buchgesellschaft, Darmstadt. ISBN 3-354-13696-9.

BROOKS, R. H. & A. T. COREY (1966). *Properties of porous media affecting fluid flow*, J. Irrig. Drainage Div., ASCE Proc. 72 (IR2): 61-88.

CAMPBELL, C. S. (1997). *Calibrating ECH$_2$O Soil Moisture Probes*, http://www.decagon.com/appnotes/echocal.pdf [Access date 03/01/05].

CARDIMONA, S. (2002). *Electrical resistivity techniques for subsurface investigation,* Department of Geology and Geophysics, University of Missouri-Rolla, Rolla, MO, U.S.A..

CARSEL, R. & R. PARISH (1988). *Developing joint probability distributions of soil water retention characteristics*, Water Resources Research., 24(5): 755-769.

CHOW, V. T., D.R. MAIDMENT & L. W. MAYS (1988). *Applied Hydrology*, McGraw-Hill, New York.

DAMIATA, B. (2001). *Assessment of the Skagafjörjur Archaeological Settlement Survey*, Cotsen Institute of Archaeology, UCLA, CA, U.S.A.. http://sass.ioa.ucla.edu /2001.

DIN (Editor) (1981). *Deutsche Einheitsverfahren zur Wasser-, Abwasser- und Schlamm-Untersuchung*, Wiley-VCH, Weinheim.

DOERNER, J. & HORN R. (2004). *Water flow in soilslopes under ecological and conventional management,* Christian Albrechts University Kiel Germany, http://www.bodenkunde.uni-freiburg.de/eurosoil/symposia/prg_sym13.htm [Access date: 03/01/2005].

DURNER, W. (1994). *Hydraulic conductivity estimation for soil with heterogeneous pore structure,* Water Resources Research., 30(2): 211-224.

DYCK, S. & G. PESCHKE (1995). *Grundlagen der Hydrologie*, Verlag für Bauwesen, Berlin.

GLA (Editor) (1981). *Erläuterungen zur geologischen Karte von Freiburg im Breisgau und Umgebung 1:50000*, Landesvermessungsamt Baden-Württemberg, Stuttgart.

GERKE, H. H. & M. T. VAN GENUCHTEN (1993). *A dual-porosity model for simulating the preferential movement of water and solute in structured porous media*, Water Resource Research 29: 305-319.

GEYER, O.F. & M.P. GWINNER (1991). *Geologie von Baden – Württemberg*, Schweizerbartsche Verlagsbuchhandlung; Stuttgart, 482 pp.

HÄDRICH F., STAHR K. (1997). *Die Böden in der Umgebung von Freiburg im Breisgau*, In Freiburger Geographische Hefte, Mäckel R, Metz B (eds). Selbstverlag des Inst. für Physische Geographie der Universität Freiburg i. Br.: Freiburg i. Br.

HEWLETT, J. D. (1961). *Watershed management*, in Report for 1961 Southeastern Forest experiment Station, US Forest Service, Ashville, N.C.

HORTON, R. E. (1933). *The role of infiltration in the hydrological cycle,* Trans. Amer. Geophys. Union 14: 446–460.

HORTON, R. E. (1945). *Erosional development of streams and their drainage basins: Hydrological approach to quantitative morphology*, Bull. Geol. Soc. Amer., 56: 275–370.

HÖLTING, B. (1996). *Hydrogeologie*, 5.Edition, Enke Verlag, Stuttgart.

HUADE, G., J. L. WILSON (2003). *Variably Saturated Water Flow Across Soil-Bedrock Interface on Conceptual Hillslopes*, Earth and Environmental Science, New Mexico Institute of Mining and Technology.

JARVIS, N. J. (1991). *MACRO- a model of water movement and solute transport in macroporous soils*, Reports and Dissertations 9, Dept. Sol., Swedish Univ. Agric., Uppsala, 58pp.

JONES, J. A. A. (1981). *The nature of soil piping-a review of research*, BGRG Research Monograph 2, GeoBooks, Norwich, 301 pp.

KEMNA ET AL. (2002). *Imaging and characterisation o subsurface solute transport using electrical resisitivity tomography (ERT) and equivalent transport models,* Journal of Hydrology, 267: 125-146. Elsevier Science Publishers B.V, Amsterdam.

KNÖDEL ET AL. (1997). *Handbuch zur Erkundung des Untergrundes von Deponien und Altlasten.* BGR, Band 3, Geophysik.SpringerVerlag, Berlin, Heidelberg, NY.

KOCH M. K. (2004). *Application of electrical resistivity tomography (ERT) together with tracer data to identify hydrological process areas at a surface / groundwater test site, St. Wilhelm, Black Forest Mountains, Germany*, Diploma thesis, University Freiburg i. Br., Institute of Hydrology, Freiburg i.Br., Germany (unpublished).

LINDENLAUB, M. (1998): *Abflusskomponenten und Herkunftsräume im Einzugsgebiet der Brugga*, PhD thesis, Institut für Hydrologie, University Freiburg i. Br.

LOKE, M. H. (2000). *Electrical imaging surveys for environmental and engineering studies - A practical guide to 2-D and 3-D surveys,* http://www.geoelctrical.com.

LORENTZ, S. (2001). *Hydrological Systems Modelling Research Programme: Hydrological Processes,* WRC Report No.637/1/01.

MCDONNELL, J. J. (1990). A *rationale for old water discharge through macropores in a steep, humid catchment*, Water Resources Research 26: 2821–2832.

MCGLYNN, B. L., J. J. MCDONNELL, D. D. BRAMMER (2002). *A review of the evolving perceptual model of hillslope flow paths at the Maimai catchments*, New Zealand. Journal of Hydrology 257: 1–26.

MEHLHORN J. (1998). *Tracerhydrologische Ansätze in der Niederschlags-Abfluss-Modellierung,* PhD thesis, University Freiburg, Freiburg.

MELCHING, C. S. (1995). *Reliability estimation*, In: V.P. Singh (Ed.), *Computer models of watershed hydrology,* Water Resources Publications, Highlands Ranch, CO, 69-118.

MEYER DE STADELHOFEN, C. (1994). *Anwendung geophysikalischer Methoden in der Hydrogeologie,* Springer-Verlag Berlin, Heidelberg, New York. ISBN 3-540-56042-4.

MILLER, E. E. & R. D. MILLER (1956) *Physical theory for capillary flow penomena*, J. Appl. Phys. 27: 324-332.

MUALEM, Y. (1976). *A new model for predicting the hydraulic conductivity of unsaturated porous media*, Water Resources Research., 12(3): 513-522.

MOSLEY, M. P. (1982). *Subsurface flow velocities through selected forest soils*, south island, *New Zealand*. Journal of Hydrology 55: 65–92.

O'BRIEN, A. L. (1977). *Hydrology of two small wetland basins in eastern Massachusetts*, Water research Bull., 13: 325-40.

PEARCE, A. J., M. K. STEWART & M. G. SKLASH (1986). *Storm runoff generation in humid headwater catchments, I. Where does the water coe from?* WRR, 22:1263-72.

REKLIP (1995). *Klimaatlas Oberrhein Mitte-Süd, Atlas Climatique du Fossé Rhénana Méridional*, Zürich-Offenbach-Strasbourg.

RICHTER, W. & W. LILLICH (1975). *Abriss der Hydrogeologie*, Schweizerbart Verlag, Stuttgart.

SCHACHTSCHABEL, P., ET AL. (2002). *Lehrbuch der Bodenkunde*, Spektrum Akademischer Verlag, Heidelberg, Berlin.

SCHEIDLER, S. (2002). *Experimentelle Untersuchung zur Grundwasserdynamik im Hang-/Talaquifer-System des St.Wilhelmer Talbachs (Südschwarzwald),* Diploma thesis, University Freiburg i. Br., Institute of Hydrology, Freiburg i.Br., Germany (unpublished).

SCHEYTT, T & F. HENGELHAUPT (2001). *Auffüllversuche in der Wassergesättigten und ungesättigten Zone – ein Vergleich unterschiedlicher Verfahren*, Grundwasser, booklet 2 Juni 2001, Publisher: Fachsektion Hydrogeologie in der deutschen Geologischen Gesellschaft, Springer Verlag, Heidelberg

SHEVNIN V. A. & MODIN I. N., (2003*). IPI2win – 1D interpretation of VES profile*, Version 3.0.1, 10/01/2003,Geological Faculty, Department of Geophysics, Moscow State University, http://geophys.geol.msu.ru/ipi2win.htm [Access date 02/01/05].

SIMUNEK, J., M. SEJNA, M. T. VAN GENUCHTEN (1998). *The HYDRUS-2D Software Package for Simulating the Two-Dimensional Movement of Water, Heat and Multiple Solutes in Variably-Saturated Media,* Version 2.0, U.S. Salinity Laboratory, USDA, ARS, Riverside, California.

SIMUNEK, J.; N. JARVIS, M. T. VAN GENUCHTEN & A. GÄRDENÄS (2003). *Review and comparison of models for describing non-equilibrium and preferential flow and transport in the vadose zone,* Journal of Hydrology, 272: 14-35.

SKLASH, M.G. & FARVOLDEN R. N. (1979). *The role of groundwater in storm runoff*, Journal of Hydrology 43: 45–65.

SKLASH, M.G., A. J. PEARCE, M. K. STEWART (1986). *Storm runoff generation in humid headwater catchments, II. A case study of hillslope and low order stream response,* WRR, 22:1273-82.

SRI NIWAS & SINGHAL (1985). *Aquifer transmissivity of porous media from resistivity data,* Journal of Hydrology, 82: 143-153. Elsevier Science Publishers B.V, Amsterdam.

STOBER, I. (1995). *Die Wasserführung des kristallinen Grundgebirges*, Ferdinand Enke Verlag, Stuttgart.

TORRES, R., W. E. DIETRICH, D. R. MONTGOMERY, S. P. ANDERSON, K. LOAGUE (1998). *Unsaturated zone processes and the hydrologic response of a steep, unchanneled catchment*, Water Resources Research 34: 1865–1879.

UCHIDA T., K. KOSUGI, T. MIZUYAMA (2001). *Effects of pipeflow on hydrological process and its relation to landslide: a review of pipeflow studies in forested headwater catchments,* Hydrological Processes, 15: 2151-2174.

UHLENBROOK, S. (1999). *Untersuchung und Modellierung der Abflussbildung in einem mesoskaligen Einzugsgebiet* (Investigating and modelling of the runoff generation in a mesoscaled catchment; in German), Freiburger Schriften zur Hydrologie, Band 10, Institute of Hydrology, University of Freiburg, Germany.

UHLENBROOK, S., M. FREY , CH. LEIBUNDGUT, P. MALOSZEWSKI (2002). *Residence time based hydrograph separations in a meso-scale mountainous basin at event and seasonal time scales*, Water Resources Research 38(6): 1–14.

VANDERBORGHT, J., D. MALLANTS, M. VANCLOOSTER & J. FEYEN (1997). *Parameter uncertainty in the mobile immobile solute transport model,* Journal of Hydrology, 190(1): 75-101.

VAN GENUCHTEN, M T., F. J. LEIJ & S. R. YATES (1991). *The RETC Code for Quantifying the Hydraulic Functions of Unsaturated Soils*, Version 6.0. US Salinity Laboratory, USDA, ARS. Riverside, California.

VOGELSANG, D. (1993). *Geophysik an Altlasten – Leitfaden für Ingenieure und Naturwissenschaftler und Juristen*. Springer-Verlag Berlin, Heidelberg, NY.

VOGEL, T. & M. CISLEROVA (1988). *On the reliability of unsaturated hydraulic conductivity calculated from soil moisture retention curve*, Transport in porous Media.3: 1-15.

WARD, R. C., M. ROBINSON (2000). *Principles of Hydrology*, McGraw-Hill Publishing Company (UK), ISBN 0077095022.

WENNINGER, J. (2002). *Experimentelle Untersuchung zur Dynamik von Hanggrundwasser und dessen Übertritt in die Talaue und den Vorfluter im Bruggaeinzugsgebiet* (Experimental investigation of hillslope groundwater and its flow into a floodplain and the channel at the Brugga basin; in Germany), Diploma thesis, University Freiburg i. Br., Institute of Hydrology, Freiburg i.Br., Germany (unpublished).

WENNINGER, J., S. UHLENBROOK, N. TILCH & CH. LEIBUNDGUT (2004). *Experimental evidence of fast groundwater responses in a hillslope/floodplain area in the Black Forest Mountains, Germany,* Hydrological Processes. 18: 3305–3322.

WHITE, P. (1988). Measurement *of groundwater parameters using salt water injection and surface resistivity*, Ground Water Vol. 26, No.2: 179-186.

ZALTSBERG, E. (1987). *Evaluation and forecasting of groundwater runoff in a small watershed in Manitoba*, Hydrological Sciences Journal 32: 69-84.

Appendix

Well	Elevation a.s.l.
A1	801,48 m
A2	798,75 m
A3	797,88 m
A4	797,74 m
B1	801,91 m
B2	797,72 m
B3	796,82 m
B4	797,23 m
B5	795,04 m
B6	794,79 m

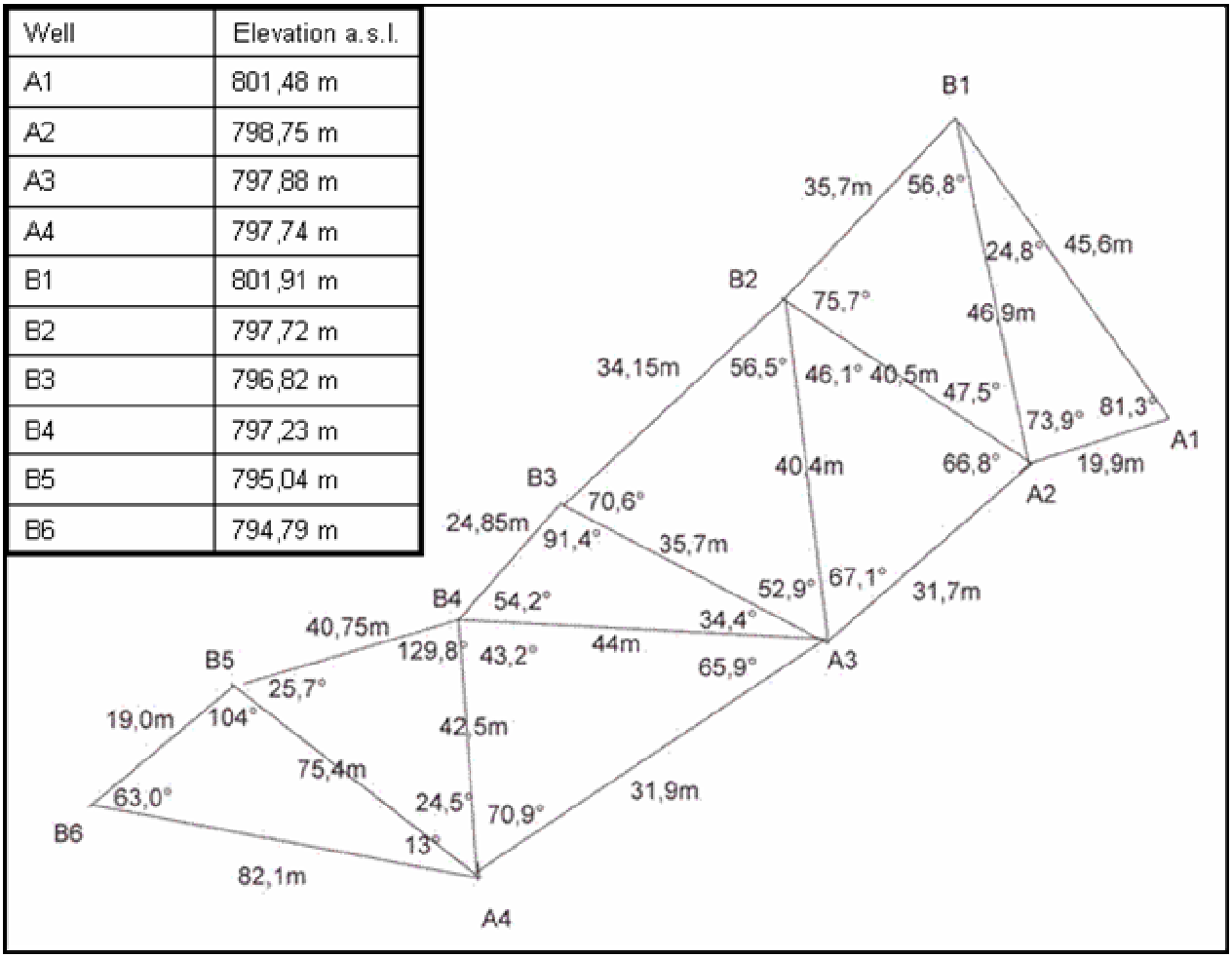

A 1: View of the location of the shallow groundwater wells (elevation, distances and angle).

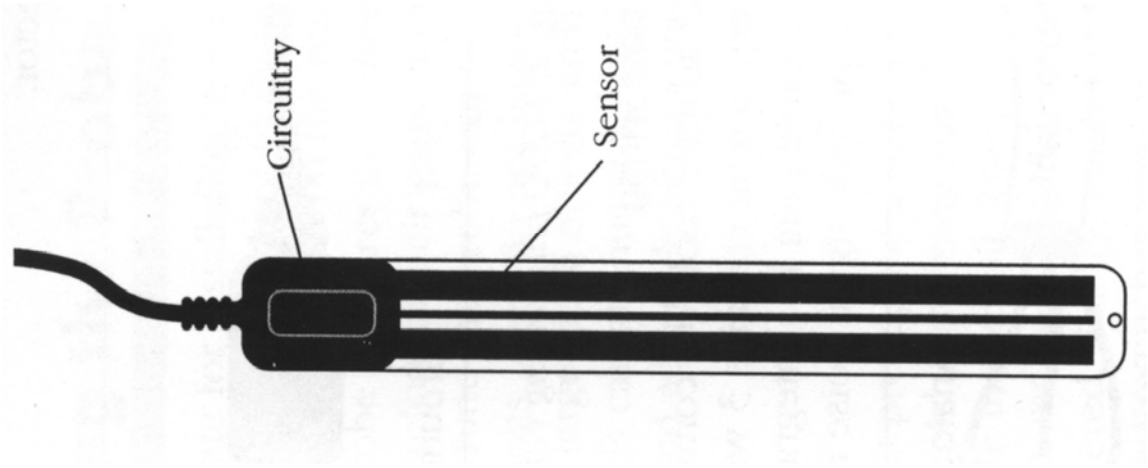

A 2: Schematically display of the ECH$_2$O soil moisture probe.

SYSCAL Kid *Switch-24*

MAJOR BENEFITS

- Attractive output parameters:
  - 200 V maximum voltage,
  - 25 W maximum power,
  - 500 mA maximum current
- Automatic fixing of the output voltage in relation with the level of the measured signal.
- Accuracy on resistivity: 1%.
- Quality control of the measurement through standard deviation and number of stacks.
- Display of measured voltage, intensity of current, apparent resistivity, and self potential.
- Serial link for transfer to PC.

ELECTRODE STRING

Made of heavy duty cable, the 12 take-out string cables are available with standard 1 or 3 meters electrode spacings. The 3 meters version is 40 m long and weights 2.5 kg. Other configuration can be made on request.

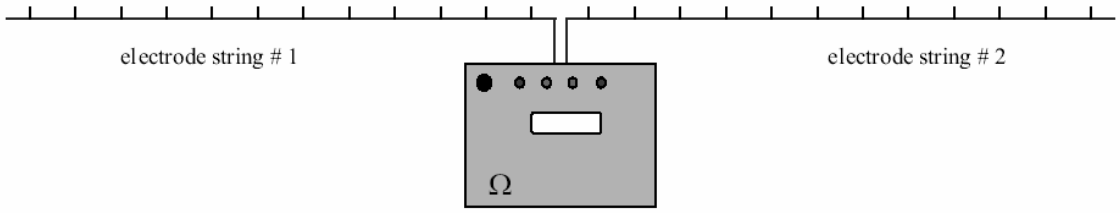

Supported arrays: pole-pole, pole-dipole, dipole-dipole and Wenner profiling

GENERAL SPECIFICATIONS

specifications subject to change

- LCD display: 4 lines of 20 characters
- Keypad: 6 functions keys
- Operating temperature range: -10 to +50 °C
- Internal rechargeable battery: 12V, 6.5 Ah with autonomy of 3000 readings typical.
- Internal memory for 1400 stations with full readings: self-potential, voltage, current, resistivity
- Dimensions: 23 x 18 x 23 cm
- Weight: 4.8 kg

TRANSMITTER

- Automatic current setting
- Output voltage: up to 200 V
- Output current: up to 500 mA
- Output power: up to 25 W
- Optional external 12V battery input
- Cycle time: 0.5, 1 or 2 s

RECEIVER

- Resistivity computation
- Automatic ranging
- SP compensation including linear drift
- Digital stacking for noise reduction
- Input voltage: protection up to 200 V
  range from - 2.5 V to +2.5 V
- Input impedance: 22 MΩ
- Resistivity range: 10^{-3} to 10^{+5} Ω.m
- Resistivity precision: 1 % typical

IRIS Instruments

IRIS Instruments - 1 avenue Buffon, B.P. 6007, 45060 Orléans Cedex 2, France
Phone: + 33 (0) 2 38 63 81 00 - Fax: + 33 (0) 2 38 63 81 82 - E-mail: irisins@attglobal.net
Web site: www.iris-instruments.com

A 3: Technical data sheet of the electrical resistivity measuring device used in the study.

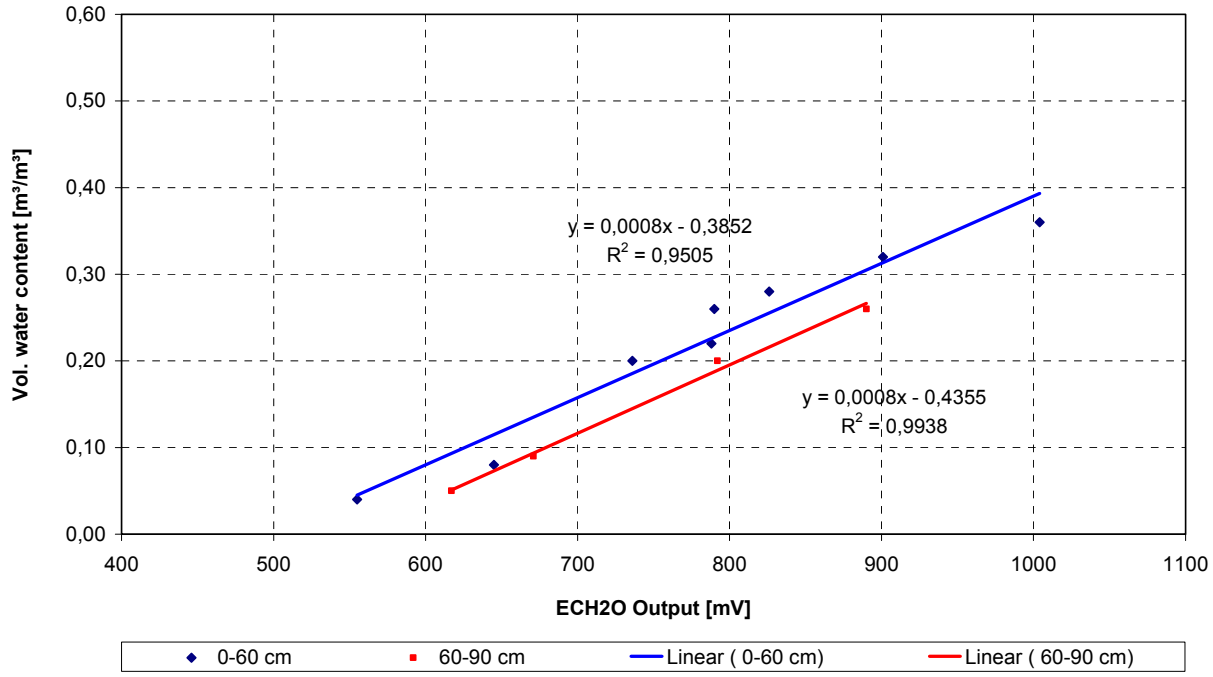

A 4: Soil moisture calibration curves (for the silty and sandy horizon).

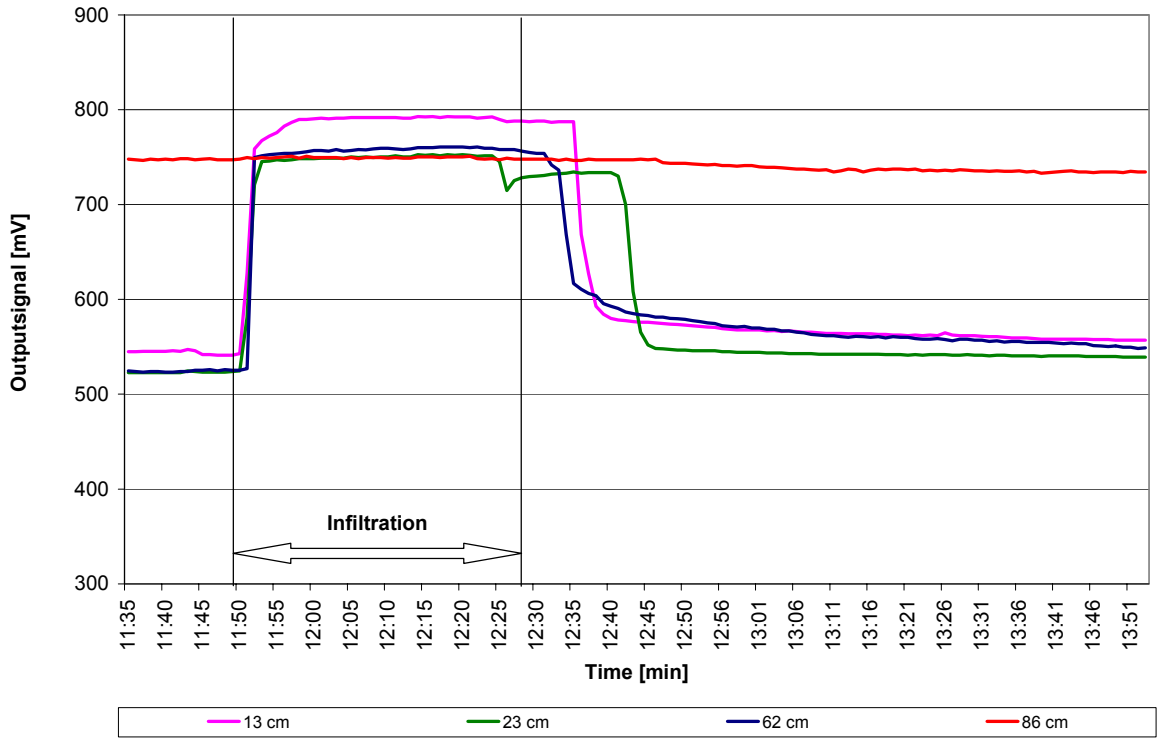

A 5: Measured signal for saturated soil moisture conditions at the test site.

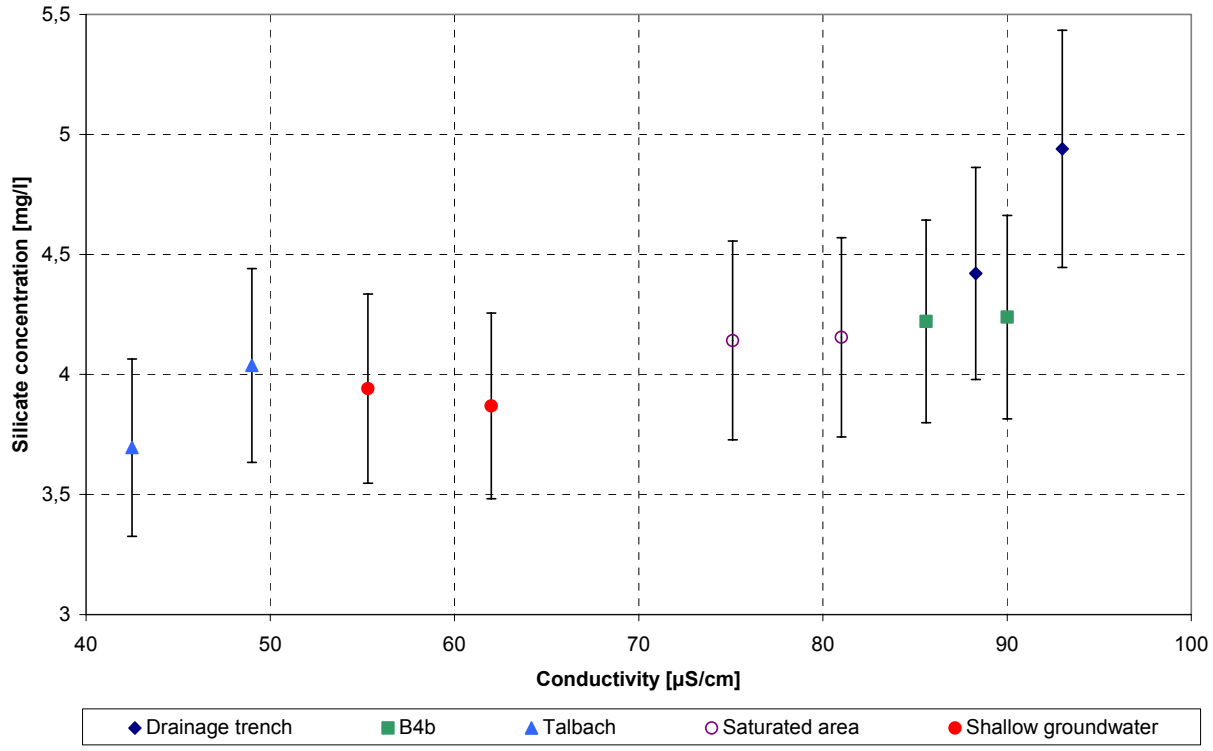

A 6: Differentiation of surface / subsurface waters by silicate concentration and electrical conductivity.

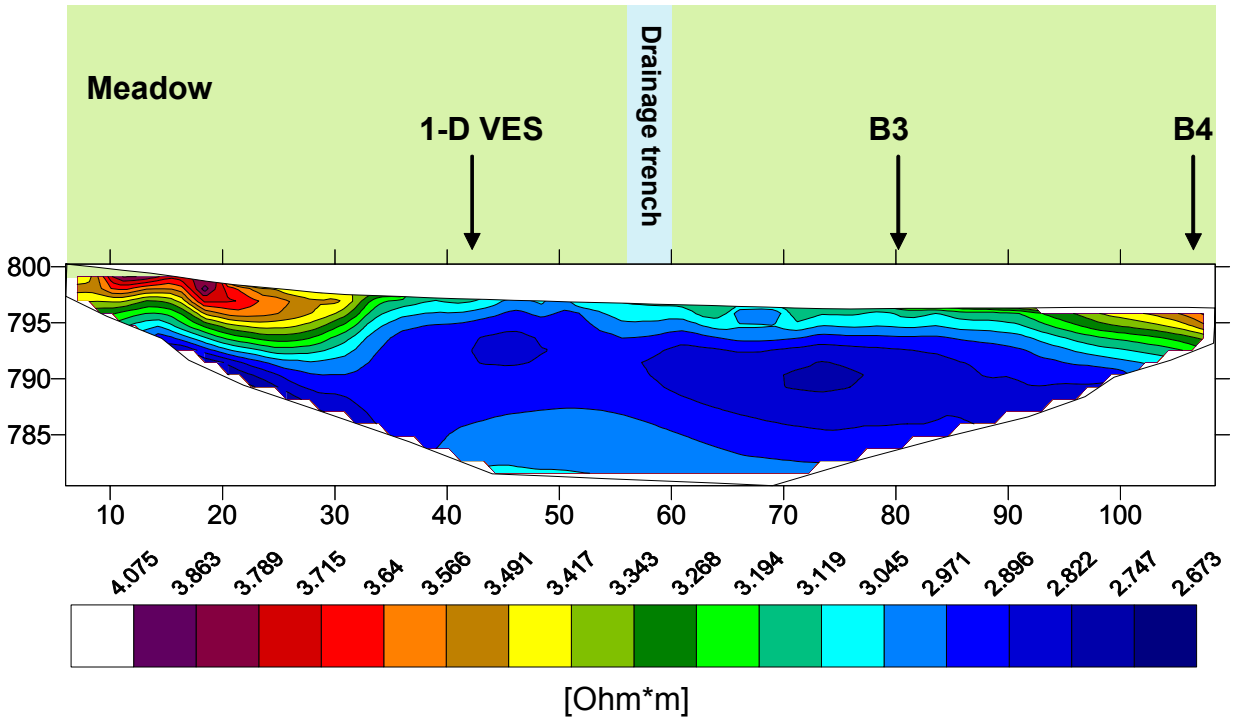

A 7: ERT Transect B (Wenner | 5 m spacing | 24 electrodes | RMS error 4,6 % | 27.07.04) with surface facts.

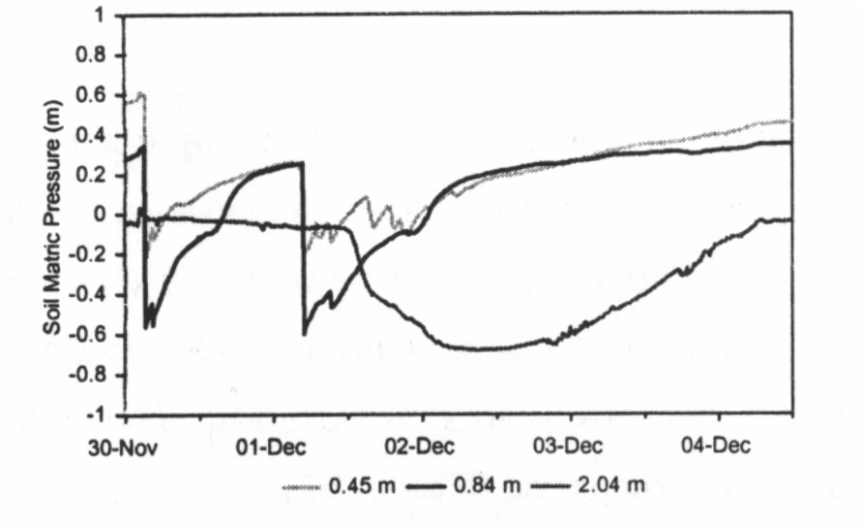

A 8: Display of tensiometer time series in different depth (where negative values indicate saturated conditions). The probes near the surface indicate the development of perched water table at the hillslope, while the probe below the phreatic water table reacts delayed (after LORENTZ, 2001).

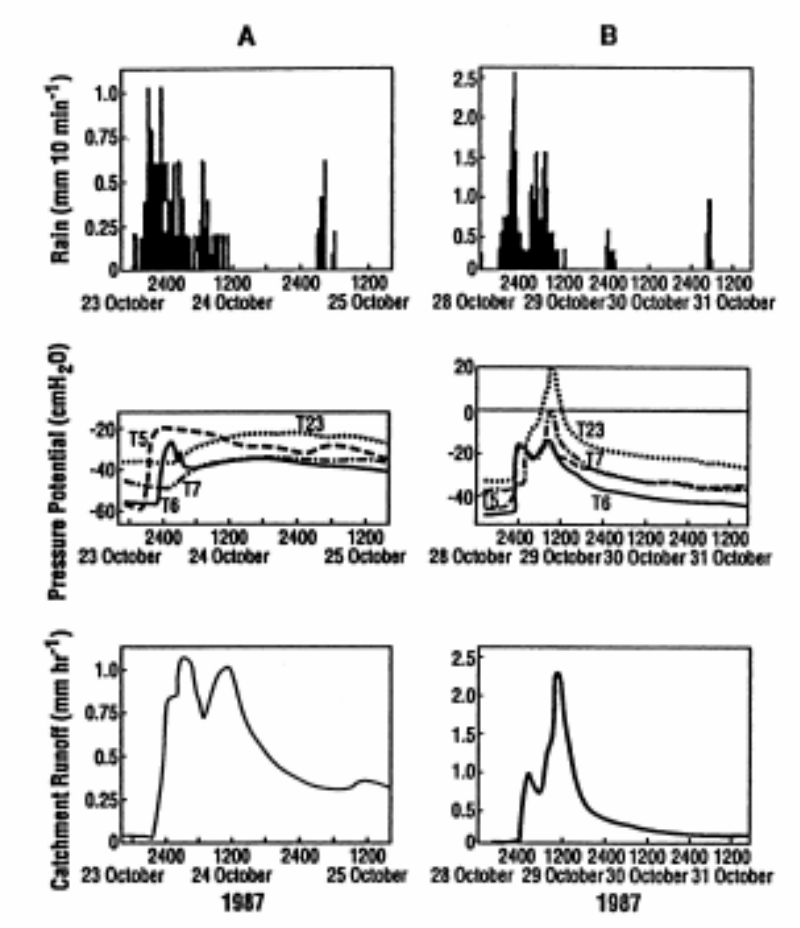

A 9: Pressure potential for tensiometers showing relationship between matric potential and rainfall – catchment runoff condition. Two storms are shown having rainfall totals on A (25 mm) and B (58 mm). Tensiometers T5, T6, T7 and T23 are inserted at 170, 410, 820 and 1080 mm below surface (after MCDONNELL, 1990).

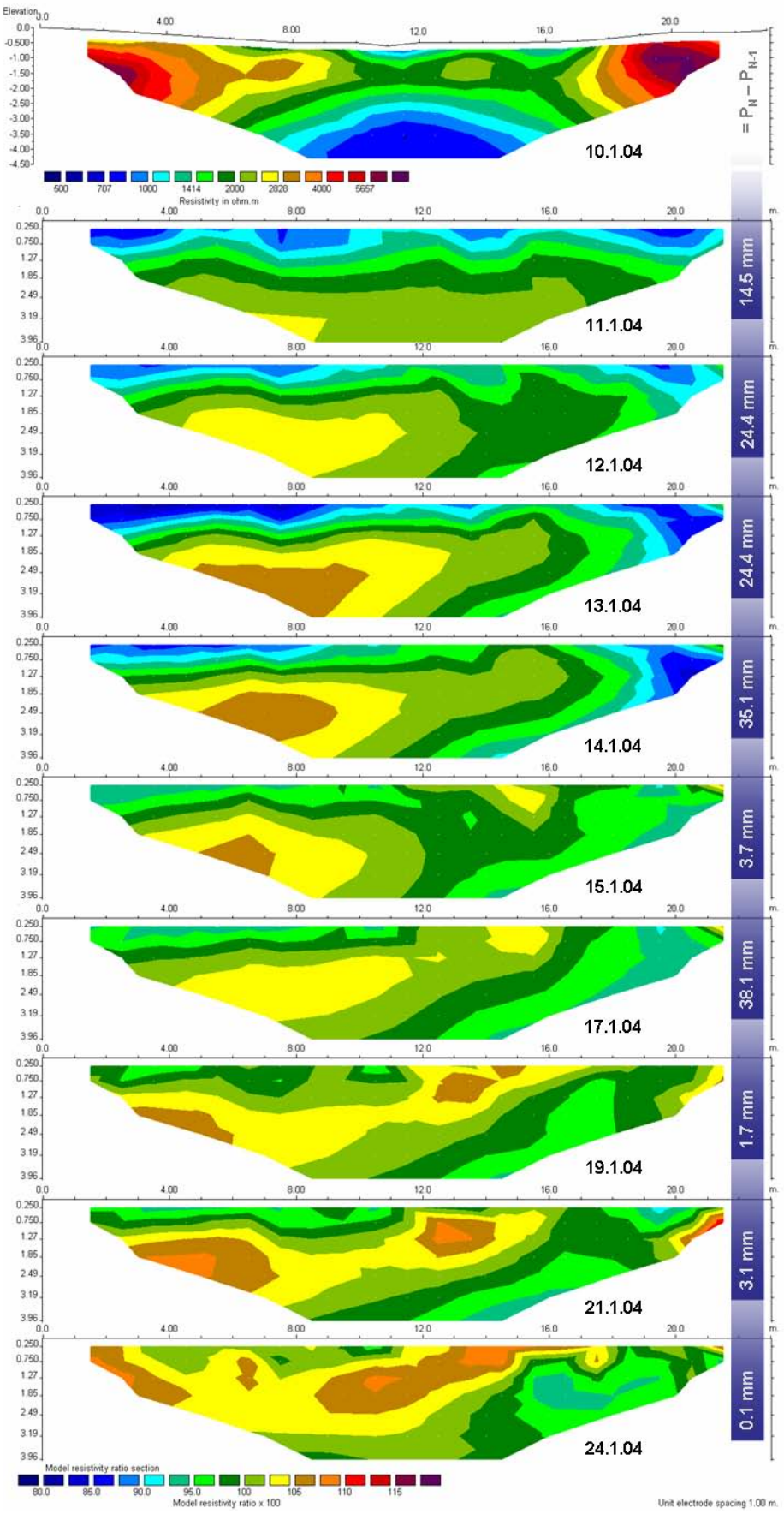

A 10: Time-lapse model calculated with the simultaneous inversion method KOCH (2004).

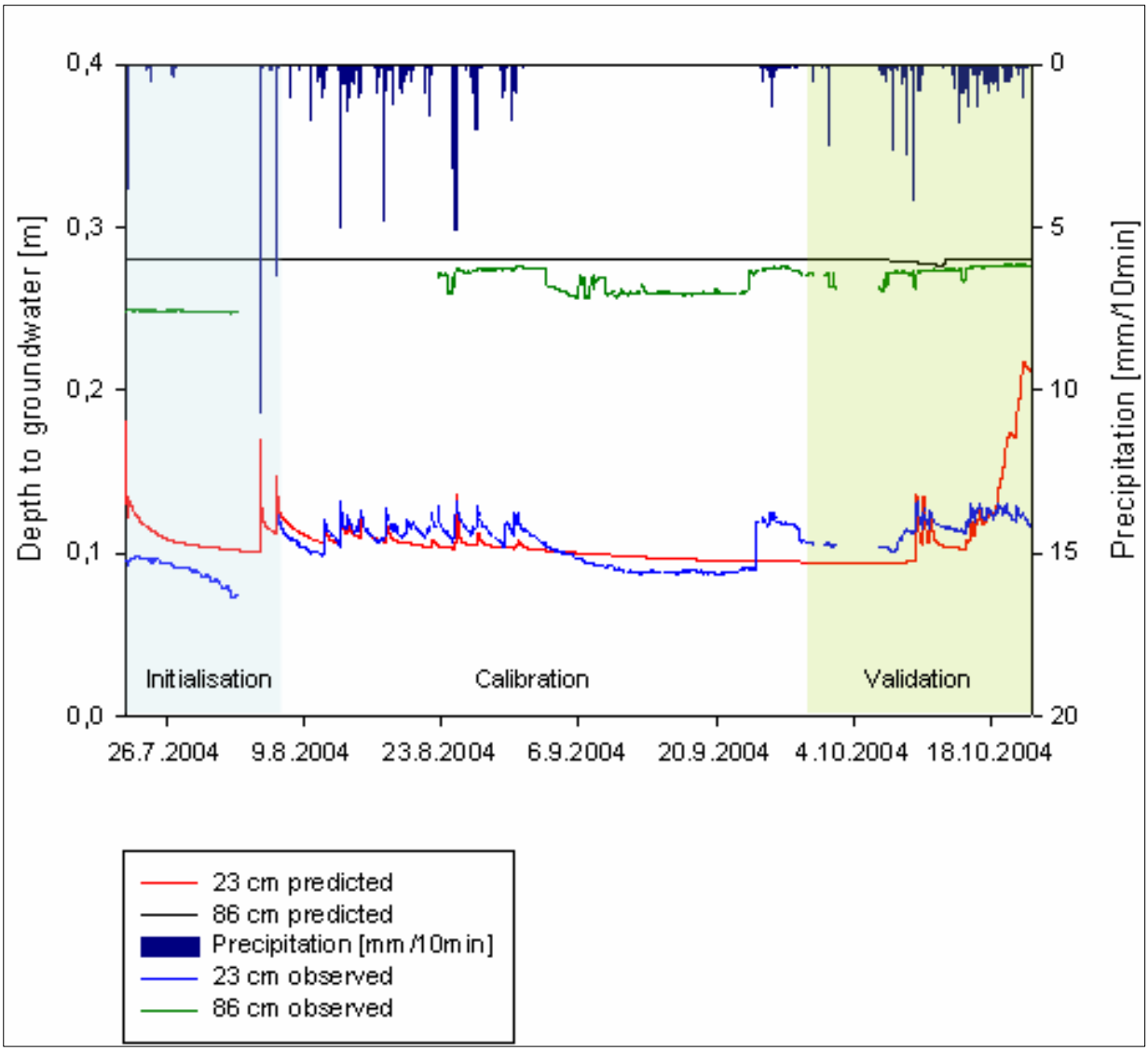

A 11: Predicted versus observed water contents for soil moisture probes in 23 cm and 86 cm depth.

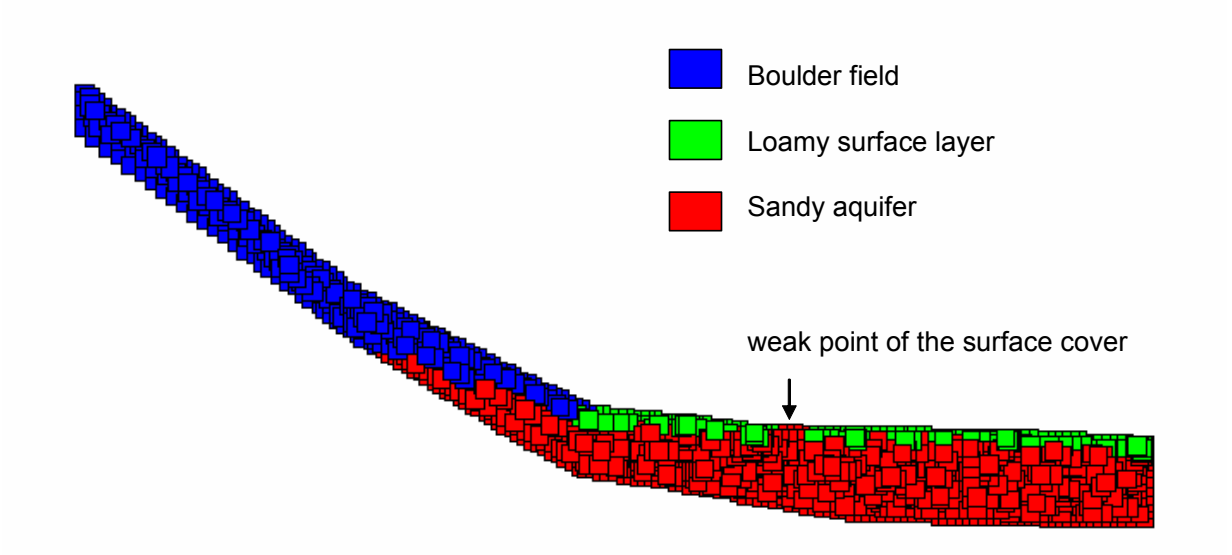

A 12: Material distribution for the vertical hillslope profile.

Ehrenwörtliche Erklärung:

Hiermit erkläre ich, dass die Arbeit selbständig und nur unter Verwendung der angegebenen Hilfsmittel angefertigt wurde.

Freiburg, den 15. Januar 2005

Katrin Meusburger